UNIVERSITAT POLITÈCNICA DE VALÈNCIA

Role of microRNAs-449 in breast cancer features: From epigenetic regulation to chemotherapy resistance

PhD THESIS

Sandra Torres Ruiz

PhD Supervisors:

Dra. Pilar Eroles Asensio

Dr. Eduardo Tormo Martín

Valencia, July 2023

“Nada en la vida es para ser temido, es sólo para ser comprendido. Ahora es el momento de entender más, de modo que podamos temer menos”

Marie Curie (1867 – 1934)

Agradecimientos

Siempre tuve claro que lo mío era la ciencia, aunque no sabía muy bien a qué correspondía este término pues era un concepto muy amplio. A medida que fui creciendo tomé mis decisiones en base a lo que tenía claro, quería estudiar y quería ser investigadora. A día de hoy puedo decir que el camino no ha sido fácil, pero sí gratificante, y durante este trayecto he aprendido que el esfuerzo y la perseverancia son clave para alcanzar tus metas. Durante el camino no he estado sola, he estado acompañada por gente que siempre ha estado y otras que han ido apareciendo. Gente sin la que, estoy convencida, no hubiera podido llegar donde estoy.

En primer lugar, gracias Pilar por haberme dado la oportunidad de llegar a este laboratorio, y gracias Juanmi por confiar en mí y permitirme seguir estando.

A la gente del labo2, que siempre ha estado ahí para escucharme y apoyarme. A ti Iris, que eres una guía y un referente. A ti Anna Adam, que, aunque ahora estás lejos sigues estando ahí para lo que se necesite, dando como siempre tu opinión más sincera. A ti Edu, que me acogiste y recibiste con los brazos abiertos. ¡Cuanto hemos hablado! Me quedo con nuestras charlas super reconfortantes que siempre me transmiten tanta positividad. Eres un gran amigo. A ti Meiri, que te prometí tendrías una mención especial. En la última etapa nos hemos llegado a conocer mucho más y he descubierto a una persona maravillosa. Siempre has estado ahí cuando lo he necesitado, pero más importante, me has ayudado a confiar más en mí misma. También, pero no menos importante, te quiero agradecer Ana Ágreda por traer aire fresco y estar siempre tan alegre, y a ti Juanjo, que para mí sigues siendo del labo 2.

En segundo lugar, gracias a mis amigas de siempre. A ti Nuria, que somos inseparables desde que nos conocimos y que nos entendemos perfectamente porque pensamos igual. A ti, Sara, por darme siempre ese otro punto de vista que

me falta para ver las cosas con otra perspectiva. A vosotras, Patri y Ari, porque, aunque estáis lejos, cuando nos vemos parece que no ha pasado el tiempo. A ti Cris, que has resultado ser fundamental en mi vida, ese “holo bonita” no me lo puede decir nadie más…. y a vosotros, Aaez y Josevi, que fuisteis una gran compañía cuando llegué.

De mi familia, ¡qué decir! Que no he podido tener más suerte y que sois imprescindibles en mi vida. Gracias a mis tíos Lolo, Pepe, Ague y Encarni, por estar siempre cuando los necesito y apoyarme incondicionalmente. Gracias a mis primos Andrea y José Andrés, que a pesar de ser totalmente diferentes me complementan a la perfección. Gracias a ti Joel, que aun siendo pequeño me has dado grandes lecciones. Sabes que eres un hermano para mí. Y cómo no, a mis padres, que han dado todo lo que tenían y más para que no me faltara de nada, y que me han dado libertad para tomar siempre mis propias decisiones sin cuestionarme nunca nada.

Por último, a ti Manuel, que me has acompañado en esta última etapa. Me has apoyado en momentos de la tesis en los que me he venido abajo, pero, además, me has impulsado hacía arriba, me has hecho creer en mí y me has dado los abrazos más reconfortantes del final del día. Hemos formado una familia junto a Misha y Mufi y no puedo estar más contenta. Te quiero.

Publications

During the completion of this PhD thesis have been obtained the following scientific publications:

- Cabello, P.; Torres-Ruiz, S.; Adam-Artigues, A.; Forés-Martos, J.; Martínez, M.T.; Hernando, C.; Zazo, S.; Madoz-Gúrpide, J.; Rovira, A.; Burgués, O.; Rojo, F.; Albanell, J.; Lluch, A.; Bermejo, B.; Cejalvo, J.M.; Eroles, P. miR-146a-5p Promotes Angiogenesis and Confers Trastuzumab Resistance in HER2+ Breast Cancer. *Cancers* ***15***, 2138 (2023).
- Torres-Ruiz S, Tormo E, Garrido-Cano I, Lameirinhas A, Rojo F, Madoz-Gúrpide J, Burgués O, Hernando C, Bermejo B, Martínez MT, Lluch A, Cejalvo JM, Eroles P. High VEGFR3 Expression Reduces Doxorubicin Efficacy in Triple-Negative Breast Cancer. *Int J Mol Sci*. **24**, 3601 (2023)
- Pattanayak B, Lameirinhas A, Torres-Ruiz S, Burgués O, Rovira A, Martínez MT, Tapia M, Zazo S, Albanell J, Rojo F, Bermejo B, Eroles P. Role of SALL4 in HER2+ Breast Cancer Progression: Regulating PI3K/AKT Pathway. *Int J Mol Sci*. **23**, 13292 (2022)
- Garrido-Cano I, Pattanayak B, Adam-Artigues A, Lameirinhas A, Torres-Ruiz S, Tormo E, Cervera R, Eroles P. MicroRNAs as a clue to overcome breast cancer treatment resistance. *Cancer Metastasis Rev*. **41**, 77-105 (2022)

Table of contents

Abbreviations and acronyms

ABCG2	ATP-binding cassette superfamily G member 2
ACACA	Acetyl-CoA carboxylase Alpha
Ac-H3	Acetyl Histone 3
ACSL4	Acyl-CoA Synthetase Long-Chain Family Member 4
AGO2	Argonaute 2
AJCC	American Joint Committee on Cancer
ATDC	Ataxia telangiectasia group D-complementing
ATE	Atelocollagen
ATG4B	Autophagy Related 4b Cysteine
ATTC	American Type Culture Collection
BC	Breast cancer
BER	Base excision repair
BMI	Body mass index
BRCA 1	Breast Cancer 1
BRCA 2	Breast Cancer 2
BSA	Bovine serum albumin
CAPN6	Calpain 6
CCNA2	Cyclin A2
CCND1	Cyclin D1
CDC25A	Cell Division Cycle 25 A
CDH1	E-cadherin

Abbreviations and acronyms

CDH2	N-cadherin
CDK4	Cyclin Dependent Kinase 4
CDK6	Cyclin Dependent Kinase 6
cDNA	Complementary DNA
CDS	Coding sequence
CI	Confidence interval
CREPT	Cell Cycle-Related and Expression-Elevated in Tumor
DFS	Disease-free survival
DGCR8	DiGeorge Syndrome Critical Region 8
DMSO	Dimethylsulfoxide
DOX	Doxorubicin
E2F3	E2F Transcription Factor 3
EGFR	Epidermal Growth Factor Receptor
EMT	Epithelial-mesenchymal transition
ER	Estrogen Receptor
ER$^{+/-}$	Estrogen Receptor positive/negative
FASN	Fatty Acid Synthase
FBS	Fetal bovine serum
FFPE	Formalin-fixed paraffin-embedded
FISH	Fluorescence *in situ* hybridization
FLOT2	Flotillin 2
FN1	Fibronectin
H3	Histone 3
HDAC	Histone Deacetylase

HDI	Human developing index
HDL	High-density lipoprotein
HEK-293T	Human embryonic kidney 293T
HER2	Human Epidermal Growth Factor Receptor Type 2
HER2$^{+/-}$	Human Epidermal Growth Factor Receptor Type 2 positive/negative
HIF1α	Hypoxia-Inducible Factor 1-Alpha
HR	Hazard ratio
HRP	Horseradish peroxidase
HT	Heterozygous
HZ	Homozygous
IARC	International Agency for Research on Cancer
IDC-NST	Invasive ductal carcinoma of no special type
IHC	Immunohistochemistry
ISH	*In-situ* hybridization
KDM3A	Lysine Demethylase 3A
LDHA	Lactate Dehydrogenase A
LGR4	Leucine Rich Repeat Containing G Protein-Coupled Receptor 4
LNA	Locked nucleic acid
MAP2K1	Mitogen-Activated Protein Kinase Kinase 1
MAPK	Mitogen-Activated Protein Kinase
miRNAs	MicroRNAs
MRI	Magnetic resonance imaging
mTOR	Mammalian Target of Rapamycin
NAC	Neoadjuvant chemotherapy

Abbreviations and acronyms

NAM	Nicotinamide
NDRG1	N-myc Downstream Regulated 1
NF90-NF45	Nuclear Factor 90-Nuclear Factor 45 complex
NGS	Next-generation sequencing
NPM1	Nucleophosmin 1
OCT4	Octamer-Binding Transcription Factor 4
OS	Overall survival
PABPC	Polyadenylate-binding protein C
PARP	Poly (adenosine-diphosphate-ribose) polymerase
PBS	Phosphate-buffered saline
pCR	Pathological complete response
PEG	Polyethylene glycol
PEI	Polyethyleneimine
PET	Polyester track etch
PFKFB3	6-Phosphofructo-2-Kinase/Fructose-2,6-Biphosphatase 3
PFS	Progression-free survival
PI3K	Phosphatidylinositol 3 kinase
PLGA	Polylactide-co-glycolic acid
POU2F1	POU Class 2 Homeobox 1
PR	Progesterone Receptor
$PR^{+/-}$	Progesterone Receptor positive/negative
PrLZ	Prostate Leucine Zipper
PSMA	Prostate Specific Membrane Antigen
RB	Retinoblastoma

RES	Reticuloendothelial system
RISC	RNA-induced silencing complex
RT-qPCR	Real-time quantitative polymerase chain reaction
SAM	S-adenyl methionine
SATB2	Special AT-Rich Sequence-Binding Protein 2
SD	Standard deviation
SDS	Sodium dodecyl sulfate
SEER	Surveillance, Epidemiology and End Results
SEM	Standard error of the mean
SGPL1	Sphingosine 1-Phosphate Lyase 1
shRNA	Short hairpin RNA
siRNA	Small-interfering RNA
SIRT1	Sirtuin 1
snoRNA	Small nuclear RNA
SOX2	SRY-Box Transcription Factor 2
TLR	Toll-Like Receptor
TNBC	Triple-negative breast cancer
TPD52	Tumor Protein D52
TRBP	TAR RNA-Binding Protein
tRNA	Transfer RNA
TSA	Trichostatin A
TUTase	Terminal uridylyl transferase
VIM	Vimentin
WHO	World Human Organization

XNR4	Exoribonuclease-4
XPO5	RanGTP-dependent exportin protein 5
YY1	Ying Yang 1

Figure index

Figure index

Figure index

Table index

Abstract

Triple-negative breast cancer accounts for 10-20% of breast cancer cases. This molecular subtype is characterized by its highly aggressive and invasive capacity being associated with a bad prognosis. The lack of hormone and HER2 receptors makes chemotherapy the main systemic effective treatment. However, several triple-negative breast cancer patients relapse after receiving chemotherapy. Therefore, deciphering the molecular characteristics and searching for new therapeutic tools for this subtype is crucial. In this sense, microRNAs are found dysregulated in several cancer types and emerge as potential prognostic molecules involved in biological processes and chemotherapy response. This thesis entitled "Role of microRNAs-449 in breast cancer features: From epigenetic regulation to chemotherapy resistance" is focused on the role of the microRNA-449 (microRNA-449a, microRNA-449b-5p, and microRNA-449c-5p) family in the modulation of breast cancer aggressiveness and chemotherapy response.

This study provided evidence of microRNAs-449 downregulation in triple-negative breast cancer cell lines and patients and suggested histone deacetylation of its promoter region as an inhibitor mechanism. Particularly, the histone deacetylases HDAC1 and SIRT1 were found upregulated in triple-negative breast cancer cells, and their genetic and chemical inhibition increased microRNAs-449 expression. In addition, a negative feedback loop modulation between microRNAs-449 and HDAC1/SIRT1 was observed, thus contributing to the homeostasis or tumoral phenotype of cells.

In silico analyses pointed out *ACSL4*, a fatty acid-activating enzyme, as target of miRNAs-449. This is in concordance with other studies that pointed out an altered

lipid metabolism to sustain cancer progression. An inverse correlation between microRNAs-449 and *ACSL4* expression was observed in triple-negative breast cancer cell lines and patients, and luciferase reporter assay confirmed this *ACSL4* direct targeting by microRNA-449a and microRNA-449b-5p for the first time. Moreover, the microRNA-449c-5p overexpression alone also produced an ACSL4 downregulation, so an indirect relationship was also suggested through the modulation of unknown molecules.

MicroRNAs-449 overexpression and *ACSL4* knockdown inhibited cell proliferation, migration by diminishing the ability to undergo the epithelial-mesenchymal transition process, and colony formation by downregulating markers of stemness. These results suggested a microRNAs-449 inhibition of breast cancer aggressiveness through *ACSL4* downregulation.

Furthermore, based on previous literature and published results by our laboratory, a microRNAs-449 implication in chemotherapy response was evaluated through this novel target. MicroRNAs-449 were downregulated in doxorubicin-resistant cells. In turn, *ACSL4* overexpression was observed in doxorubicin-resistant cells and patients who relapsed after chemotherapy-containing treatment. Subsequent doxorubicin treatment increased microRNAs-449 but decreased ACSL4 expression in doxorubicin-sensitive, but not in resistant cells, thus suggesting a microRNAs-449 and ACSL4 implication in chemotherapy response. In this study, we observed that microRNAs-449 overexpression produced doxorubicin sensitivity through ACSL4 downregulation by viability and apoptosis assay. In addition, ACSL4 inhibition decreased the drug extrusion pump ABCG2's expression, leading to an increased doxorubicin accumulation in cells.

The involvement of microRNAs-449 in the inhibition of aggressiveness and sensitivity to doxorubicin suggests its potential use as a therapeutic tool in triple-negative breast cancer.

Resumen

El cáncer de mama triple negativo representa el 10-20% de los casos de cáncer de mama. Este subtipo molecular se caracteriza por su capacidad altamente agresiva e invasiva asociándose a un mal pronóstico. La ausencia de receptores hormonales y HER2 hace que la quimioterapia sea el principal tratamiento sistémico eficaz. Sin embargo, muchas pacientes con cáncer de mama triple negativo recaen tras recibir quimioterapia. Descifrar las características moleculares y la búsqueda de nuevas herramientas terapéuticas de este subtipo en particular resulta crucial. En este sentido, los microRNAs se encuentran desregulados en varios tipos de cáncer, y emergen como potenciales moléculas pronósticas implicadas en procesos biológicos y en la respuesta a la quimioterapia. Esta tesis titulada "Papel de los microRNAs-449 en las características del cáncer de mama: De la regulación epigenética a la resistencia a la quimioterapia" se centró en el papel de la familia de microRNA-449 (microRNA-449a, microRNA-449b-5p y microRNA-449c-5p) en la modulación de la agresividad del cáncer de mama y la respuesta a la quimioterapia.

Este estudio aportó pruebas de la regulación negativa de los microRNAs-449 en líneas celulares y pacientes de cáncer de mama triple negativo, y sugirió una desacetilación de histonas de su región promotora como un mecanismo inhibidor. En particular, las histonas desacetilasas HDAC1 y SIRT1 se encontraron sobreexpresadas en células de cáncer de mama triple negativo, y su inhibición genética y química aumentó la expresión de los microRNAs-449. Además, se observó una modulación de retroalimentación negativa entre los microRNAs-449 y HDAC1/SIRT1, contribuyendo así a la homeostasis o fenotipo tumoral de las células.

Análisis *in silico* apuntaron a ACSL4, una enzima activadora de ácidos grasos, como diana de los microRNAs-449. Esto concuerda con otros estudios que apuntaban a una alteración del metabolismo lipídico para sostener la progresión del cáncer. Se observó una correlación inversa entre la expresión de los microRNAs-449 y *ACSL4* en líneas celulares de cáncer de mama triple negativo y en pacientes, y el ensayo reportero de la luciferasa confirmó esta interacción directa de *ACSL4* por los microRNA-449a y microRNA-449b-5p por primera vez. Además, la sobreexpresión del microRNA-449c-5p por separado produjo una regulación negativa de ACSL4, por lo que también se sugirió una relación indirecta a través de la modulación de moléculas desconocidas.

Tanto la sobreexpresión de los microRNAs-449 como el silenciamiento de *ACSL4* inhibieron la proliferación celular, la migración mediante la disminución de la capacidad de someterse al proceso de transición epitelio-mesénquima, y la formación de colonias mediante la regulación negativa de los marcadores de troncalidad. Estos resultados sugirieron una inhibición de la agresividad del cáncer de mama por los microRNAs-449 a través de la regulación negativa de ACSL4.

Además, basándonos en la literatura previa y en los resultados publicados por nuestro laboratorio, se evaluó la implicación de los microRNAs-449 en la respuesta a la quimioterapia a través de esta nueva diana. Los microRNAs-449 se encontraron infraexpresados en las células resistentes a la doxorrubicina. A su vez, se observó una sobreexpresión de ACSL4 en células resistentes a la doxorrubicina y en pacientes que recayeron tras el tratamiento con quimioterapia. El tratamiento posterior con doxorrubicina aumentó la expresión de los microRNAs-449 pero disminuyó la de ACSL4 en células sensibles a la doxorrubicina, aunque no en las resistentes, sugiriendo así una implicación de los microRNAs-449 y ACSL4 en la respuesta a la quimioterapia. En este estudio, observamos que la sobreexpresión de los

microRNAs-449 produjo sensibilidad a la doxorrubicina a través de la regulación negativa de ACSL4 mediante ensayos de viabilidad y apoptosis. Además, la inhibición de ACSL4 disminuyó la expresión de la bomba de extrusión de fármacos ABCG2, lo que condujo a un aumento de la acumulación de doxorrubicina en las células.

La implicación de los microRNAs-449 en la inhibición de la agresividad y la sensibilidad a la doxorrubicina sugiere su uso potencial como herramienta terapéutica en cáncer de mama triple negativo.

Resum

El càncer de mama triple negatiu representa el 10-20% dels casos de càncer de mama. Aquest subtipus molecular es caracteritza per la seua capacitat altament agressiva i invasiva associant-se a un mal pronòstic. L'absència de receptors hormonals i HER2 fa que la quimioteràpia siga el principal tractament sistèmic eficaç. No obstant això, moltes pacients amb càncer de mama triple negatiu recauen després de rebre quimioteràpia. Desxifrar les característiques moleculars i la cerca de noves eines terapèutiques d'aquest subtipus en particular resulta crucial. En aquest sentit, els microRNAs es troben desregulats en diversos tipus de càncer, i emergeixen com a potencials molècules pronosticades implicades en processos biològics i en la resposta a la quimioteràpia. Aquesta tesi titulada "Paper dels microRNAs-449 en les característiques del càncer de mama: De la regulació epigenètica a la resistència a la quimioteràpia" es va centrar en el paper de la família de microRNAs- 449 (microRNA-449a, microRNA-449b-5p i microRNA-449c-5p) en la modulació de l'agressivitat del càncer de mama i la resposta a la quimioteràpia.

Aquest estudi va aportar proves de la regulació negativa dels microRNAs-449 en línies cel·lulars i pacients de càncer de mama triple negatiu, i va suggerir una desacetilació d'histones en la seua regió promotora com a mecanismo inhibidor. En particular, les histones desacetilases HDAC1 i SIRT1 es van trobar sobreexpresades en cèl·lules de càncer de mama triple negatiu, i la seua inhibició genètica i química va augmentar l'expressió dels microRNAs-449. A més, es va observar una modulació de bucle de retroalimentació negativa entre els microRNAs-449 i HDAC1/SIRT1, contribuint així a l'homeòstasi o fenotip tumoral de les cèl·lules.

Anàlisi *in silico* van apuntar *ACSL4*, enzima activadora d'àcidos grassos, com a diana dels microRNAs-449. Això concorda amb altres estudis que apuntaven a una alteració del metabolisme lipídic per a sostindre la progressió del càncer. Es va observar una correlació inversa entre l'expressió dels microRNAs-449 i *ACSL4* en línies cel·lulars de càncer de mama triple negatiu i en pacients, i l'assaig reporter de la luciferasa va confirmar aquesta interacció directa d'*ACSL4* pels microRNA-449a i microRNA-449b-5p per primera vegada. A més, la sobreexpressió del microRNA-449c-5p per separat va produir una regulació negativa d'ACSL4, per la qual cosa també es va suggerir una relació indirecta a través de la modulació de molècules desconegudes.

Tant el guany de funció dels microRNAs-449 com el silenciament d'*ACSL4* van inhibir la proliferació cel·lular, la migració mitjançant la disminució de la capacitat de sotmetre's al procés de transició epiteli-mesènquima, i la formació de colònies mitjançant la regulació negativa dels marcadors de troncalitat. Aquests resultats van suggerir una inhibició de l'agressivitat del càncer de mama pels microRNAs-449 a través de la regulació negativa d'ACSL4.

A més, basant-nos en la literatura prèvia i en els resultats publicats pel nostre laboratori, es va avaluar la implicació dels microRNAs-449 en la resposta a la quimioteràpia a través d'aquesta nova diana. Els microRNAs-449 es van trobar infraexpressats en les cèl·lules resistents a la doxorrubicina. Al seu torn, es va observar una sobreexpressió d'*ACSL4* en cèl·lules resistents a la doxorrubicina i en pacients que van recaure després del tractament amb quimioteràpia. El tractament posterior amb doxorrubicina va augmentar l'expressió dels microRNAs-449 però va disminuir la d'ACSL4 en cèl·lules sensibles a la doxorrubicina, encara que no en les resistents, suggerint així una implicació dels microRNAs-449 i ACSL4 en la resposta a la quimioteràpia. En aquest estudi, observem que la sobreexpressió dels microRNAs-

449 va produir sensibilitat a la doxorrubicina a través de la regulació negativa d'ACSL4 mitjançant assajos de viabilitat i apoptosi. A més, la inhibició d'ACSL4 va disminuir l'expressió de la bomba d'extrusió de fàrmacs ABCG2, la qual cosa va conduir a un augment de l'acumulació de doxorrubicina en les cèl·lules.

La implicació dels microRNAs-449 en la inhibició de l'agressivitat i la sensibilitat a la doxorrubicina suggereix el seu ús potencial com a eina terapèutica en càncer de mama triple negatiu.

CHAPTER 1 |

Introduction

1.1 Cancer

According to the International Agency for Research on Cancer (IARC), 1 in 5 people develop cancer throughout their lives, being also one of the leading causes of death in developed countries. Specifically, recent data published by GLOBOCAN point out a total of 19,300,000 new cancer cases and 10,000,000 cancer deaths in 2020[1]. In the United States, a total of 1,958,310 cases and 609,820 deaths are expected to occur in 2023[2].

Due to the great relevance of this disease, different studies have focused on the origin and progression of cancer. A malignant transformation of healthy cells due to genetic and epigenetic mutations, as well as the presence of cancer stem cells capable of giving rise to tumorigenic cells are two explanations for its origin[3]. Among the characteristics of this disease are its high proliferative capacity, dysregulation of metabolism, resistance to cell death, genomic instability, sustained angiogenesis, invasion and metastasis, unlimited replicative potential, tumor-promoting inflammation, evasion of the immune system and insensitivity to growth suppressants[4] (**figure 1**).

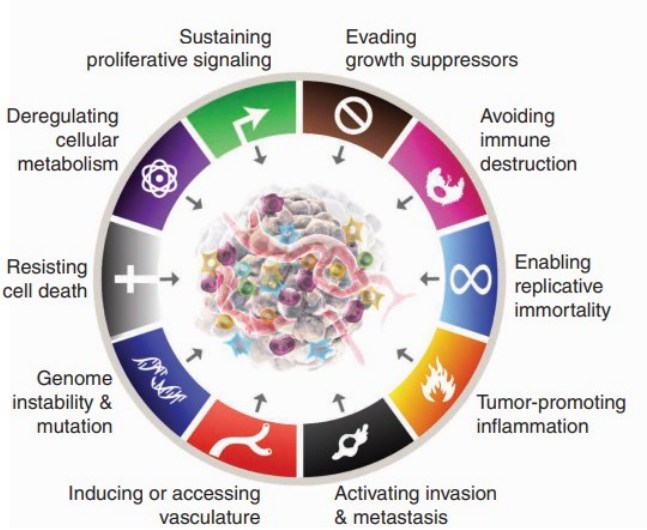

Figure 1: Representation of cancer hallmarks. Source: Hanahan *et.al.*[4]

Concretely, this thesis focuses on the study of the molecular basis of breast cancer (BC), as well as its progression and treatment response.

1.2 BC epidemiology

According to the most recent published data by GLOBOCAN, BC is the most common cancer diagnosed with 2,261,419 cases, representing 11.7% of all cancer cases worldwide in 2020[1] (**figure 2**). In the United States, a total of 300,590 new cases are expected to occur in 2023[2]. Concretely, BC is mainly diagnosed in women, with males being less than 1% of all cases[5]. The incidence rate presents a different distribution in the world population associated with the human developing index (HDI). In this sense, developed countries have an 88% higher incidence rate (55.9 per 100,000) than developing countries (29.7 per 100,000)[1] (**figure 3**). This increment in developed countries is commonly attributed to changes in hormonal, reproductive, and lifestyle risk factors[6].

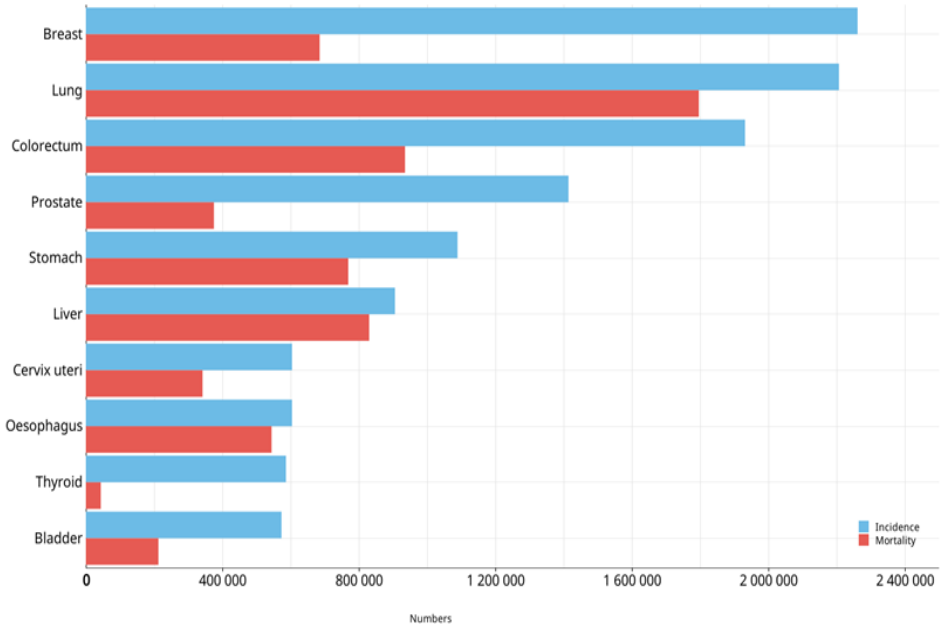

Figure 2: Number of incident cases and deaths worldwide in 2020, including both sexes and all ages. Source: Globocan 2020

Analysis of the trend in incidence rate between 1975 and 2018 in the United States evidences a peak of incidence in the 90s due to the increasingly widespread use of mammographic screening, and has been increasing since then with a rate of 0.5% per year[7]. Based on this slightly increased, 4,4 million cases are expected to be reached by 2070[8].

Regarding mortality, BC is the fifth cause of cancer death worldwide with a record of 684,996 deaths in 2020 (**figure 2**), which represents 6.9% of all cancer deaths, and is the leading cause of cancer death in women. In the United States, a total of 43,700 deaths are expected to occur in 2023[2]. Contrary to the incidence rate, developing countries have a 17% higher mortality rate (15 per 100,000) than developed countries (12.8 per 100,000) associated with delay in early detection and lack of

effective treatments[1,9] (**figure 3**). In addition, an analysis of the trend in mortality rate between 1975 and 2018 in the United States evidences a decrease in mortality since the 90s due to early detection and effective treatment[7]. However, this drop in mortality has been decreasing in recent years probably related to a higher incidence rate, advanced treatments, and widespread use of mammography screening[10].

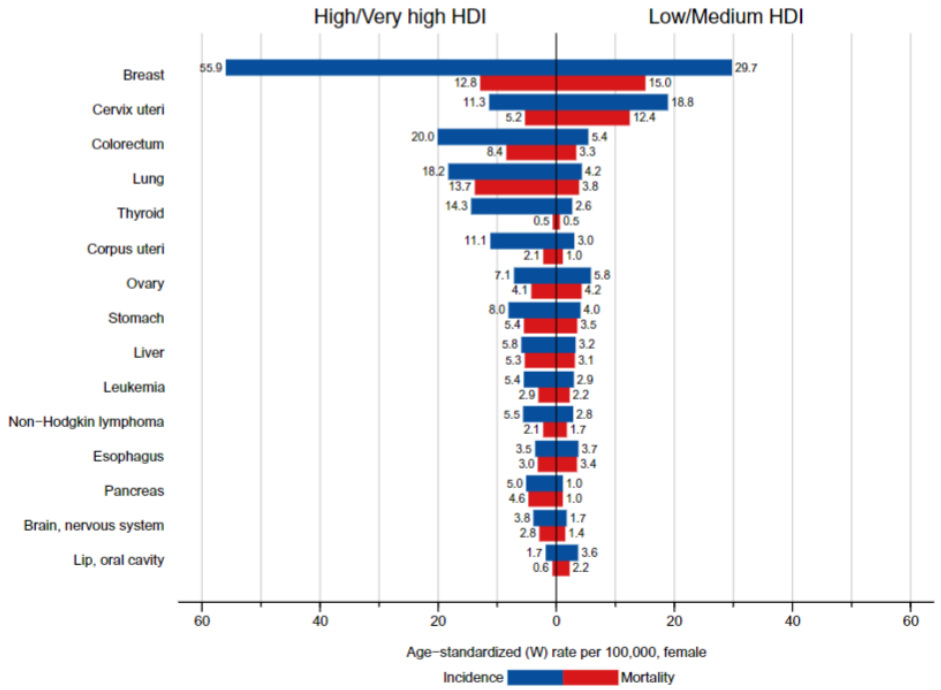

Figure 3: Estimated age-standardized incidence and mortality rates in 2020 for high/very high and low/medium HDI countries in females and all ages. Source: Globocan 2020

Considering this data, establishing effective screening programs in the population to diagnose BC early-stage and searching for effective treatments is crucial for improving BC mortality. In addition, it is necessary to raise awareness among the population of cancer health to prevent the risk factors that lead to increased incidence.

1.3 BC risk factors

Different factors that can be classified as non-modifiable and modifiable factors have been associated with BC risk.

1.3.1 Non-modifiable risk factors

1.3.1.1 Family history and genetic factors

A total of 5-10% of BC cases are hereditary. Regarding these, it is known that 2 or more family cases with BC in women under 50 and 3 or more cases of any age are 10 times more likely to have BC[6]. Twenty-five percent of these hereditary BCs are due to mutations in the *Breast Cancer 1* (*BRCA1)* and *Breast Cancer 2* (*BRCA2)* tumor suppressor genes. Moreover, *de novo* mutations also occur, thus accounting for up to 10% of all BC cases[11]. The incidence of BC for women with *BRCA1* mutations is higher and increases up to 40 years, however, women with *BRCA2* mutations have the same incidence as women who do not have this mutation[12]. Furthermore, it is known that *BRCA1* and *BRCA2* mutations represent approximately 65% and 45%, respectively, of BC risk at age 70[13], and are associated with more aggressive tumors. Specifically, some studies associate *BRCA* mutations with worst overall survival (OS) and lower disease-free survival (DFS)[14,15]. Other germline mutations in *TP53, PTEN, PALB2, ATM, CHEK2,* and *STK11* genes are found in less than 1% of hereditary BCs[11].

1.3.1.2 Age

The risk of BC is known to increase with age, which is associated with changes in different reproductive factors such as menarche, menopause, and related to pregnancy. However, younger women (characterized as younger than 45 years in

most studies) are associated with diagnosis in more advanced stages[16,17], more unfavorable biology, more aggressive subtypes, and a higher risk of distant recurrence after treatment. Additionally, 50% of women under the age of 30 have *BRCA1, BRCA2*, and *TP53* mutations[18,19].

1.3.1.3 Menarche and menopause

BC risk is associated with estrogen and progesterone exposure that occurs during the reproductive years and directly affects breast function. In this sense, a longer reproductive lifespan has been associated with higher BC risk[20]. Specifically, a meta-analysis based on epidemiologic studies in different countries points out a 5% of risk increase for each younger year of menarche and a 3% of risk increase for each older year of menopause[21]. These results are related to the observed protective effect of early oofectomy[12].

1.3.1.4 Breast density

It refers to mammography appearance due to different amounts of fat that are reflected as black spots, leading to potential misdiagnosis. Different studies demonstrate a positive association between breast density and BC risk[22,23] with an approximate increment of 3.4% risk for each 1% of greater breast density[6].

1.3.2 Modifiable risk factors

1.3.2.1 Reproductive factors

Having a child and breastfeeding are associated as protective factors against BC in different prospective studies. A meta-analysis combining 47 epidemiological studies demonstrated that having a child decreases the risk of BC in women under 30,

assuming a decrease of 3% for each year younger and 7% for each child[24]. In addition, pregnancies of more than 34 weeks reduce the relative risk even more compared to pregnancies of shorter duration [25]. Breastfeeding further decreases the relative BC risk compared to those who have not breastfed, with a greater decrease with longer a duration of breastfeeding[24,26,27].

1.3.2.2 Hormone factors

Hormone replacement therapy and hormonal contraception are also associated with BC risk. Two formulations are used to treat the symptoms of menopause, one is estrogen therapy and the other is combined estrogen and progestin therapy. Different studies show discrepancies regarding the risk associated with estrogen treatment alone. Some prospective studies point out a decreased risk of BC due to a lower incidence and mortality rate observed in this group, while others point out a higher risk. However, combined hormone therapy points to a generalized increased BC risk[28–30]. This increased risk is also greater with prolonged use of hormonal treatment and in high-risk groups of women, such as those with *BRCA1* and *BRCA2* mutations [12,30].

Hormonal contraception is associated with BC risk in different studies, with higher risk with longer hormonal exposure in women who use or have recently used it. However, this increase seems to disappear after 10 years of cessation[31–34].

1.3.2.3 Lifestyle factors

Obesity, increased body fat, alcohol consumption, smoking, and lack of exercise have been associated with BC risk factors.

Body mass index (BMI) ≥ 30 kg/m^2 is associated with an increased risk of BC incidence, especially in postmenopausal women, and with a higher relative risk of BC mortality[35–37]. In addition, increased whole-body fat is associated with higher BC risk in women with normal BMI. This latter is because BMI is an inaccurate measurement that does not distinguish between body fat and muscle[38]. This increased risk due to obesity is explained by metabolic alterations such as insulin resistance, increased expression of aromatase, and increased levels of free estradiol that end up stimulating cell proliferation and survival[36,37].

Alcohol consumption and smoking also increase BC risk in a dose and time-dependent manner. Different meta-analyses point out an increase of up to 10% and 13% of the risk in women who consume 1 alcoholic drink a day or smoke 10 to 20 cigarettes a day, respectively[39–41]. Higher mortality has also been associated with the consumption of more than 3 alcoholic drinks a day and in current and former smokers[40–43].

However, physical exercise and a healthy diet based on vegetables, fruits, legumes, and cereals have been widely associated with a decrease in BC risk[44–47].

1.4 BC screening

According to data from Surveillance, Epidemiology and End Results (SEER), BC survival is lower at more advanced stages of diagnosis, changing the 5-year survival rate from 98% for stage I to 92% for stage II, 75% for stage III, and 27% for stage IV[48]. In this sense, screening aims to detect asymptomatic BC in early-stage to improve the patient's prognosis and reduce its mortality rate.

Mammography is the most common BC screening method implemented in different European and American screening programs. Specifically, the World Human

Organization (WHO) strongly recommends population-based mammography screening programs for women aged 50-69 years each two years. This recommendation is based on different strong and moderate evidences. Randomized trials carried out in different countries showed a reduction in mortality of 15-32% in women who have undergone mammography screening programs after 13 years of follow-up compared to those who have not[49–51]. However, mammography also has negative aspects such as false positives, overdiagnosis, and overtreatment that have been analyzed in different prospective studies. A higher number of false positives have been associated with annual screening compared to biennial screening, earliest ages at first screening, and women with dense breasts, leading to unnecessary biopsies[49,52]. In addition, the estimate of overdiagnosis varies in different randomized controlled trials depending on the calculation method used, with a range of 1 to 50% in different world populations, thus resulting in possible unnecessary treatment[53–55]. Dense breast tissue has also been shown to mask the presence of tumors[56].

Due to the negative effects of mammography, different methods have been evaluated to establish them in screening programs. In women at high risk for BC, magnetic resonance imaging (MRI) showed a sensitivity of 90-93%, compared to 50% for mammography[57]. Moreover, its use in combination with mammography was also shown to detect BC in earlier stages than the use of individual mammography[58]. European Commission Initiative on Breast Cancer and American College of Radiology has established recommendations based on such evidence that support its use in women at high risk, with a history of familial breast cancer, with or without BRCA mutations, and with dense breasts[58,59]. Other methods such as ultrasound, tomosynthesis, shear wave elastography, and spectral mammography are being

evaluated for screening implementation, but no evidence has yet been seen in mortality reduction.

As indicated above, prevention programs, early detection, and improved treatments are crucial to increase survival rates and reduce mortality rates, calculating also a saving of 60% of total expenses compared to only the implementation of treatment programs in all world regions[60]. These strategies are not feasible in short and middle-income countries, where self-examination and clinical examination take on special importance.

1.5 BC classification

BC is a heterogeneous disease, so different classification systems have been developed to better understand tumor biology and establish a prognostic and predictive value that determines the best treatment strategy to follow for each patient.

1.5.1 Histological and anatomical classification

The previously specified imaging tests together with the physical examination guide the diagnosis. However, the final pathological diagnosis is based on the biopsy according to the classification of the WHO and the eighth edition of the American Joint Committee on Cancer (AJCC) tumor, node, metastasis (TNM) staging system[58].

BC is histologically classified according to the fourth edition of the WHO. Breast carcinomas are mainly divided according to whether the tumor is limited to the epithelial component (*in situ* carcinoma) or has invaded the stroma (invasive carcinoma). In addition, the morphological characteristics of the cells and the epithelial origin are taken into account, the latter referring to whether it has

originated in the mammary ducts (ductal carcinoma) or lobules (lobule carcinoma)[61–63]. Invasive carcinoma is the most commonly diagnosed histological subtype and with a less favorable prognosis, being invasive ductal carcinoma of no special type (IDC-NST) up to 75% of all cases and with a higher risk of recurrence[64–66]. However, morphologic markers are limited due to intratumorally variations.

Moreover, AJCC TNM system classification divides BC into four different anatomic stages: I (early stage)-IV (advanced stage). This staging system is based on the size and location of the tumor (T), the number of affected lymph nodes (N), and distant metastases (M), thus giving a view of tumor progression. A description of TNM stage system classification is specified in **table 1**. Regarding prognostic value, advanced stages presented poor relapse-free survival (RFS) compared to early-stages[67]. Nevertheless, the prediction of clinical outcome and prognosis solely based on the TNM stage is insufficient due to tumor heterogeneity[68,69].

Table 1: American Joint Committee on Cancer (AJCC) anatomic stage groups. Source: AJCC cancer staging manual, eighth edition

T	N	M	Anatomic stage
Tis	N0	M0	**0**
T1	N0	M0	**IA**
T0	N1mi	M0	**IB**
T1	N1mi	M0	**IB**
T0	N1	M0	**IIA**
T1	N1	M0	**IIA**
T2	N0	M0	**IIA**
T2	N1	M0	**IIB**
T3	NO	M0	**IIB**
T0	N2	M0	**IIIA**
T1	N2	M0	**IIIA**
T2	N2	M0	**IIIA**
T3	N1	M0	**IIIA**
T3	N2	M0	**IIIA**

Table 1: (Continued)

T4	N0	M0	**IIIB**
T4	N1	M0	**IIIB**
T4	N2	M0	**IIIB**
Any T	N3	M0	**IIIC**
Any T	Any N	M1	**IV**

The last edition of the AJCC TNM system also incorporates the tumor grade as an additional anatomic prognostic factor along with the determination of three different molecular prognostic factors: Estrogen Receptor (ER), Progesterone Receptor (PR), and Human Epidermal Growth Factor Receptor Type 2 (HER2)[70]. Tumor grade determination is currently performed according to the Nottingham system. This system assigns a score from 1 to 3 on the analysis of nuclear polymorphism, tubule formation, and mitotic activity, being 3 farthest from the normal breast. The sum of these scores gives rise to 3 different tumor grades: grade 1 (well-differentiated), grade 2 (moderately differentiated), and grade 3 (poorly differentiated) (**Table 2**)[71].

Table 2: Nottingham histological grade criteria of scoring. Adapted from Santos *et.al.* [72]

Parameter	**Score 1**	**Score 2**	**Score 3**
Tubule formation	>75%	10-75%	<10%
Nuclear polymorphism	Absent	Moderate	Marked
Mitotic activity	<9	9-17	>17
Final score	3-5 (**Grade I**)	6-7 (**Grade II**)	8-9 (**Grade III**)

Integration of the TNM system and molecular markers determination results in different clinical and pathological prognostic stages, that can be applied to all

patients or those who have surgical resection as initial treatment, respectively. A study from the University of Alabama in 2018 showed that the application of prognostic stages upgraded 27.7% and downgraded 24.7% of BC cases compared to anatomic staging[67]. The use of the prognostic stage has been validated in different patient cohorts, demonstrating a better prediction of BC prognosis[73–75].

1.5.2 Pathological classification

The 12th St Gallen International Breast Cancer Conference established a surrogate intrinsic BC classification based on immunohistochemical (IHC) determination of PR, ER, HER2 (also known as ERBB2), and the Ki67 proliferation marker that should be into account for BC treatment decisions[76]. This IHC analysis is made from formalin-fixed paraffin-embedded tumor samples in routine clinical practice. In addition, fluorescence *in situ* hybridization (FISH) for borderline positive IHC cases is used to determine HER2 status. One of the limitations of IHC analysis is the lack of a uniform cut-off for each biomarker. In this sense, ASCO/CAP guidelines recommend to considered ER and PR positive when ≥1% of tumor cells present nuclear staining by Allred scoring and histochemical score (H-score) method. Additionally, HER2 is recommended to be considered positive when ≥10% of tumor cells present a membrane staining[58,77]. Ki67 is also determined to measure cell proliferation, and a cut-off of 14% is commonly used to differentiate between high and low-proliferation tumors. However, some studies point out a cut-off of 20% due to better BC surrogate classification and sensitivity to discriminate between luminal subtypes[76,78–80]. According to the expression of these biomarkers, BC is clinically divided into four different surrogate intrinsic subtypes: Luminal A (ER+, PR+, HER2-, Ki67 low), luminal B (ER+, PR+/-, HER2+/-, Ki67 any), HER2+ (ER-, PR-, HER2+. Ki67 high) and triple-negative (ER-, PR-, HER2, Ki67 high)[62] (**table 3**).

Table 3: Pathological BC classification.

Subtype	ER	PR	HER2	Ki67
Luminal A	+	+	-	<14%
Luminal B-HER2-	+	-/low	-	≥14%
Luminal B-HER2+	+	-/+	+	Any
HER2+	-	-	+	≥14%
Triple-negative	-	-	-	≥14%

Based on this clinical classification, luminal A is the most common subtype (40-50%), followed by luminal B (20-30%), HER2+ (15-20%), and triple-negative (10-20%)[62]. Regarding prognosis, luminal A present the best 5-year survival rate (92%), followed by luminal B (89%), HER2+ (83%), and triple-negative (77%)[48].

1.5.3 Molecular classification

The molecular classification of BC based on multigenic analysis has been developed in recent years and has gained special relevance in decoding tumor biology and establishing a more accurate predictive value.

Perou *et.al.* was the pioneer in the 2000s. They evaluated a set of 'intrinsic genes' by microarray cDNA on a total of 43 individuals (40 BC samples and 3 normal breast samples) and distinguished four different intrinsic molecular subtypes: luminal, HER2-enriched, basal-like, and normal-like[81]. However, different studies considered the normal-like subtype as an artifact due to expression genes from adipose tissue and normal breast tissue[81,82]. In 2001, Sorlie *et.al.* evaluated this `intrinsic genes' list in 85 individuals (78 BC samples and 7 normal breast samples) and differentiated the luminal subtype into luminal A and luminal B[83]. Subsequent integrative analysis on

mammary and murine tumors by Herschkowitz *et.al.* in 2007 and mammary cell lines by Prat *et.al.* in 2010 revealed the claudin-low subtype[84,85]. Based on this data, five molecular intrinsic molecular subtypes are strongly recognized and present different characteristics:

Luminal A is the most common subtype and accounts for 50-60% of all BC[86]. It is characterized by high expression of *ER* and luminal cell genes and low expression of proliferation-related genes[81,83]. In addition, it presents a great diversity of mutated genes, *PIK3CA* being the most frequent[77]. This subtype is frequently associated with low histological grade and well-differentiated tumors[86]. Regarding the metastatic sites, bone is the most common one[87]. It presents the better prognosis, but the lowest rate of pathological complete response (pCR) to neoadjuvant chemotherapy[83,88]. However, it presents high benefits from endocrine therapy[89].

Luminal B represents 15-20% of all BC[86]. It is characterized by high expression of *ER* and proliferation-related genes, less expression of luminal cell genes than luminal A, and, low or no expression of *PR*, together with *TP53* and *PIK3CA* mutations[77,83]. In addition, studies carried out by Parker and Rouzier *et.al.* where they compared the intrinsic subtypes with the clinical status found that not all tumors with HER2 amplification were HER2-enriched, but some were luminal B[82,88]. This subtype is frequently associated with intermediate histological grade and moderately differentiated tumors[62]. Regarding metastatic sites, bone is also the most frequent followed by liver, lung, and pleural/peritoneal[87]. It presents poor prognosis than luminal A[83]. Moreover, it shows the same pCR rate to neoadjuvant chemotherapy with anthracyclines and paclitaxel and a higher pCR rate to anthracycline and taxane-based chemotherapy[88,90], but worst response to endocrine therapy than luminal A subtype[89].

HER2-enriched accounts for 15-20% of all BC[86]. It presents a high expression of *ERBB2*, proliferation-related genes, and other genes related to the HER2 pathway, but no expression of *ER* nor *PR*[77,81]. In addition, it shows a high frequency of *TP53* and *PIK3CA* mutations[77]. This subtype is frequently associated with high histological grade and poorly differentiated tumors[62]. Bone is also the most common metastatic site followed by lung, liver and pleural/peritoneal[87]. As for the prognostic and predictive value, it presents a poor prognosis, but a higher pCR rate to neoadjuvant chemotherapy than luminal A and luminal B subtypes, and it also presents a high benefit from anti-HER2 therapies[83,88–90].

Basal-like accounts for 8-37% of all BC cases[86]. It is characterized by no expression of *ER*, *PR* nor *HER2*, high expression of basal epithelial cell genes as cytokeratin 5/6 and 17, and proliferation-related genes[81,89]. Furthermore, it presents high genetic instability and a high frequency of *BRCA1* and *TP53* mutations[83,91]. This subtype is frequently associated with high histological grade and poorly differentiated tumors[62]. The most common metastatic site is the lung, but bone and distant nodal are also high frequent[87]. Regarding prognostic and predictive value, it has a poor prognosis and higher pCR rate to neoadjuvant chemotherapy compared to the other molecular subtypes, this last being almost the only treatment available in primary tumor[88,90].

Claudin-low represents 7-14% of all BC cases[90]. It is mainly ER, PR, and HER2 negative but 29-39% express one of these molecular markers. It is characterized by low expression of cell adhesion genes as claudins 3/4/7, low expression of luminal and proliferation-related genes, high expression of epithelial-mesenchymal transition (EMT) and stem-cell-like features, and high immune infiltration[84,85]. Clinical outcome studies show that this subtype has a poor prognosis than luminal A but is similar to

the rest[85]. In addition, there is a lower pCR rate to neoadjuvant chemotherapy than basal-like but higher than luminal A[90].

The lack of standardization and the high costs involved make the determination of intrinsic subtypes by gene analysis not feasible in clinical practice. Different commercial tests have been developed to solve this problem and provide a more accurate prognostic and predictive value [77,92]. PAM50 classifier identifies the main molecular intrinsic subtypes (luminal A, luminal B, HER2-enriched, basal-like, and normal-like) from formalin-fixed paraffin-embedded tissues using a 50 gene-signature[82]. In addition, multigenic tests such as Oncotype DX, Mammaprint, UPA, and PAI-1, including PAM50 provide a recurrence score and risk of distant recurrence. Patients with a high recurrence score had benefited from chemotherapy in different clinical trials. Furthermore, these multigene tests have been shown to reduce the administration of chemotherapy in those groups of patients classified as high risk according to clinicopathological factors, but low risk according to said recurrence score[71,92–94].

It should be noted that the intrinsic molecular subtypes do not exactly match the surrogate ones. Different studies suggest that the triple-negative BC (TNBC) and basal-like subtypes are the same, but only 56% of the gene expression profiles of both subtypes overlap[95]. This is because basal-like intrinsic subtype is mostly ER, PR, and HER2 negative but approximately 17% express one of these biomarkers. In this sense, Prat *et.al.* found that 83% of basal-like were triple-negative, 8% were HER2+, 7% were luminal A and 2% were luminal B. In addition, only 51%, 72%, and 87% of HER2-enriched, luminal B, and luminal A match with their surrogate classification. This data reflects that the analysis of only 4 biomarkers by IHC is therefore not sufficient to represent the intrinsic molecular subtypes (**figure 4**)[90].

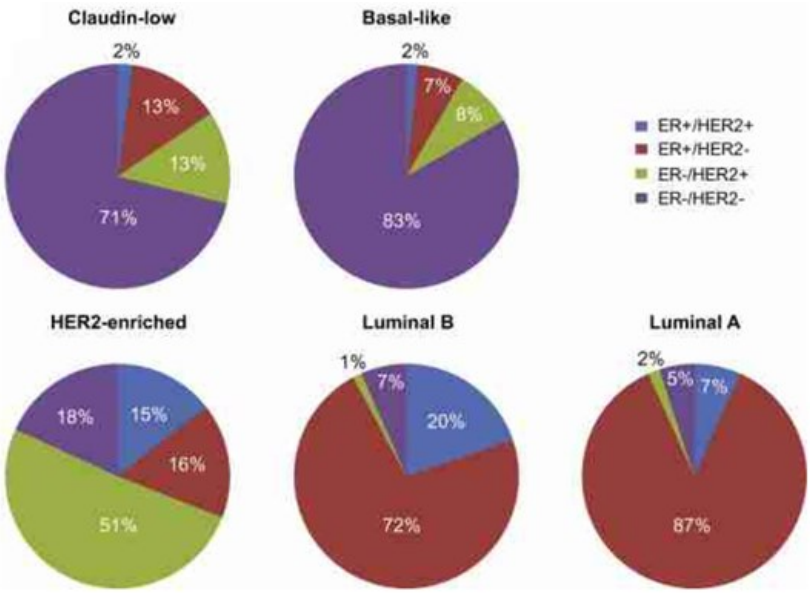

Figure 4: Distribution of pathological subtypes relative to the intrinsic ones. Adapted from Prat *et.al.* [90]

1.6 BC treatment

Treatments can be classified as local therapies (surgery, radiation) and systemic therapies (chemotherapy, hormone therapy, targeted drug therapy, and immunotherapy), which affect only tumor mass or can reach almost any cell of the body, respectively. These treatments can be also applied in neoadjuvant (before surgery) or adjuvant (after surgery) configurations. The goal of adjuvant and neoadjuvant settings is to reduce the recurrence rate and improve long-term survival[96]. In addition, neoadjuvant therapy pretends to reduce the tumor mass to make it operable and assess treatment response. Patients' treatment decisions are based on different clinicopathological factors such as BC stage, molecular subtype, age, and menopause status among others.

The goal of early-stage BC treatment is to prevent relapse. Metastatic BC is considered an incurable disease and the treatment aims to prolong patient survival and prevent tumor progression, in addition to palliating symptoms and improving quality of life[48]. The different most common local and systemic therapies for both configurations are specified below.

1.6.1 Surgery and radiotherapy

Surgery is the first decision to treat early-stage BC patients, being able to perform a breast-conserving surgery (lumpectomy) or a mastectomy. Mastectomy should be performed in case of the inability of achieving negative margins after various surgeries and in those who have received prior radiation to the breast[97]. Those patients who undergo a mastectomy have the option of breast reconstruction, which can be done immediately or delayed. Regarding metastatic BC, surgery is not the first option, being only palliative with clear benefits in the patient's survival[98,99] .

Sentinel lymph node biopsy is also performed to evaluate regional lymph node status in those patients who show a high risk of invasion[97]. In addition, whole-breast radiotherapy is recommended after lumpectomy since it has been shown to reduce ipsilateral recurrence risk by 50%, and a significant reduction of BC mortality in higher-risk patients[100–102]. The addition of impulse radiotherapy in women with lumpectomy and whole breast radiotherapy has been shown to reduce the ipsilateral risk recurrence, being greater in younger than older patients in phase III EORTC trial[103], and is currently indicated for patients under 50 years of age, grade 3 tumors and vascular invasion. Radiotherapy is also performed in those cases with inoperable metastatic BC to make it resectable[97].

1.6.2 Chemotherapy

There are no differences in adjuvant and neoadjuvant chemotherapy (NAC) configurations in terms of OS and DFS. However, with the neoadjuvant treatment, value information is obtained with the pathology response. The adjuvant treatment could change depending on the pCR, especially in HER2+ and TNBC patients. In this sense, HER2+ and TNBC have been demonstrated to present the highest pCR[104]. Different multigenic tests such as Oncotype DX and Mammaprint can also calculate a recurrence score in luminal BC patients to determine those more likely to benefit from chemotherapy[71,105,106]. Adjuvant chemotherapy is usually performed in higher-risk recurrence patients and those with residual disease after NAC, as it is known to reduce the risk of recurrence and BC mortality[107,108]. Regarding early-stage TNBC, NAC is the standard of care[109,110].

Chemotherapeutic drugs are used alone and combined. Standard practice is based on the use of anthracyclines (doxorubicin (DOX), epirubicin) followed by taxanes (paclitaxel, docetaxel)[111]. Capecitabine is approved for paclitaxel or anthracycline-resistant patients and those who anthracycline administration is not possible, as the addition of capecitabine adjuvant therapy is shown to prolong DFS and OS compared to placebo in phase III JBCRG trial[112]. Platinum agents (cisplatin, carboplatin) are considered in TNBC, as they showed better clinical response compared to docetaxel in *BRCA*-mutation patients in phase III TNT trial, and compared to anthracycline, taxane, and targeted therapy alone in phase II GeparSixto trial[113,114].

1.6.3 Hormone therapy

It is applied in hormone receptor-positive subtypes. These subtypes are estrogen and progesterone dependent, which after binding to their receptor induce BC cell

proliferation[115]. Based on this fact, different strategies have been developed to target HR. In this sense, tamoxifen competes with estrogen to prevent its binding to ER and is commonly used in ER+ patients for 5 years. Tamoxifen used for 5 years has been shown to reduce recurrence risk by 4% and BC mortality by 3%, however, its use is being implemented for 10 years due to the greater benefits observed in ATLAS trial[116]. In addition, fulvestrant is an ER antagonist approved to treat postmenopausal patients with advanced BC, and toremifene is a tamoxifen analog approved for postmenopausal women with metastatic BC[117]. Aromatase inhibitors are other hormone treatments that block estrogen synthesis. An example is anastrozole, which is approved for postmenopausal women with early-stage BC due to the better clinical response in terms of recurrence rate and DFS compared to tamoxifen in phase III ATAC trial[118]. The latter is because the estrogen in postmenopausal women may be produced in the fatty body by the enzyme aromatase[117].

1.6.4 Anti-HER2 therapy

The HER2 receptor is a membrane tyrosine kinase member of the Epidermal Growth Factor Receptors (EGFRs) family. Homodimerization or heterodimerization results in autophosphorylation of tyrosine residues in the cytoplasmic domain, which activates different signaling mechanisms such as the Phosphatidylinositol 3 Kinase (PI3K)/AKT or Mitogen-Activated Protein Kinase (MAPK) pathways that promote cell proliferation and survival[119,120]. Given that this receptor is overexpressed in 20% of BC and is associated with more aggressive disease and a higher recurrence rate, different therapeutic strategies have been developed to target it[121]. Anti-HER2 treatments are used in early-stage and metastatic BC, usually in conjunction with chemotherapy, and can be divided into monoclonal antibodies (trastuzumab,

pertuzumab), tyrosine kinase inhibitors (lapatinib, neratinib, tucatinib) and antibody-drug conjugates (trastuzumab-emtansine, trastuzumab-deruxtecan).

The most commonly used treatment is trastuzumab for 1 year, a monoclonal antibody that targets the extracellular domain of HER2. Its use in conjunction with chemotherapy is known to have greater recurrence and survival benefits than the use of chemotherapy alone in both neoadjuvant and adjuvant settings[122–125]. The addition of pertuzumab, which inhibits HER2 dimerization, is established as the first-line treatment in a neoadjuvant setting, as it has been shown to improve pCR compared to trastuzumab plus chemotherapy alone[126,127].

The administration of the tyrosine kinase inhibitors lapatinib and, more recently, neratinib were approved for advanced and early-stage BC, respectively, based on results shown in different clinical trials. In case of disease progression after trastuzumab plus chemotherapy-based treatment, lapatinib in combination with capecitabine showed an increase in DFS in advanced BC compared to capecitabine alone[128]. Furthermore, neratinib after trastuzumab adjuvant treatment showed an increase in DFS compared to placebo in early-stage BC according to phase III ExteNET trial[129].In addition, tucatinib is approved for metastatic BC in combination with trastuzumab plus capecitabine, as it has been shown to increase progression-free survival (PFS) and OS compared to placebo in phase II HERCLIMB trial[130].

Regarding antibody-drug conjugates, trastuzumab-emtansine is a monoclonal antibody covalently linked to DMI, a microtubular inhibitor, and is approved in advanced BC previously treated with trastuzumab and chemotherapy, as it has been demonstrated to increase PFS and OS compared to administration of lapatinib plus capecitabine in phase III EMILIA trial[131]. Moreover, Trastuzumab-deruxtecan consists of trastuzumab, a cleavable linker, and topoisomerase I inhibitor, and is indicated for

unresectable and metastatic BC previously treated with other anti-HER2 drugs based on phase II DESTINY-Breast01 trial results[132].

1.6.5 PI3K inhibitors

PI3K pathway activation promotes cell proliferation and survival, protein synthesis and DNA repair[133]. *PIK3CA* mutations are found in 25-40% of BC cases and are known to be associated with worst prognosis, tumor progression and drug resistance, especially in hormone receptor-positive/HER2- tumors[134,135]. In this sense, alpelisib was the first *PIK3CA* inhibitor approved for *PIK3CA*-mutated hormone receptor-positive/HER2- advanced BC patients who received prior endocrine therapy, as it increased PFS compared to placebo in phase III SOLAR-1 trial[136]. Other PI3K inhibitors as GDC-0077 and Inavolisib are under evaluation in BC (NCT03006172, NCT04191499).

1.6.6 PARP inhibitors

Poly (adenosine-diphosphate-ribose) polymerase (PARP) is part of the base excision repair (BER) complex and is responsible for repairing single-strand breaks in DNA. BRCA is also involved in DNA repair mechanisms. Therefore, PARP inhibitors have been developed in *BRCA*-deficient cells to reduce the integrity of DNA strands during DNA replication, thus resulting in lethal[117]. Adjuvant olaparib is approved in early-stage and HER2- patients with *BRCA* mutation and high risk of recurrence who received prior chemotherapy, as it showed an increase in invasive and distant DFS compared to placebo in phase III OlympiA trial[137]. This PARP inhibitor is being evaluated in metastatic and HER2- patients with *BRCA*-mutation who received chemotherapy, based on longer PFS compared to standard chemotherapy observed in phase III OlympiAD trial[138]. Talazoparib is approved for advanced or metastatic,

HER2- patients with *BRCA* mutation who received chemotherapy, as it showed longer PFS compared to standard chemotherapy in phase III EMBRACA trial[139].

1.6.7 CDK4/6 inhibitors

The Cyclin-Dependent Kinases 4 (CDK4) and 6 (CDK6) are involved in G_1 to S cell cycle checkpoint, and upon activation promote cell cycle progression. Overexpression of cyclin D1, the binding partner of CDK4/6, is known to correlate with worse prognosis and endocrine resistance in ER+ tumors[140,141]. In this sense, CDK4/6 inhibitors have been developed to slow cancer growth. Palbociclib, robociclib and amebaciclib are used in advanced or metastatic, hormone receptor-positive/HER2- patients in combination with hormone therapy, based on benefits observed in different phase III clinical trials[142–145]. Recently, amebaciclib has also been approved in combination with endocrine therapy in early-stage configuration and high recurrence patients, based on results of phase III monarchE trial[146].

1.6.8 mTOR inhibitors

The Mammalian Target of Rapamycin (mTOR) acts as a nutrients and growth factors cellular sensor, but it is also an effecter of PI3K signaling, promotes cell growth, and is implicated in endocrine therapy resistance[147]. Everolimus is an mTOR inhibitor approved for advanced, hormone receptor-positive/HER2- and postmenopausal patients in combination with hormone therapy, based on longer PFS observed compared to endocrine therapy alone in phase III BOLERO-2 trial[148].

1.6.9 Immunotherapy

Immunotherapy boosts the own immune system to recognize and attack tumor cells. It is known that lymphocyte T cells play a critical role in killing tumor cells. However, the expression of the ligand PD-L1 by some tumor cells is recognized by the PD-1 receptor of T cells, thus leading to tumor immunosuppression[149]. In this sense, pembrolizumab is a PD-1 inhibitor monoclonal antibody approved in combination with chemotherapy for TNBC patients with high-risk early-stage, inoperable or metastatic BC, based on the better clinical results observed in comparison with chemotherapy alone in phase III KEYNOTE-522 and KEYNOTE-355 trials[149,150].

The lack of ER, PR, and HER2 in TNBC makes it not sensitive to any hormonal therapy or anti-HER2 drugs, being chemotherapy the main systemic effective treatment. However, approximately 50% of TNBC patients relapse after receiving NAC[151]. Lack of knowledge of its genetic and molecular bases makes it necessary a better understanding of the pathways involved to find new molecular targets for this subtype.

1.7 MicroRNAs

MicroRNAs (miRNAs) are small non-coding RNAs of 19-25 nucleotides that bind by sequence complementarity with seed sequence to the 3'UTR of their target mRNAs, leading to gene silencing by mRNA degradation or translational inhibition. Among some of the functions that they modulate are development, cell proliferation and differentiation, embryogenesis, metabolism, apoptosis, and intercellular communication[152]. In addition, miRNAs dysregulation has been seen to play a critical role in different pathological conditions such as cardiovascular and renal diseases, epilepsy, neurodegenerative disorders, or cancer[153–157].

Lin-4 was the first miRNA to be discovered in *C.elegans* in 1993[158], being let-7 the first to be discovered in humans seven years later[159]. Since then, many miRNAs have been studied in different species that are highly conserved among them. Currently, more than 2600 sequences of mature miRNAs are known in humans, and different studies have been carried out to understand their functionality.

1.7.1 Biogenesis

More than half of human miRNAs genes are located in intragenic regions (intronic or exonic) and may share or not promoter with their host genes, while other miRNAs are located in intergenic regions and are transcribed as an independent unit. In addition, some miRNAs are nearby, thus forming clusters that are co-transcribed (called polycistronic transcripts) but processed as individuals at the post-transcriptional level[160].

MiRNA biogenesis is mostly produced by canonical pathway. In this pathway, miRNAs transcription is carried out by RNA polymerase II, and in some cases by RNA polymerase III, which presents binding with transcription factors and epigenetic modulators that help control their expression. After transcription, a long primary miRNA (pri-miRNA) over 1kb in length is generated. This pri-miRNA consists of one or few stem-loop structures based on a terminal loop, a stem of double-stranded RNA where miRNA mature sequence is located, a 5'-methylated cap, and 3'-adenylated tail of single-stranded RNAs. This pri-miRNA is then processed by the microprocessor complex, made up of a double-stranded RNA binding protein named DiGeorge Syndrome Critical Region 8 (DGCR8) and the RNAse III enzyme called Drosha. As a result, stem-loop miRNAs precursor (pre-miRNA) about 70 nucleotides in length, with 2-3 nucleotides overhang in the 3’ end and a monophosphate group at the 5’ end are generated. As the seed sequence of miRNAs is situated 2-7 positions

from the 5’ end and Drosha defines miRNA terminus, it determines miRNA specificity.

The pre-miRNA is then transported to the cytoplasm through the RanGTP-dependent exportin protein 5 (XPO5) localized in nuclear membrane. Once in the cytoplasm, this pre-miRNA is cleaved by the RNAse III enzyme called Dicer, which is bound to the TAR RNA-Binding Protein (TRBP), to form double-stranded RNA (dsRNA). This dsRNA joins to RNA-induced silencing complex (RISC) with the help of ATP-dependent chaperone proteins. The catalytic component of this multiprotein complex is the Argonaute 2 protein (AGO2), which is responsible for producing the single-stranded mature miRNA, being the passenger strand degraded. Depending on the guide strand chosen, miRNA-5p or miRNA-3p arise, depending on whether it is from the 5' or 3' end of the pre-miRNA, respectively[161–163]. RISC complex finally guides miRNAs to their mRNA targets for its posttranscriptional regulation. The scheme of the canonical pathway biogenesis of miRNAs is specified in **figure 5**.

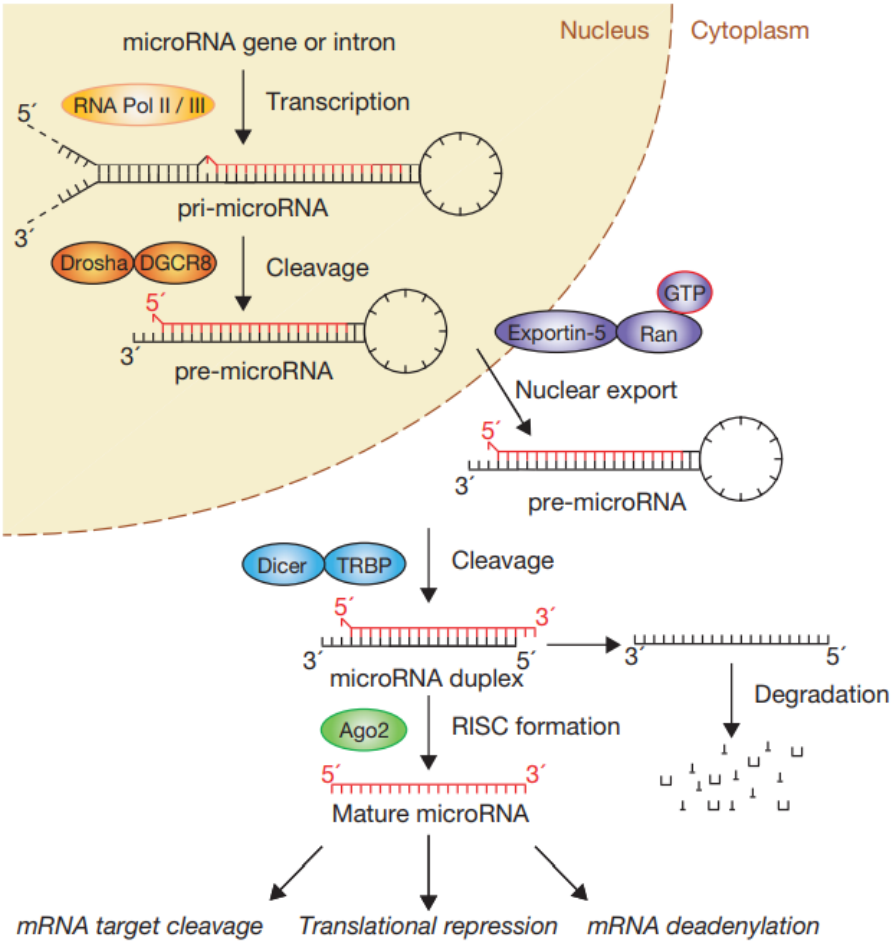

Figure 5: Canonical pathway of miRNAs biogenesis. Source: Winter *et.al.* [163]

However, approximately 1% of conserved miRNAs follow non-canonical biogenesis pathways that are Drosha or Dicer independent or terminal uridylyl transferases (TUTase) dependent. One of the Drosha-independent pathways is generated from miRNATrons (entire intronic sequences of protein-coding genes) through mRNA splicing, while other miRNAs derived from short hairpin RNAs (shRNAs), transfer RNAs (tRNAs), small nuclear RNAs (snoRNAs) or snoRNAs-like viral RNAs. Regarding TUTase dependent pathway, it appears in those pre-miRNAs such as pre-let-7 that

present a shorter 3' region than the rest and need to be extended by monouridylation through TUTase to be processed by Dicer[161,164].

1.7.2 Target regulation

MiRNAs bind by sequence complementarity with seed sequence to their target mRNA sites, thus leading to posttranscriptional repression by mRNA degradation or translational inhibition. In this sense, it is known that each miRNA is capable of regulating hundreds of different mRNAs and each mRNA can be regulated by various miRNAs, thus creating a complex network of post-transcriptional regulation. miRNAs target sites are mostly located in 3'UTR mRNA regions, but also in 5'UTR and protein-coding sequences (CDS)[152,165]. Depending on where miRNA target sites are located and how base-pair complementarity is produced, different mechanisms of mRNA silencing appear.

In plants, base-pair complementarity by perfect pairing is produced. This induces endonucleolytic cleavage through the AGO protein. mRNA degradation then happens as a result of exosome and exoribonuclease-4 (XNR4) activity on the fragments with 3' and 5' ends generated, respectively. In addition, mRNA translational inhibition may also be produced through unknown mechanisms, although this has rarely been seen[165,166].

In animals, binding of miRNAs to their target mRNAs mainly occurs by partial pairing[165,166]. For years it has been believed that this partial binding leads to translational inhibition, but *in vitro* studies also support mRNA degradation. The mechanisms of mRNA repression in animals are based on the development of mechanisms that interfere with the stability of the mRNA and the different steps of translation. mRNAs have a 5'cap and poly(A) tail structure necessary for translation. The 5'cap binds to the eukaryotic initiation factor (eIF) 4A (eIF4F) complex, which

interacts with polyadenylate-binding protein C (PABPC) that binds to the poly(A) tail, thus allowing the eIF3 translation initiating factor to be recruited[166].

It should be noted that target regions found in CDS have been related to translational inhibition but not mRNA degradation[167]. The mRNA degradation mechanism observed in animals is based on the GW182 protein that interacts with AGO. This GW182 protein has a PABPC binding domain in addition to the CAF1-CCR4-NOT1 deadenylation complex. After binding of GW182 to PABPC, deadenylation of the poly(A) tail is promoted, followed by decapping through DCP2 and mRNA degradation by 5'-to-3' exonuclease activity XRN1. GW182 binding to PABPC is known to not only promote mRNA degradation but also inhibit translational initiation[166]. A study of the domain sequence of the protein AGO also showed that it has a binding site for eIF4E, thus interfering with its binding to the 5`cap of the mRNA and inhibiting the initiation of translation[168]. Co-sedimentation studies of miRNAs with polysomes made also translation inhibition evident after initiation, by slowing elongation or causing translation premature termination by ribosomes drop-off. Peptide proteolysis has also been proposed although no protease has been identified yet[165,166].

On the contrary, activation of the target mRNAs has been observed, either promoting the translation of the target gene or activating its gene transcription[169].

In addition, microRNAs have also been shown to act as ligands by binding to Toll-Like Receptors (TLRs), thus enhancing the antitumor activity of natural killer cells or promoting signaling pathways that culminate in cell proliferation and metastasis[170,171].

1.7.3 Cancer implication

The first evidence of miRNAs in cancer was discovered by Colin *et.al.* in 2002, who observed that miRNA-15a and miRNA-16-1 were found in the chromosomal region 13q14 commonly deleted in B-cell chronic lymphocytic leukemia[172]. Subsequent studies have shown the deregulation of miRNAs in various types of cancer, presenting a key role in diagnosis, prognosis, and therapeutic tools. Depending on the regulation of their targets, these miRNAs can act as oncogenes or as tumor suppressors through the modulation of different cancer pathways hallmarks such as cell proliferation, evasion of growth suppressors, apoptosis evasion, invasion and metastasis, deregulation of cellular metabolism, evasion of immune destruction, and angiogenesis (**figure 6**). Treatment response is also known to be modulated by miRNAs[173], so studying its deregulation and implication in cancer progression and treatment response is crucial to better understanding this disease molecularly.

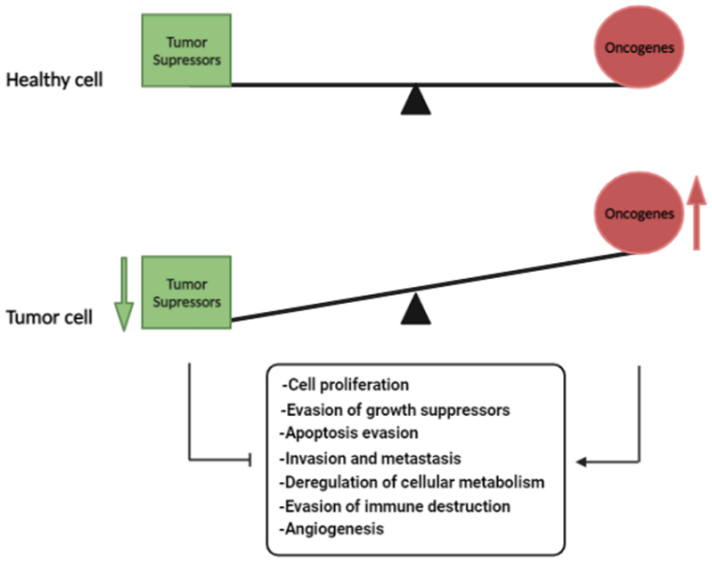

Figure 6: Representation of miRNAs in cancer. MiRNAs can function as tumor suppressors or oncogenes. In tumor cells, tumor suppressors are frequently downregulated, while oncogenes are upregulated. Tumor suppressors and oncogenes are known to inhibit or induce, respectively different cancer hallmarks (cell proliferation, evasion of growth suppressors, apoptosis evasion, invasion and metastasis, deregulation of cellular metabolism, evasion of immune destruction, and angiogenesis).

MiRNAs deregulation has been extensively studied. The different mechanisms that explain it are detailed below and are summarized in **figure 7:**

Genomic alterations: Genomic mutations, amplifications, deletions, and translocations in loci containing miRNAs genes have been widely associated with miRNAs cancer dysregulation in several studies. Zhang et .al found that 31.7, 72.8, and 85.9% of miRNAs in ovarian, breast, and melanoma cancers, respectively, were located in regions that present DNA copy number alterations[174]. Two examples are the miRNA-15 and miRNA-16-1 commented before, located in the chromosomal region 13q14 frequently deleted in chronic lymphocytic leukemia[172]. On the

contrary, the miRNA-17-92 cluster is located in the 13q31 locus, which has been associated with DNA amplification in lymphoma [172,175], but DNA deletion in ovary, breast, and melanoma cancers[174]. This suggests that there are genomic alterations in regions that code for miRNAs that are tumor-specific type. In addition, t(4;14) translocation in multiple myeloma leads to miRNA-146a and miRNA-135b decreased expression, thus promoting tumor progression[176].

Epigenetic alterations: MiRNA expression can also be modulated by epigenetic factors, such as DNA methylation and histone modifications. DNA methylation is characterized by the addition of a methyl group from S-adenyl methionine (SAM) to the cytosine residue predominantly found in CpG islands. This DNA modification inhibits gene expression by recruiting repression transcription factors or impairing activator transcription factors binding[177]. miRNA-424, miRNA-34b/c, and miRNA-148a are some of the tumor suppressor miRNAs that are negatively regulated in various cancer types due to DNA hypermethylation in the promoter region. However, treatment with demethylating agents has been shown to restore their expression[178–180].

As known, DNA is associated with histone proteins, which can also present methylation and acetylation reversible marks that modulate miRNA expression. Histone acetylation is based on the addition of the acetyl-CoA group to the lysine residue of the histone tail. This leads to the neutralization of the base charge of lysine and subsequent chromatin decondensation, thus giving way to a transcriptionally active chromatin state[181]. The first evidence of miRNAs modulation by histone modifications was published by Scott *et.al.* in BC, who showed 27 miRNAs deregulated after treatment with a histone deacetylase (HDAC) inhibitor drug in SKBR3 cell line[182]. Regarding the miRNAs of study of this thesis, induction of the

tumor suppressor miRNA-449a expression after HDAC inhibitor treatment was observed in hepatocellular carcinoma, skeletal muscle cells, and TNBC[183–185].

Histone methylation is based on the addition of a methyl group to the lysine or arginine residues of histone tails. This modification interferes with transcription factors binding to DNA, thus giving rise to gene expression or repression[181]. One example is miRNA-449a and b-5p, which are epigenetically repressed by histone methylation in the BC cell line MCF7, thus treatment with a histone-demethylating agent being able to induce their expression[186].

Alterations in miRNAs transcriptional control: Transcription factors are known to regulate gene expression, and their abnormal expression has been implicated in miRNAs cancer deregulation. The proto-oncogene c-Myc is overexpressed in most human cancers and is known to act as a transcription factor, thus activating the expression of the miRNA-17-92 oncogene cluster, and inhibiting miRNA-15a/16, miRNA-26, and miRNA-34a tumor suppressors among others[187]. In addition, P53 is a tumor suppressor frequently mutated in cancer, that is known to induce the expression of various tumor suppressors such as miRNA-34 family, miRNA-107, miRNA-145, and miRNA-192[188].

Alterations in miRNAs biogenesis machinery: As previously mentioned, the miRNAs biogenesis machinery is a complex process that integrates the action of different enzymes and proteins, so mutations and alterations in the expression of the different components can lead to an abnormal expression of these miRNAs. Torrezan *et.al.* detected mutations in miRNAs processing machinery (DROSHA, DGCR8, DICER1, XPO5, and TARBP2) in 33% of Wilms tumors, and *DROSHA* E1147K mutation was associated with a predominant mature miRNAs downregulation[189]. In addition, low expression of DICER1, DROSHA, DGCR8, and AGO2 was found in clear renal cell

carcinoma by Lee *et.al.*[190]. The low expression of DROSHA and/or DICER has been widely associated with poor prognosis and cancer progression in different tumor types[191–193], including BC[194]. This correlation between miRNAs machinery deficiency and prognosis may be due to general negative regulation of miRNAs found in tumors, thus suggesting that most of the miRNAs act as tumor suppressors[195].

Melo *et.al.* found that *XPO5*-inactivating mutations are associated with tumors with microsatellite instability and with cancer progression. A truncated form of XPO5 is unable to form a complex with miRNAs, thus retaining them in the nucleus and avoiding being processed by DICER. However, the introduction of *XPO5* wild-type rescued its function and caused upregulation of tumor suppressors as miRNA-200 family[196]. Moreover, Sun *et.al.* found that phosphorylation of XPO5 in hepatocellular carcinoma also impairs its function and causes miRNAs global downregulation, thus promoting tumor development and poor prognosis[197].

RNA binding proteins (RBP) also modulate miRNA biogenesis. In this sense, Higuchi *et.al.* found that the Nuclear Factor 90-Nuclear Factor 45 Complex (NF90-NF45) is upregulated in hepatocellular carcinoma and reduces miRNA-7 mature levels by inhibiting pri-miRNA-7 processing[198].

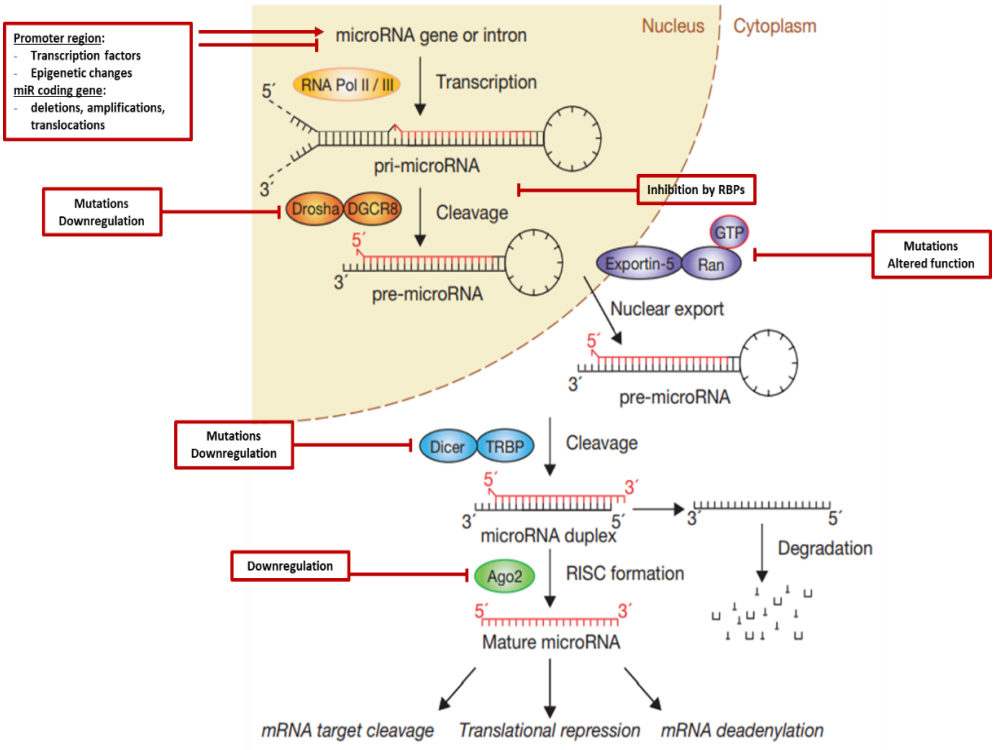

Figure 7: Representation of different mechanisms of miRNAs deregulation in cancer. Adapted from Winter *et.al.* [163]

1.7.3.1 MiRNA-449 family

This thesis focuses on the miRNA-449 family, formed by miRNA-449a, miRNA-449b-5p, and miRNA-449c-5p. These miRNAs are located in the second intron of the CDC20B gene within the 5q11.2 region of chromosome 5[199], which has been associated with an increased risk of BC in genome-wide association studies[200].

As for their role in physiological conditions, they are highly expressed in multiciliate cells such as those present in the trachea, testicles, brain, lung, and ovaries. MiRNAs-449 have been involved in the differentiation process of multiciliate cells, where they

show a spatial-temporal expression pattern. More specifically, they inhibit components of the Notch pathway (Notch1 receptor and Delta-like 1 ligand) overexpressed in progenitor cells, produce the cell cycle exit of these dividing cells to compromise their differentiation and promote early stages of differentiation[201]. In this sense, Wu *et.al.* generated knockout mice for this family and observed that they died at postnatal day 27, they were also smaller, with smaller basal forebrain structures, not fertile, and with air obstruction due to the absence of mucus production[202].

Regarding miRNAs-449 in cancer, they have been underexpressed in several cancer types, including BC, and are suggested to act as tumor suppressors by targeting several genes, thus inhibiting cell proliferation, migration, invasion, and promoting apoptosis and cell cycle arrest. MiRNA-449a and miRNA-449b-5p show similar patterns of regulation, while miRNA-449c-5p seems to act more independently[203–211]. However, most studies focus only on miRNA-449a role in cancer. MiRNA-449 family role in cancer hallmarks is summarized below.

Proliferation: MiRNA-449a overexpression is known to inhibit cell proliferation and mouse tumor growth through multiple gene modulation in several cancer types. It is known to negatively modulates the expression of various transcription factors, such as POU Class 2 Homeobox 1 (POU2F1) in liver cancer, MYC Associated Zinc Zinger (MAZ) protein in glioblastoma, E2F Transcription Factor 3 (E2F3) in gastric cancer, Special AT-rich Sequence-binding Protein 2 (SATB2) in colorectal cancer, SATB1 in hepatocellular carcinoma, c-Myc in prostate cancer and mutant P53 in BC, this last leading to a decrease of cell proliferation by inhibition of PI3K/AKT/mTOR pathway[212–218]. In addition, it is known to directly downregulate cell cyclin-related proteins such as Cyclin Dependent Kinase 6 (CDK6) and Cell Division Cycle 25 A (CDC25A) in bladder cancer, and CCNE2 in gastric cancer, which are essential for cell

cycle progression from G1 phase to S phase[205,219]. Moreover, miRNA-449a is observed to directly downregulate some enzymes known to act as oncogenes, such as Calpain 6 (CAPN6) in liver cancer and Sphingosine 1-Phosphate Lyase 1 (SGPL1) in gastric cancer, and other proteins as N-myc Downstream Regulated 1 (NDRG1) in endometrial cancer, the specific protein Prostate Leucine Zipper (PrLZ) in prostate cancer and the Tumor Protein D52 (TPD52) in BC [212,220–223]. MiRNA-449a is also observed to inhibit cell proliferation through the downregulation of two transmembrane receptors known to promote tumor progression, Notch 1 in lung and ovarian cancer, and c-Met in hepatocellular and endometrial cancer [224–227]. Li *et.al.* showed that miRNA-449a inhibits cell proliferation by inhibiting the β-catenin/TCF/CD44 signaling pathway by direct Ataxia Telangiectasia Group D-complementing (ATDC) downregulation in pancreatic cancer[211]. Furthermore, Hu *et.al.* demonstrated that the same miRNA decreases cell proliferation and mice tumor growth by inhibiting Lysine Demethylase 3A (KDM3A)/Hypoxia-Inducible Factor 1-Alpha (HIF-1α) axis in lung cancer[209]. Cancer cells have also been linked with metabolism deregulation, as higher aerobic glycolysis and fatty acid synthesis, to give a proliferative advantage to cells. In this sense, Zhang *et.al.* showed that miRNA-449a suppresses cell proliferation by targeting Sirtuin 1 (SIRT1), leading to the inactivation of the transcription factor SREBP-1c and consequent downregulation of the Fatty Acid Synthase (FASN)[228].

Regarding miRNA-449b-5p, it is also known to suppress cell proliferation by directly inhibiting two transcription factors, Ying Yang 1 (YY1) and E2F3, and Cyclin D1 (CCND1) in colorectal cancer [203,229]. In addition, Jiang *et.al.* showed that this miRNA inhibits cell growth through downregulation of the Wnt/ β-catenin/TCF-4 axis by directly targeting the Cell Cycle-Related and Expression-Elevated in Tumor (CREPT) in BC[230]. Yang *et.al.* also demonstrated that miRNA-449b-5p overexpression

produces an inhibition of cell proliferation through leucine Rich Repeat Containing G Protein-Coupled Receptor 4 (LGR4) downregulation[231].

MiRNA-449c-5p is the least studied and is known to inhibit cell proliferation through direct c-Met and c-Myc downregulation in gastric cancer and osteosarcoma, respectively[232] . Information is summarized in **figure 8**.

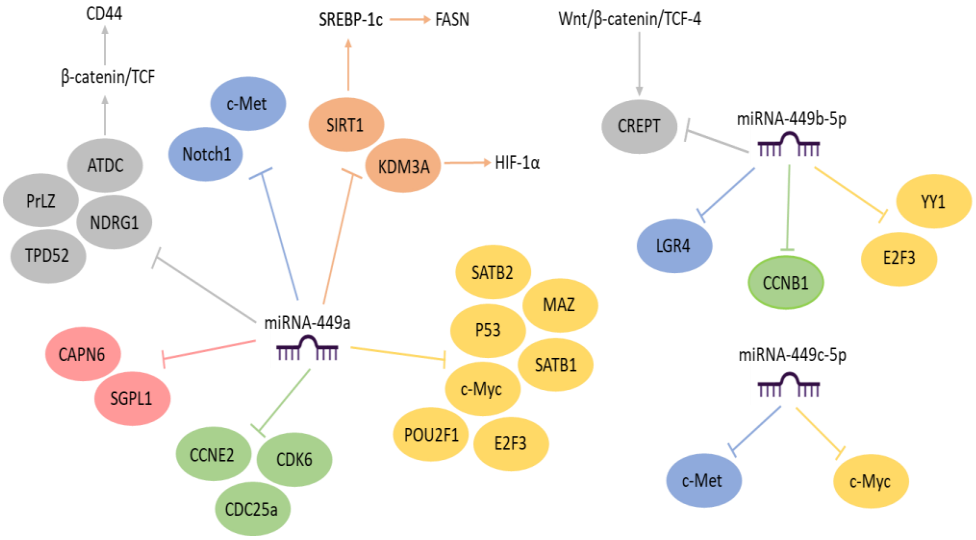

Figure 8: MiRNA-449 family implication in inhibition of cell proliferation. Orange boxes: epigenetic enzymes; yellow boxes: transcription factors; green boxes: cell-cycle related proteins; blue boxes: transmembrane receptors; red boxes: diverse enzymes; gray boxes: other proteins.

Cell-cycle: MicroRNAs-449a and b-5p are also known to produce cell cycle arrest through different gene modulation. Both miRNAs are known to directly downregulate E2F3 transcription factor in different cancer types, while miRNA-449a is also known to directly inhibit c-Myc in prostate cancer and Lymphoid Enhancer Binding Factor 1 (LEF1) in neuroblastoma [214,217,229,233]. In addition, downregulation of CCND1 and CDK6 by both miRNAs and CDC25a by miRNA-449a is known to dephosphorylate Retinoblastoma (RB), which in turn inhibits the well-known miRNA-

449 family activator transcription factor E2F1 [205,233,234]. Shekhar *et.al.* also demonstrated that miRNA-449a produces cell cycle arrest through the downregulation of Cyclin A2 (CCNA2) in osteosarcoma[210]. Moreover, miRNA-449a is known to produce the same effect through the downregulation of two epigenetic enzymes, HDAC1 in prostate cancer and KDM3A in lung cancer, the last leading to HIF-1α repression[209,234]. Notch1 is another miRNA-449a target, which after its negative regulation by this miRNA not only inhibits cell proliferation but also produces cell cycle arrest in lung cancer[224]. Regarding miRNA-449c-5p's role in the cell cycle, no studies have been conducted to date. Information is summarized in **figure 9**.

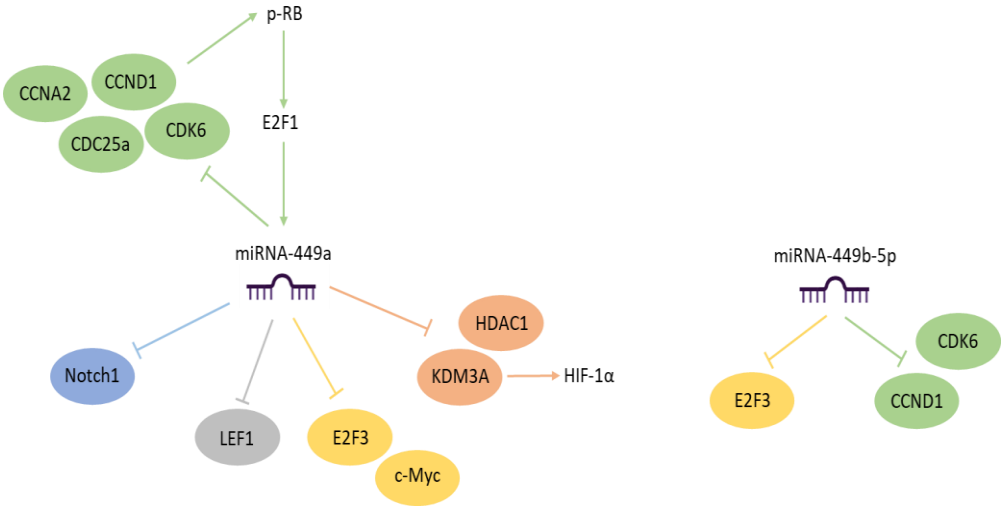

Figure 9: MiRNA-449 family implication in cell-cycle arrest. Orange boxes: epigenetic enzymes; yellow boxes: transcription factors; green boxes: cell-cycle related proteins; blue boxes: transmembrane receptors; gray boxes: other proteins.

Apoptosis: MiRNA-449 family is also studied to be involved in promoting apoptosis. Many studies point out the activation of apoptosis through transcription factors downregulation, such as SATB1, SATB2, POU2F1, MAZ, and E2F3 by miRNA-449a,

and YY1 by miRNA-449b-5p in colorectal cancer[203,212–216]. In addition, both miRNA-449a and miRNA-449b-5p are known to directly downregulate SIRT1 and HDAC1 in several cancer types. These are two histone deacetylases that deacetylase not only histones but also some proteins such as P53. Its absence, therefore, produces acetylation and consequent activation of P53, a known tumor suppressor involved in the activation of apoptosis[219,235,236]. Chen *et.al.* also observed that miRNA-449a overexpression produces apoptosis by direct BCL2 downregulation in osteosarcoma, a widely studied oncogene that acts inhibiting apoptosis[237]. Moreover, miRNA-449a produces the same effect through downregulation of the cell cycle-related protein CDC25a in endometrial and prostate cancer[207,236]. Apart to be involved in proliferation, c-Met inhibition by miRNA-449a and miRNA-449c-5p is also known to promote apoptosis in hepatocellular and gastric cancer, respectively, while Notch1 downregulation by miRNA-449a is observed to promote apoptosis in lung and ovarian cancer[225,226,232]. Activation of apoptosis is also known to be produced through inhibition of different enzymes by miRNA-449a, such as CAPN6 in liver cancer, KDM3A and Lactate Dehydrogenase A (LDHA) in lung cancer, and Autophagy Related 4b Cysteine peptidase (ATG4B) in T-cell lymphoma[209,212,238,239]. Moreover, *Chen et.al.* observed induction of apoptosis and suppression of cancer progression via PrLZ downregulation in prostate cancer, while Duan *et.al.* demonstrated the same via TPD52 downregulation in BC by miRNA-449a overexpression[223,240]. Information is summarized in **figure 10**.

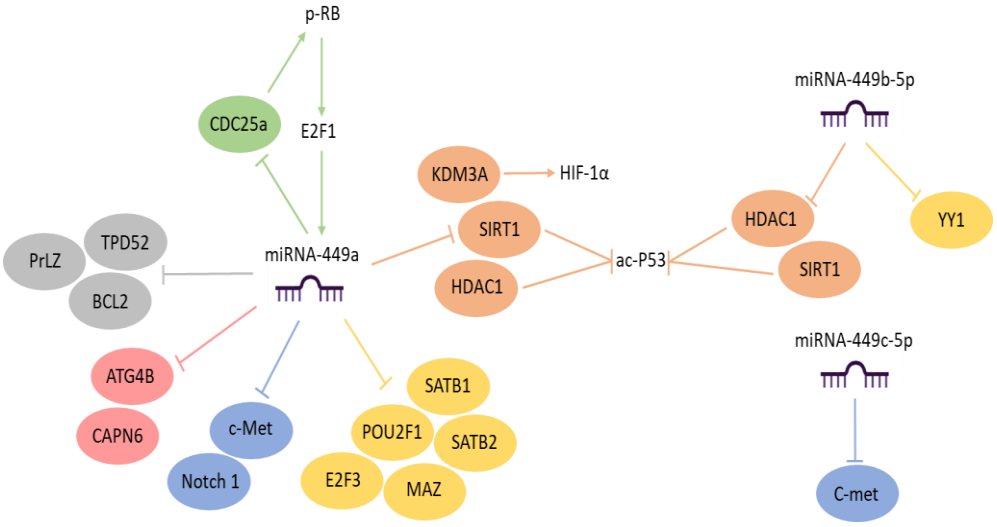

Figure 10: MiRNA-449 family implication in apoptosis. Orange boxes: epigenetic enzymes; yellow boxes: transcription factors; green boxes: cell-cycle related proteins; blue boxes: transmembrane receptors; red boxes: diverse enzymes; gray boxes: other proteins.

Invasion/migration: MiRNA-449 family has also been implicated in cell migration and invasion suppression, thus inhibiting metastasis in different mouse tumor models. Downregulation of transcription factors by miRNA-449a and miRNA-449b-5p are not only involved in inhibiting proliferation and promoting cell cycle arrest and apoptosis but also in inhibiting cell migration and invasion. In this sense, suppression of TGF-β via SOX4 direct targeting by both miRNAs in liver cancer, SATB1, MAZ, FOS, PLAG1 Like Zinc Finger 2 (PLAGL2), PI3K/AKT/mTOR pathway via P53 by miRNA-449a, and YY1 by miRNA-449b-5p have been described[203,208,213,216,218,241,242]. In addition, *Jiang et.al.* demonstrated the same effect through Wnt/β-catenin/TCF-4 axis suppression via direct CREPT downregulation by miRNA-449b in BC[230]. c-Met and AXL by miRNA-449a in different cancer types, and LGR4 suppression by miRNA-449b-5p in lung cancer are transmembrane receptors whose downregulation have also been implicated in cell migration and invasion inhibition[208,227,231,243,244]. MiRNA-449a

overexpression is also known to produce the same effect through two enzymes downregulation, SGPL1 in gastric cancer and ERK1/2/c-Jun axis suppression via Mitogen-Activated Protein Kinase Kinase 1 (MAP2K1) downregulation in lung cancer, while miRNA-449c does so through 6-Phosphofructo-2-Kinase/Fructose-2,6-Biphosphatase 3 (PFKFB3) modulation[220,245,246]. Moreover, miRNA-449a directly downregulates two epigenetic enzymes, SIRT1 in pancreatic cancer and KDM3A in lung cancer, the last leading to HIF-1α suppression and consequent cell migration and invasion inhibition[209,247]. Suppression of other proteins by miRNA-449a as NDRG1 in endometrial cancer, Flotillin 2 (FLOT2) in gastric cancer, PrLZ in prostate cancer, ADAM10 in lung cancer, and β-catenin/TCF/CD44 axis via ATDC downregulation in pancreatic cancer, are also known to act in the same way[211,221,240,248,249]. Information is summarized in **figure 11**.

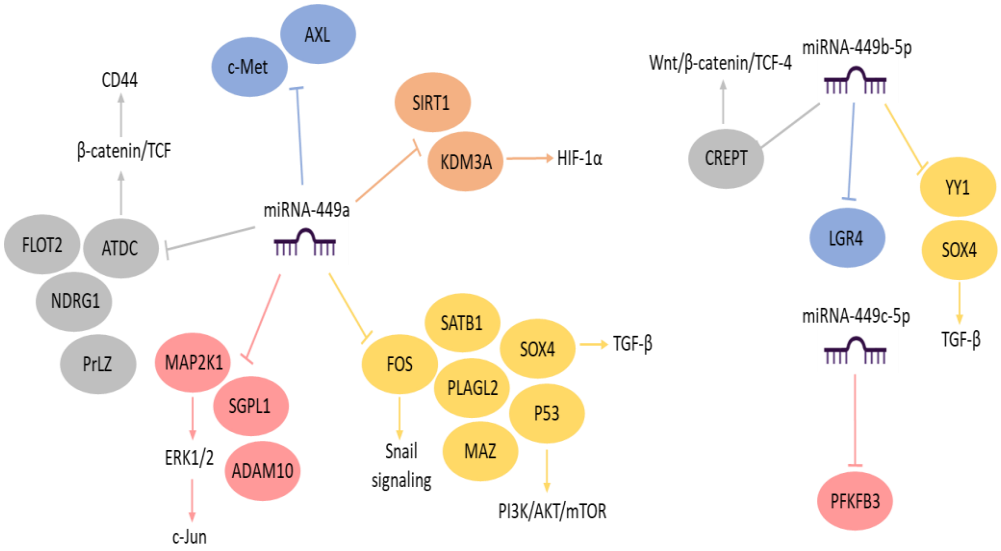

Figure 11: MiRNA-449 family implication in cell migration and invasion. Orange boxes: epigenetic enzymes; yellow boxes: transcription factors; blue boxes: transmembrane receptors; red boxes: diverse enzymes; gray boxes: other proteins.

Treatment response: MiRNA-449a overexpression is known to sensitize to different cancer treatments. Mao *et.al.* showed that miRNA-449a mimic transfection sensitizes to ionizing radiation through CDC25a, HDAC1, and c-Myc downregulation in prostate cancer, and LDHA expression and activity suppression in lung cancer[217,236,239]. Moreover, Notch1 downregulation by the same miRNA is known to sensitize to cisplatin in ovarian cancer[225]. Regarding BC, miRNA-449a is known to sensitize to tamoxifen through ADAM22 downregulation and sensitize to olaparib through survivin/BRCA2 suppression via E2F3 knockout[250]. A study carried out by our group also observed a greater sensitivity to DOX through a negative feedback loop with the cell cycle-dependent cyclins CDK4/6, CDC25a, and CCNE2[251]. Information is summarized in **figure 12**.

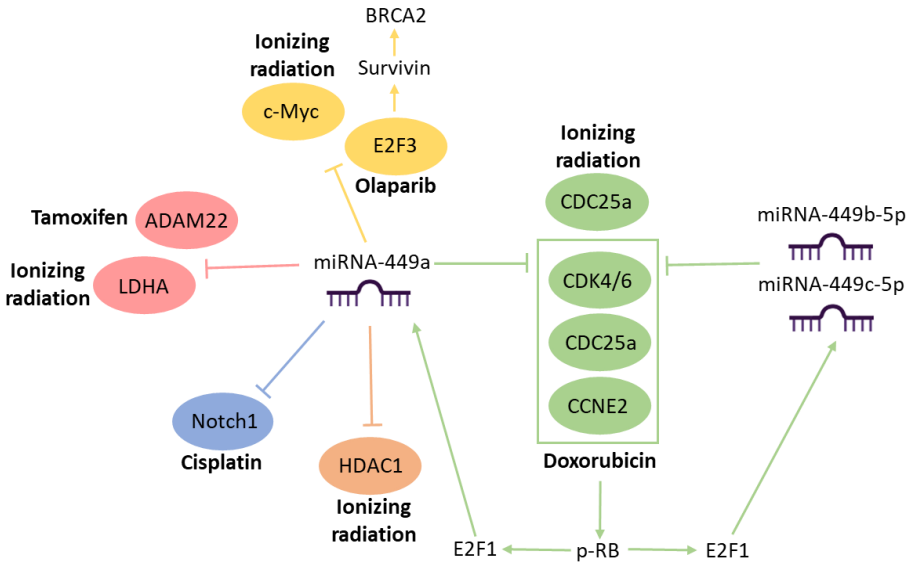

Figure 12: MiRNA-449 implication in treatment response. Orange boxes: epigenetic enzymes; yellow boxes: transcription factors; green boxes: cell-cycle related proteins; blue boxes: transmembrane receptors; red boxes: diverse enzymes.

1.7.4 MiRNAs clinical applicability

1.7.4.1 Biomarkers

Biomarkers are known as molecules that are found in various body fluids and whose presence or absence points to a specific biological state, and can also be detected in medical laboratories. To be considered as such, it must be easily accessible, present high specificity and sensitivity, and be applicable to clinical practice[252].

In this sense, miRNAs have been found in almost all the body fluids that have been analyzed, such as plasma, serum, urine, tears, or breast milk, among others. Cui *et.al.* found that miRNAs profiles in body fluids are influenced by the surrounding tissues so miRNAs from plasma and serum show a greater positive correlation with miRNAs from the pericardium, adipose tissue, spleen, and liver, as well as miRNAs of the urine with the miRNAs of the kidneys, or the miRNAs of the intestines with those of the feces[253]. In addition, the expression of circulating miRNAs is known to vary depending on various normal conditions such as pregnancy or different pathological conditions such as diabetes or cancer[254,255]. On the other hand, miRNAs present high stability and resistance to various storage conditions that degrade most RNAs. The latter may be due to the mechanisms involved in the release of these into body fluids.

MiRNAs are released to extracellular space by passive leakage from broken cells, as caused by tissue injury or apoptotic cells, or by active secretion. One of the most commonly studied active secretion mechanisms is exosome-enclosed secreted miRNAs. Multivesicular bodies are formed by endocytosis that subsequently fuse with the plasma membrane, thus releasing small 50-100nm intraluminal vesicles known as exosomes that contain miRNAs. This release mechanism is also known to

depend positively on the activity of the neutral sphingomyelinase 2 (nSMase2). Other known mechanisms are through transport by binding to circulating High-Density Lipoprotein (HDL), or RNA binding proteins such as Nucleophosmin 1 (NPM1) or AGO2, which protect miRNAs from being degraded by RNase activity. The mechanism through HDL transport also negatively depends on the activity of nSMase2 (**figure 13**). These miRNAs, released by different mechanisms, finally reach the recipient cells and influence their gene expression, thus establishing cell-to-cell communication[256–259].

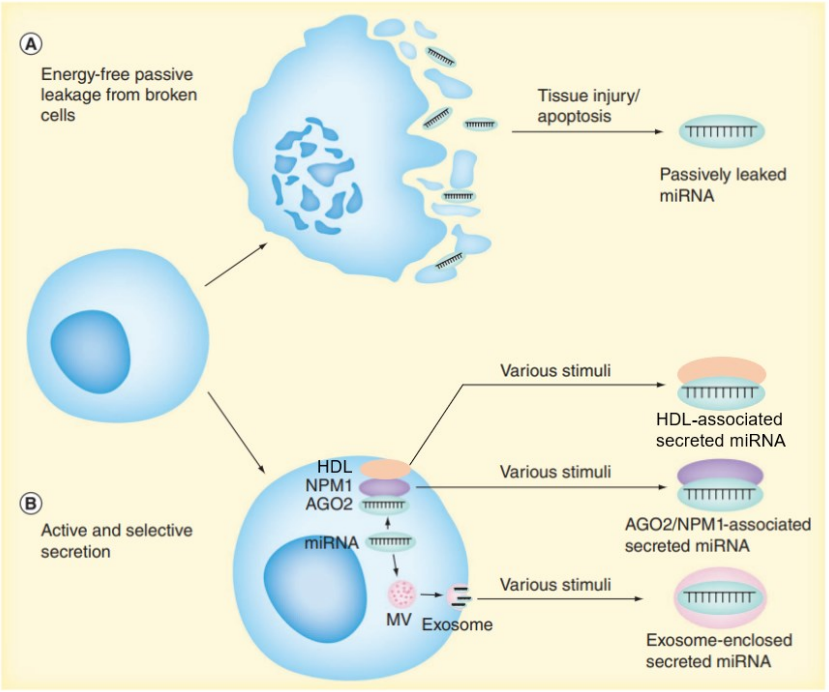

Figure 13: Representation of the different proposed miRNA release mechanisms. There are different mechanisms of miRNA released to extracellular space. **A.** Energy-free passive leakage from broken cells caused by tissue injury/apoptosis. **B.** Active and selective secretion due to exosome-enclosed secreted miRNA, or HDL/AGO2/NPM1-associated miRNA. Adapted from Redova *et.al.*[258]

As previously mentioned (*1.3 Screening*), the current diagnostic tools present some limitations, so new diagnostic tools are required for early BC detection to improve the patient's prognosis. In this sense, the deregulation of miRNAs has been seen to play a key role in cancer initiation and progression, and its ease of collection and characterization describe above provide an opportunity to circumvent the problems associated with invasive tissue biopsy procedures. All these advantages make miRNAs to be proposed as biomarkers for diagnosis, prognosis, and treatment response. Lawrie *et.al.* first proposed miRNAs as biomarkers in cancer in 2008. It was observed that miRNA-155, miRNA-210, and miRNA-21 are overexpressed in serum from patients with diffuse large B-cell lymphoma and these levels are correlated with worse RFS[260]. Since then, many other studies have arisen mainly with circulating miRNAs in plasma and serum. One example is miRNA-30b and miRNA-99a, which are overexpressed in plasma from BC patients compared to healthy samples and are proposed as diagnostic biomarkers for very early BC[261]. MiRNA-155 is another example, which is overexpressed in BC tissue compared to healthy and its levels diminish after chemotherapy treatment in patients who respond, thus allowing monitoring of the effectiveness of the treatment[262]. Regarding miRNA-449a, it is lower expressed in tissue and serum samples from gastric and colorectal cancer patients compared to healthy ones, and this lower expression is related to lower cancer-specific survival and 5-year OS, thus proposing it as a potential prognostic biomarker[263,264].

Despite the advances in research, circulating miRNAs have not been yet applied in clinical practice. Different studies present inconsistencies for the same miRNA, which may be due to the lack of protocol standardization in both sample processing and detection and analysis methods[256]. Regarding miRNA detection methods, these are minimally invasive, such as microarray, next-generation sequencing (NGS), *in-situ*

hybridization (ISH), northern-blot, and more commonly real-time quantitative polymerase chain reaction (RT-qPCR), but all of them present some limitations[252]. Therefore, these problems need to be solved to be able to take them to clinical practice.

1.7.4.2 Therapeutic tools

Knowledge of the role of miRNAs in cancer initiation and development makes them attractive for miRNA-based therapies. Replacement therapy to replenish endogenous miRNAs, and suppression therapy to reduce their effects are the two exploring possibilities. In addition, different options have been considered for each of the configurations. Regarding replacement therapy, miRNA mimics are double-stranded oligonucleotides that mimic and act as endogenous miRNAs, when these nucleic acids present chemical modifications, they are known as agomirs. MiRNA precursors are also used and transformed inside cells by Dicer in mature miRNAs, also miRNA-expressing plasmids. Regarding suppression of miRNAs-based therapy, miRNA inhibitors are single-strand oligonucleotides that bind and inhibit specifically endogenous miRNA. Similarly, they can present chemical modifications in which case are known as antagomirs. MiRNA masks are also single-stranded miRNAs but they do not bind directly to the miRNA but to their binding sequence in the 3'UTR of the mRNA, thus competing with them. MiRNA sponges are also used, these are coding plasmids for fragments complementary to the seed region that manage to inhibit the function of endogenous miRNAs[265] (**figure 14**). More recently, selective inhibitors of miRNAs and their processing machinery have been explored, such as diazobenzene for miRNA-21 inhibition, a widely studied miRNA that has been seen to be overexpressed in many types of cancer, including BC[266,267].

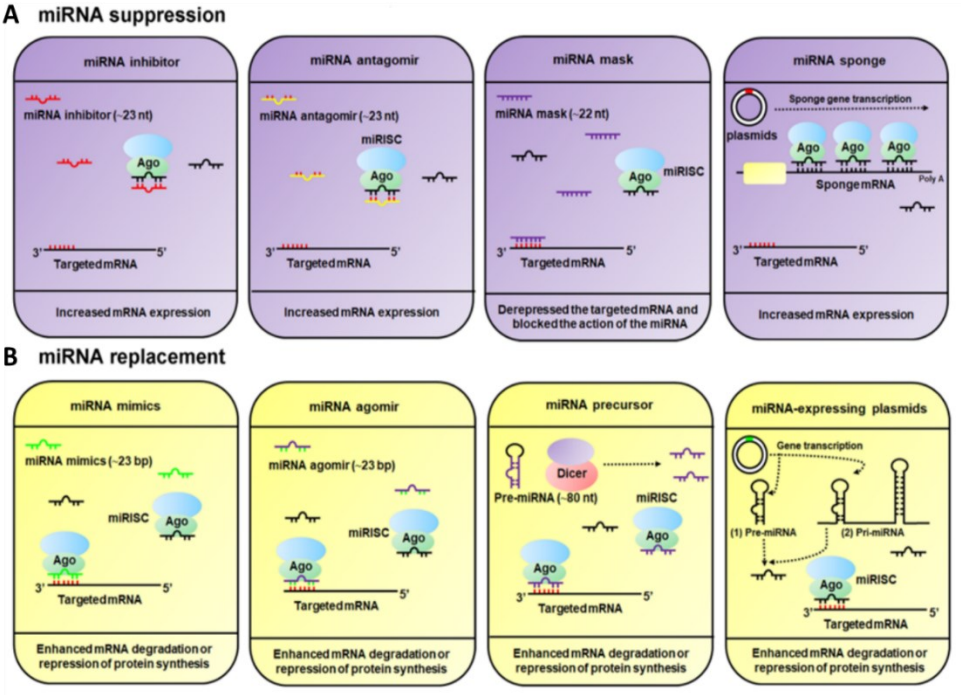

Figure 14: MiRNA-based therapies. A. miRNA suppression therapy: miRNA inhibitor, miRNA antagomir, miRNA mask, and miRNA sponge. **B.** miRNA replacement therapy: miRNA mimics, miRNA agomir, miRNA precursor, and miRNA-expressing plasmids. Adapted from Fu *et.al.* [265]

However, miRNAs present limitations in terms of their bioavailability, tissue permeability, intracellular activity, and secondary effects. On one side, they are rapidly degraded in the bloodstream by the action of nucleases, and rapidly eliminated in the urine and the reticuloendothelial system (RES), drastically reducing their half-life in the blood. The leaky structure of blood vessels, increased interstitial fluid pressure, as well as the presence of immune cells in the microenvironment that can capture miRNAs also limit their penetration into tumor cells. These oligonucleotides enter the cell by endocytosis mechanisms, although most end up being degraded in lysosomes. Those miRNAs that cross the lysosomal barrier may present off-target effects due to imperfect pairing with their targets, and in some

cases, a saturation of the enzymes involved in their processing can occur. All this limit miRNAs activity. On the other hand, they can induce immunotoxic and neurotoxic effects[268,269] (**figure 15**).

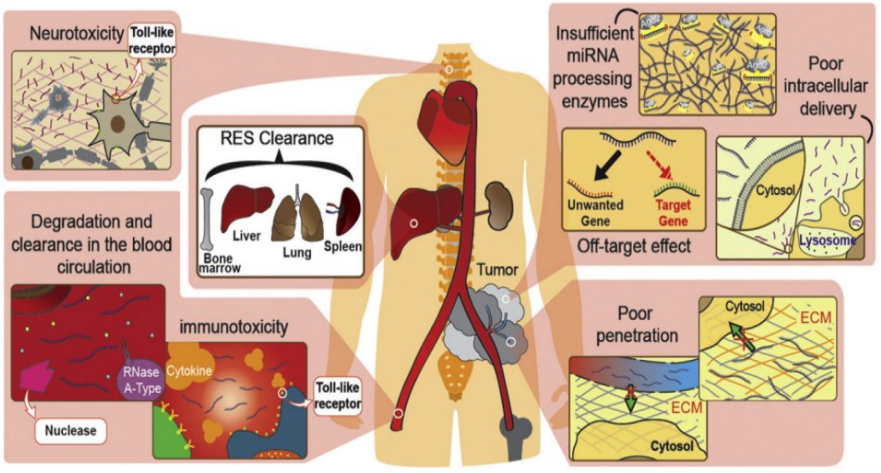

Figure 15: *In vivo* limitations for miRNA-based therapy. Source: Chen *et.al.* [268]

Local delivery can be performed, although it cannot be applied in case of metastatic cancer, so systemic delivery has also been developed. Chemical modifications and delivery systems have been designed to overcome all these limitations and enable clinical applicability. 2'-o-methoxyethyl, 2'-o-methyl, 2'-fluoro, locked nucleic acids (LNAs), phosphorodiamidate morpholino oligomers (PMO), peptide nucleic acids (PNAs), and terminal modifications as the addition of cholesterol or biotin, are some chemical modifications that have been applied and have demonstrated to increase miRNA stability and activity[265,270,271]. Regarding delivery systems, they can be divided into viral and non-viral vectors. Among the non-viral vectors are the inorganic, lipid, polymeric, and cell-derived vectors[265,269,270,272–276] (**figure 16**).

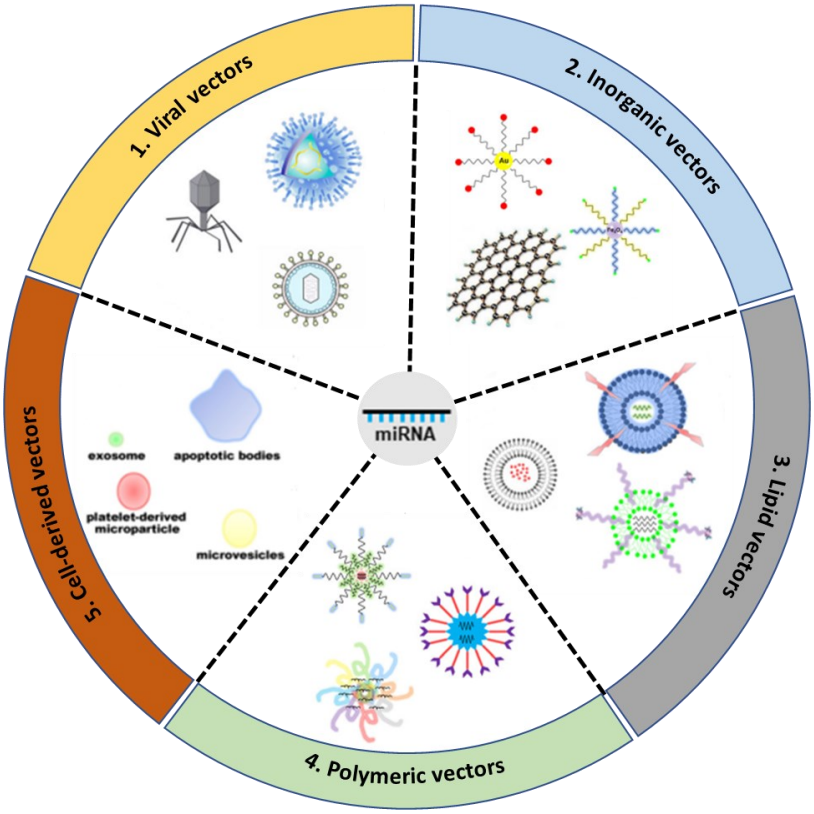

Figure 16: MiRNAs-based delivery systems: 1. Viral vectors. 2. Inorganic vectors. 3. Lipid vectors. 4. Polymeric vectors. 5. Cell-derived vectors.

The first miRNA-based clinical trial was performed in 2013 with a liposomal formulation of miRNA-34 (MRX34) for solid advanced tumors. However, strong immune-related effects forced this phase I trial to end[277]. Other phases I clinical trials have been developed since then, as minicells (targomiRs) containing miRNA-16 for malignant pleural carcinoma and non-small cell lung cancer, or LNA-based anti-miRNA-155 for cutaneous T-cell lymphoma (NCT02580552), both of them with safe and positive results[278]. Nevertheless, more preclinical studies are needed to overcome instability, toxicity, and off-target miRNA-derived effects. In addition,

miRNAs and chemotherapeutic agents cotreatment have been demonstrated to potentiate cytotoxic effects, so joint encapsulation is proposed as an effective strategy[273].

CHAPTER 2 |

Objectives

Based on the limitations of TNBC treatment and previous results published in our laboratory, this thesis focuses on the dysregulation of the miRNA-449 family and its involvement in the different biological capacities of TNBC. This work hypothesizes that the miRNA-449 family is dysregulated and modulates TNBC aggressiveness and chemotherapy response. The specific objectives are:

1. To study the epigenetic regulation of the miRNA-449 family in TNBC cell lines.

2. To elucidate new miRNA-449 family targets and to study their involvement in TNBC aggressiveness.

3. To uncover the involvement of the miRNA-449 family in DOX resistance through *ACSL4* targeting.

CHAPTER 3

Materials and methods

3.1 Cell lines and proceedings

3.1.1 Cell lines

TNBC (MDA-MB-231 and MDA-MB-436), non-tumorigenic cell line (MCF10A) and human embryonic kidney 293T (HEK-293T) cell lines were used for this study. All cell lines were collected from American Type Culture Collection (ATCC, Manassas, USA) and grown in basal media supplemented with 10% (v/v) of heat-inactivated fetal bovine serum (FBS; Gibco, Carlsbad, USA), 1% (v/v) sterile filtered penicillin-streptomycin (Biowest, Nuaillé, France) and 1% (v/v) L-glutamine 100X 200mM (Biowest, Nuaillé, France) in a humidified incubator at 37°C and 5% CO_2. Culture conditions and characteristics of cell lines are specified in **table 4**.

Table 4: Characteristics of cell lines.

Cell line	MCF10A	MDA-MB-231	MDA-MB-436	HEK-293T
Growth Media	DMEM F12 (Biowest)	DMEM F12 (Biowest)	DMEM+Gluta MAX (Gibco)	DMEM F12 (Biowest)
Growth properties	Adherent	Adherent	Adherent	Adherent
Cell type	Epithelial	Epithelial	Epithelial	Unknown
Morphology	Cuboidal	Fibroblast-like	Fibroblast-like	Epithelial
Tissue origin	Fibrocystic	Metastatic mammary adenocarcino ma	Metastatic mammary adenocarcino ma	Embryonic kidney
Age	36	51	43	Fetus
Ethnicity	White	White	White	-
Gender	Female	Female	Female	-
Tumorigenic	No	Yes	Yes	Yes
BC biomarkers expression	ER-/PR-/HER2-	PR-/ER-/HER2-	PR-/ER-/HER2-	Unknown

Table 4: (Continued)

Subtype	Healthy	Triple-negative	Triple-negative	-
Mutations	NO	BRAF/KRAS/CD79A/CRTC3/PDGFRA (HT), NF2/TP53 (HZ)	BRCA1 (HZ), TP53 (Unknown)	NO

HT: heterozygous; HZ: homozygous

The acquired DOX-resistant (MDA-MB-231R) cell line was kindly provided by Federico Rojo's group at the *Fundación Jiménez Díaz* (Madrid). Briefly, MDA-MB-231R was obtained from the MDA-MB-231 cell line in the presence of increased doses of DOX, starting at 0.5 µM. IC_{50} value was determined for each dose to evaluate the resistance acquisition and compared it with the parental cell line. DOX resistance was then periodically verified by WST-1 cell viability assay by comparing MDA-MB-231R IC_{50} value with MDA-MB-231 one (**Figure S1**).

Regarding maintenance, all cell lines were passaged when reached 70-90% confluence and culture media was refreshed 3 days a week. When confluence is reached, the cells establish contacts with each other that inhibit their proliferation, so at this point, a subculture is necessary. For passage, cells were washed with Dulbecco's Phosphate-Buffered Saline (PBS; Biowest, Nuaillé, France) and incubated for 2-3 min at 37°C with trypsin-EDTA 1X (Biowest, Nuaillé, France). Trypsin is a protease used to detach cells from the culture dish and separate cells from each other. Next, trypsin was neutralized with the same volume of corresponding supplemented media and centrifuged at 1,500 rpm for 5 min before subculturing.

3.1.2 Cell counting

Once the cell pellet was obtained after being raised with trypsin and centrifuged, it was resuspended in the corresponding supplemented culture media, and 10 µl of volume was used to count cells using a Neubauer chamber. Neubauer's chamber has a central square made up of 25 squares, each of which has 16 quadrants. It also has 4 large squares in the corners formed by 16 quadrants and used for cell counting. To know the number of cells/mL that we have, the average of the four corner squares is taken and multiplied by 10^4, which corresponds to the volume of $0.1mm^3$ of the Neubauer chamber. In the event of a high cell density, a dilution was carried out before counting, which must be taken into account for the calculations following the formula specified below.

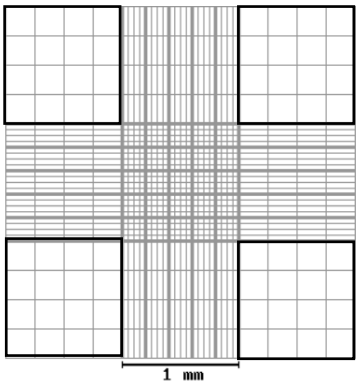

Neubauer chamber volume = 1mm×1mm×0.1mm= 10^{-4} ml

Concentration (cells/ml) = (total number of cells× 10^4× dilution concentration factor)/ 4

Figure 17: Schematic representation of Neubauer chamber and cell count.

3.1.3 Cryopreservation

The cells were frozen in low passages to ensure a good cell stock before starting the experiments. For this, the cell pellet was resuspended in FBS at 10% dimethylsulfoxide (DMSO; Sigma-Aldrich, St. Louis, USA) to prevent crystal formation that breaks down the membrane, and placed at -80^{o}C in a freezing cooler with isopropanol (AppliChem, Monza, Italy), allowing a slow and gradual drop in temperature. After at least one day, the vials were transferred to the liquid nitrogen tank for long-term storage.

On the other hand, cell thawing must be carried out quickly to avoid the formation of intracellular crystals and the known cytotoxicity of DMSO at room temperature. In this case, the vials were rapidly transferred from the nitrogen tank to 37^{o}C, and the content was diluted with the appropriate supplemented media. Cells were then centrifuged at 1,500 rpm for 5 min and transferred to a culture dish.

3.2 Drugs

3.2.1 Trichostatin A

Trichostatin A (TSA) inhibits class I and II of HDACs by chelating zinc ions necessary for their enzymatic activity[279].

MDA-MB-231 and MDA-MB-436 cell lines were seeded to reach 70-90% of confluence and treated with 10nM of TSA for 24 h (#T8551, Sigma-Aldrich, St. Louis, USA). The cell pellet was then divided for gene and protein expression analyses as specified in the *3.6 Gene expression analysis and 3.7 Protein expression analysis* sections. A stock solution of 5 µM TSA in DMSO was prepared and stored at -80°C until use. DMSO at 0.2% was used as a control.

3.2.2 Nicotinamide

Nicotinamide (NAM) inhibits the class III of HDACs. Class III HDACs are NAD+-dependent enzymes and NAM inhibits them in a non-competitive manner by binding to another pocket different from NAD+, thus diminishing their activity[280].

MDA-MB-231 and MDA-MB-436 cell lines were seeded to reach 70-90% of confluence and treated with 300 µM of NAM for 24h (#N0636, Sigma-Aldrich, St. Louis, USA). The cell pellet was then divided for gene and protein expression analyses as specified in the *3.6 Gene expression analysis and 3.7 Protein expression analysis* sections. A stock solution of 250mM NAM in distilled water was prepared and stored at -80°C until use. Distilled water at 0.12% was used as a control.

3.2.3 DOX

DOX is a chemotherapeutic drug that intercalates with DNA and inhibits topoisomerase II, thus producing DNA damage by a double-strand break and ultimately leading to apoptosis[281]. A stock solution of 3.67 mM was obtained from Pfizer and stored at -4°C until use. The concentration of DOX used is specified in each section.

3.3 miRNA and siRNA transient transfections

Cell lines were seeded the day before transfection to reach 70-90% of confluence and transfected with 100 nM of small-interfering RNAs (siRNA) or 50 nM of miRNAs-449 mimics specified in **table 5**.

Table 5: List of siRNAs and miRNAs mimics used in this study

siRNA or miRNA name	Identification number
ACSL4 siRNA	#122222
HDAC1 siRNA	#120419
SIRT1 siRNA	#136457
miRNA-449a mimic	#MC11127
miRNA-449b-5p mimic	#MC11521
miRNA-449c-5p mimic	#MC15616

All siRNAs and miRNA mimics were purchased from Ambion (Austin, USA). Lipofectamine 2000 reagent (Invitrogen, Carlsbad, USA) was used for transfection following the manufacturer's instructions. Lipofectamine is a cationic lipid molecule able to entrap nucleic acid molecules and fuse with the negatively charged cell membrane. Briefly, an appropriate amount of lipofectamine 2000 and siRNAs or miRNA mimics molecules were diluted in Opti-Mem (Thermo Fisher Scientific, Waltham, USA) media and incubated for 20 min before the addition of unsupplemented recommended cell media. The transfection medium was replaced after 4-6h with recommended complete medium.

A scramble was used as negative transfection control. For miRNA transfection, a random sequence miRNA molecule (#4464059, Ambion, Austin, USA) was used. For siRNA transfection, a siRNA molecule with no significant sequence similarity to mouse, rat, or human genetic sequences (#4390844, Ambion, Austin, USA) was used.

Transfection efficiency was verified after 48h and 72h by RT-qPCR and Western blot, respectively (**Figure S2**).

3.4 Gene expression analysis

To evaluate the changes in gene expression, three steps were followed: first, the extraction of total cellular RNA, followed by reverse transcription to complementary DNA (cDNA), and finally gene evaluation by RT-qPCR.

3.4.1 RNA extraction and quantification

Total RNA, including miRNAs, was extracted using TRIZOL reagent (Invitrogen, Carlsbad, USA) following the manufacturer's instructions. 500 µl of TRIZOL was added to the cell pellet to lyse the cells and incubated for 5 min at 4ºC to permit complete dissociation of the nucleoproteins complex. Next, 100 µl of chloroform (Sigma-Aldrich, St. Louis, USA) was added and centrifuged at 13,200 rpm for 15 min at 4ºC. At this point, 3 phases were formed: a lower red phenol-chloroform (proteins), an interphase (DNA), and a colorless upper aqueous phase (RNA). The aqueous phase was transferred to a new tube and 250 µl of isopropanol (AppliChem, Monza, Italy) was added to precipitate RNA overnight at -20ºC. 24 h later, samples were centrifugated at 13,200 rpm for 15 min at 4ºC and 500 µl of 75% ethanol (Sigma Aldrich, St. Louis, USA) was added to wash. After other centrifugation at 13,200 rpm for 15 min at 4ºC, the supernatant was discarded and cell pellets were allowed to dry. Finally, RNA pellets were resuspended in 20-30 µl of RNase-free water and the concentration and purity of isolated RNA were assessed using NanoDrop 2000 spectrophotometer (Thermo Fisher Scientific, Waltham, USA). 260/280 and 260/230 ratios were taken into account to assess the purity of RNA, being 1.8-2 accepted as pure RNA. RNA absorbs at 260 nm, while proteins and phenols absorb at 280 nm, and carbohydrates, phenols, and other contaminants absorb at 230 nm.

3.4.2 Retro-transcription

1 µg of RNA was retro-transcribed to cDNA using High-Capacity cDNA Reverse Transcription Kit (#4368813, Applied Biosystems, Waltham, USA) for mRNA and Taqman™ MicroRNA Reverse Transcription Kit (#4366597, Applied Biosystems, Waltham, USA) for miRNA, following manufacturer's instructions. RNU43 and miRNAs-449 specific primers obtained from Applied Biosystems were used to generate cDNA from miRNA, as specified in **table 6**, and 2 mixes were prepared as described in **table 7**. RNA was then retro-transcribed to cDNA at either 25 °C for 10 min and 37 °C for 2h for mRNA or 16 °C for 30 min, 42 °C for 30 min, and 85 °C for 5 min for miRNA.

Table 6: List of specific primers used in retro-transcription.

Primer name	Identification number
miRNA-449a	#001030
miRNA-449b-5p	#001608
miRNA-449c-5p	#241086_mat
RNU43	#001095

Table 7: Description of prepared MIX for mRNA and miRNA retro-transcription.

	MIX for mRNA	MIX for miRNA
RNA	1µg	1µg
Primers	4µl random primers	6µl (1:100 specific primers in RNase-free water)
Buffer	4µl	1.5µl
Reverse transcriptase	2µl	3µL
dNTPs	1.6µl	0.3µl
RNase inhibitor	-	0.2µl
RNase-free water	until 20µl	until 15µl

3.4.3 RT-qPCR

The resulting cDNA was amplified using TaqMan® Universal Master Mix (#M3004E, Applied Biosystems, Waltham, USA) and TaqMan® 20× assays (Applied Biosystems, Waltham, USA) specific for the genes of interest (specified in **table 8**) following manufacturer's instructions on 9700HT Fast Real-Time PCR system (Applied Biosystems, Waltham, USA). Briefly, RT-qPCR preparation is described in **table 9**.

Table 8: List of TaqMan-specific assays used for RT-qPCR.

TaqMan assay's name	Identification number
miRNA-449a	#001030
miRNA-449b-5p	#001608
miRNA-449c-5p	#241086_mat
RNU43	#001095
HDAC1	#Hs02621185_s1
SIRT1	#Hs01009006_m1
ACSL4	#Hs00244871_m1
GAPDH	#Hs03929097_g1

Table 9: Description of prepared MIX for RT-qPCR.

MIX
2 µl cDNA
5 µl Master Mix 2X
2.5 µl RNase-free water
0.5 µl TaqMan assay 20X

The RT-qPCR assay using TaqMan probes is based on the use of two primers (forward and reverse) that flank the sequence to be amplified and a TaqMan probe that hybridizes with the sequence of interest, which has a FAM dye label at the 5' end

and a non-fluorescent suppressor at the 3' end. When an RT-qPCR cycle occurs, the 5'-3' exonuclease activity of Taq polymerase releases the FAM dye, allowing fluorescence release. The amount of final fluorescence detected is directly proportional to the amount of initial cDNA.

The PCR conditions were 50 °C for 2 min, 95 °C for 10 min, 40 cycles of 95 °C for 15 sec, and 60 °C for 1 min. Expression of housekeeping *GAPDH* mRNA or *RNU43* miRNA was used as an internal control and data was analyzed following the comparative critical threshold ($2^{-\Delta\Delta CT}$) method.

3.5 Protein expression analysis

Protein expression analysis was performed by Western blot. For this, the extraction of protein and quantification of the samples to be analyzed was first carried out.

3.5.1 Protein extraction and quantification

The cells pellets were collected and lysed on ice using Pierce® RIPA buffer (#89900, Thermo Fisher Scientific, Waltham, USA) supplemented with protease and phosphatase inhibitor cocktail (#A32961, Thermo Fisher Scientific, Waltham, USA) according to manufacturer's instructions. Briefly, a volume of supplemented RIPA buffer was added depending on the size of the cells pellets, and samples were incubated on ice for 30 min before being sonicated by the Sonics Vibra Cell VC 505 (Sonics&Materials, Newtown, USA) (40% pulse and 10 seconds). After 15 min of 13,200 rpm at 4˚C, proteins were collected and quantified using a Pierce™ BCA Protein Assay Kit (#23227, Thermo Fisher Scientific, Waltham, USA). The quantification of proteins by the BCA method is a colorimetric detection based on two reactions: in the first step, in an alkaline environment, peptides with three or more amino acid residues form a complex with cupric ions and go from Cu^{2+} to Cu^{1+}.

Next, the BCA reagent reacts with Cu^{1+} and a reaction is generated that gives a purple color. The more intensity of color, the greater the concentration of protein available in the sample.

Protein quantification was performed by duplicate in a 96-well plate. Briefly, a 1:10 dilution of the sample in distilled water was done in a final volume of 25 µl in each well, and 200 µl of BCA was added (1 part of reagent B in 50 parts of reagent A). A calibration curve was also performed with known concentrations of bovine serum albumin (BSA) to interpolate sample concentration. The plate was incubated for 30 min in the dark before absorbance was measured at 562 nm in Spectra Max Plus (Thermo Fisher Scientific, Waltham, USA).

3.5.2 Protein preparation

A total of 30 µg of protein was mixed with laemmli loading buffer 2X (Sigma-Aldrich, St. Louis, USA) and distilled water until reaching a final volume of 30 µl. Laemmli buffer contains tris(hydroxymethyl)aminomethane (tris base), sodium dodecyl sulfate (SDS) which denatures proteins and gives negative charges necessary to separate the proteins only but their molecular weight, glycerol to give density to the sample, 2-mercapto-ethanol that breaks the disulfide bridge of proteins, and bromophenol blue to visually locate the samples in the gel. After preparation, samples were then incubated for 5 min at 95^{o}C for protein denaturalization.

3.5.3 Western blot

Protein samples were separated in 6, 10, or 15% SDS-polyacrylamide gels, depending on the size of the proteins to be analyzed at constant 120V until the forward front reached the end of the gel, and transferred to nitrocellulose membranes (#1620115, BIO-RAD, Hercules, USA) for 2 h at constant 120V.

Membranes were then blocked for 1h with 5% of BSA in 0.1% TBS-Tween20 and incubated with specific antibodies described in **table 10** in a shaker at 4°C overnight. Described GAPDH was used as an internal control.

Table 10: List of primary antibodies used for Western blot.

Primary antibody	Dilution	Identification number
Anti-SIRT1	1:1000	#MA5-15677, Invitrogen
Anti-HDAC1	1:1000	#PA1-860, Invitrogen
Anti-ACSL4	1:1000	#PA5-27137, Invitrogen
Anti-Acetyl H3 (K9 + K14 + K18 + K23 + K27)	1:1000	#ab47915, Abcam
Anti-Total H3	1:1000	#9715S, Cell Signaling
Anti-CDH1	1:1000	#610181, BD Biosciences
Anti-CDH2	1:1000	#4061S, Cell Signaling
Anti-Vimentin	1:1000	#550513, BD Biosciences
Anti-Fibronectin	1:1000	#ab32419, Abcam
Anti-ABCG2	1:1000	#4477S, Cell Signaling
Anti-SOX2	1:1000	#3579, Cell Signaling
Anti-Nanog	1:1000	#4903, Cell Signaling
Anti-OCT4	1:1000	#2840, Cell Signaling
Anti-GAPDH	1:2000	#MA5-15738, Thermo Fisher Scientific

The following day, membranes were washed for 10 min 3 times with 0.1% TBS-Tween20 and incubated for 1 hour with IgG horseradish peroxidase (HRP)-linked secondary antibodies (**table 11**) at room temperature.

Table 11: List of secondary antibodies used for Western blot.

Secondary antibody	Dilution	Identification number
Anti-rabbit	1:2000	#7074S, Cell Signaling
Anti-mouse	1:2000	#7076S, Cell Signaling

After incubation, membranes were washed as specified above and signals were developed using Pierce™ ECL Western blotting reagent (#32106, Thermo Fisher Scientific, Waltham, USA) or ultra-sensitive ECL Super Signal West Femto (#34095, Thermo Fisher Scientific, Waltham, USA) according to the manufacturer's instructions in the ImageQuant Lass 400 system (GE-Healthcare Bioscience, Chicago, USA). A chemiluminescence signal was then obtained and images were analyzed with ImageJ-win64 for Windows to build the figures.

3.5.4 Western blot quantification

Western blot quantification was performed by band densitometry using ImageJ. A rectangle was first drawn around one protein band, and the same area was used for the other conditions, including loading control. Mean, maximum, and minimum pixel intensity was subsequently measured. The mean minus maximum was then calculated to know the protein value in each band and was next normalized to the loading control value to obtain relative protein values. To compare between different conditions, a final relative protein value was calculated compared to their respective control. Band densitometry for Western blots is represented in **figure S3-14**.

3.6 Luciferase reporter assay

The putative miRNA-449 binding site at the 3'UTR of the Acyl-CoA Synthetase Long-Chain Family Member 4 (*ACSL4)* mRNA (NM_004458.2) was cloned into pEZX-MT06 plasmid (Genecopeia, Guangzhou, China). pEZX-MT06 empty vector was used as a negative control plasmid. HEK293T cell line was seeded in a 24-well plate at 10^5 cells/well and cultured 24 h before transfection. Cells were co-transfected with 5ng/µl of plasmid or control plasmid pEZX-MT06, and 100 nM of miRNA-449a

(#MC11127, Ambion, Austin, USA), miRNA-449b-5p (#MC11521, Ambion, Austin, USA) or miRNA-449c-5p (#MC15616, Ambion, Austin, USA) mimic using lipofectamine 2000 reagent (Invitrogen) following manufacturer's instruction (same as *3.4 miRNA and siRNA transient transfections* section). Scramble served as a miRNA-negative transfection control (#4464059, Ambion, Austin, USA). 24h after transfection, luciferase activity was then measured using Luc-Pair™ Duo-Luciferase Assay Kit 2.0 (#217LF002, Genecopeia, Guangzhou, China) following manufacturer's instructions, and luminescence was detected in a luminescence microplate reader (LUMIstar Omega, BMG Labtech, Ortenberg, Germany). Relative luciferase activity was normalized to r-luc activity and relative to scramble control.

Briefly, 3'UTR of specific mRNA is fused with the reporter gene luciferase, and a hybrid LUC-3'UTR transcript is produced. If the miRNA of interest does not directly bind to 3'UTR of the specific mRNA, then luciferase oxidizes D-luciferin thus resulting in a fluorescent product that can be quantified. However, if a direct interaction is produced, the activity of luciferase is interrupted, so there is a drop in its signal (**figure 18**).

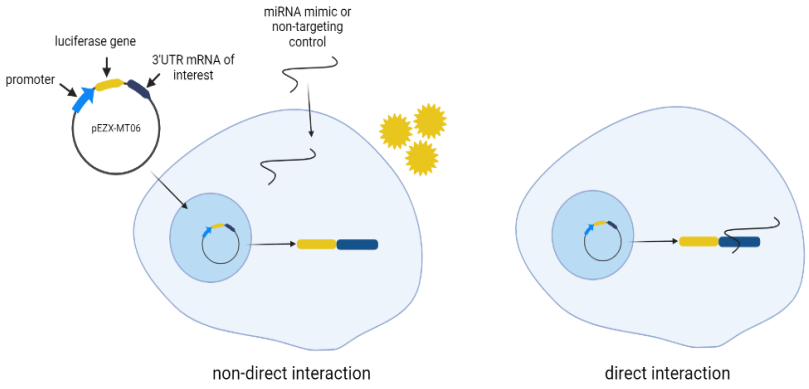

Figure 18: Schematic representation of luciferase reporter assay. Created by using BioRender

3.7 Cell proliferation and viability assay

After transfection specified in *3.5 miRNA and siRNA transient transfections* section, cells were seeded in 96-well plate at 5×10^3 cells/well for cell proliferation analyses at different periods (0, 24, and 48h post-transfection) and 10^4 cells/well for IC_{50} determination. The following day, cells were exposed to 48h of different doses of DOX (Pfizer, New York, USA) (0, 10^{-3}, 10^{-2}, 0.1, 0.25, 0.5, 1, 2.5, 5, 10, 50, 100 µM) to determine IC_{50} values. Cell proliferation at different time points specified above and viability for IC_{50} determination were then measured with Colorimetric Cell Viability kit II (WST-1) (#K304-2500, Deltaclon, Madrid, Spain) according to the manufacturer's instructions. Briefly, 100 µl of 7% WST-1 reagent in phenol red-free media was added to each well for 3h at 37°C. Absorbance was then measured at 450 nm in a microplate reader background corrected at 650 nm in Spectra Max Plus (Thermo Fisher Scientific, Waltham, USA).

Mitochondrial dehydrogenases can cleavage WST-1 to formazan which absorbs at 450nm. A more viable cells, more formazan formation, and more absorption at 450 nm.

3.8 Colony formation assay

A colony formation assay was performed to analyze anchor-independent proliferation after transfection specified in the *3.5 miRNA and siRNA transient transfections* section. Cells were seeded in a 6-well plate at 500 cells/well and cultured for 15 days at 37°C to form colonies. The medium was first gently removed from the dish and cells were then fixed for 20 min with 100% methanol (AppliChem, Monza, Italy). Next, cells were washed with distilled water and stained for 5 min with 0.5% crystal violet (Sigma-Aldrich, St. Louis, USA) in 25% methanol at room

temperature. Excess dye was removed by washing cells with distilled water and colonies were then allowed to dry and counted manually. A colony is considered when there are more than 50 cells together.

3.9 Transwell assay

Transwell assay was performed to study the migration ability of cells after transfection specified in the *3.5 miRNA and siRNA transient transfections* section. 72h after transfection, 5×10^4 cells were seeded in upper chambers of transparent polyester track etch (PET) membrane 24 well 8.0 μm pore size (#35307, Corning, New York, USA) in DMEM-F12 serum-free media. DMEM-F12 supplemented with 10% of serum was added in the lower chamber to act as a chemoattractant and the plate was incubated at 37°C for 24h to allow cell migration. The following day, cells were fixed for 2 min with 70% ethanol (Sigma-Aldrich, St. Louis, USA), permeabilized for 15 min with 100% methanol (AppliChem), and stained for 10 min with 0.5% crystal violet (Sigma-Aldrich, St. Louis, USA) in 25% methanol at room temperature. After drying, pictures of at least 3 different regions were captured under an inverted microscope (10X) (DMi1, Leica Microsystems, Wetzlar, Germany) and quantified using ImageJ-win64 for windows.

3.10 Quantification of intracellular DOX uptake

Intracellular DOX uptake was analyzed by confocal microscopy after transfection specified in the *3.5 miRNA and siRNA transient transfections* section. 48h post-transfection, 5×10^4 cells were seeded in an 8-well chamber (#30108, SPL Life Sciences, Gyeonggi-do, South Korea) and incubated at 37°C. The following day, cells were exposed to 5μM of DOX for 3h. After incubation, cells were fixed for 10 min with 4% paraformaldehyde (VWR BDH Chemicals, Matsonford, USA), counterstained

with DAPI (1:500 in PBS, Merck, Darmstadt, Germany), and mounted with glycerol (1:1 in PBS, Sigma-Aldrich, St. Louis, USA). 15 pictures per well were taken at the Central Medicine Research Unit (UCIM-UV) using a Leica DMi8 inverted fluorescence microscope (Wetzlar, Germany) with a PE4000 LED light source and DFC9000GT camera at 40X magnification. DOX and DAPI fluorescence was excited at 550 and 365, and the emission was 590 and 435-485, respectively. Mean DOX fluorescence intensity per cell was analyzed with ImageJ-win64 for windows and results were normalized to scramble control condition, keeping the same analysis settings for all pictures.

3.11 Apoptosis assay

Apoptosis was analyzed 96h after transfection as specified in the *3.5 miRNA and siRNA transient transfections* section and 48h 1µM DOX treatment by using Annexin V-FITC apoptosis detection kit (#ANXVKF-100T, Immunostep, Salamanca, Spain). Briefly, 4.8×10^4 cells/well were seeded in a 24-well plate and treated or not with 1µM of DOX for 48h. After the incubation time, the medium was removed and the cells were washed with 250 µl PBS (Biowest, Nuaillé, France), which was added together with the removed medium. Next, 250 µl of trypsin-EDTA 1X (Biowest, Nuaillé, France) was added for 5 min at 37^{o}C to detach the cells, and their action was then inhibited with the previously removed medium. Subsequently, pellets were centrifuged at 1,500 rpm for 5 min and the cells were incubated for 10 min in the dark with 200µl of 0.5% FITC Annexin V (#556419, BD Pharmingen) and 10% binding buffer (#ANXVKF-100T, Immunostep, Salamanca, Spain) in PBS. Samples were passed through BD LSR Fortessa cytometer (BD Biosciences, New Jersey, USA) and data were analyzed using BD FACSDiva X20 Software.

The apoptotic process presents certain morphologic features that can be analyzed by flow cytometry. One of the earliest events is the translocation of the phospholipid phosphatidylserine (PS) from the inner to the outer plasma membrane, which presents a high affinity for Annexin V that can be detected because it presents the binding of the FITC fluorochrome.

3.12 *In silico* analysis

3.12.1 Kaplan-Meier curves

Kaplan-Meier plotter software (https://kmplot.com/analysis/) was used to evaluate the prognostic value of the miRNA-449 family (hsa-miRNA-449a, hsa-miRNA-449b-5p, hsa-miRNA-449c-5p) and *ACSL4*. OS for the miRNAs-449 family was analyzed based on the expression of TNBC patients from the TCGA group (*n*=97) with auto-selected best-cut-off. DFS for *ACSL4* mRNA was analyzed based on the expression of TNBC patients (*n*=53) with auto-selected best cut-off. The Hazard ratio (HR) and log-rank P-value are calculated by the software and curves are plotted[282].

3.12.2 MiRWalk analysis

The online biological database miRWalk 2.0 (http://zmf.umm.uni-heidelberg.de/mirwalk2) was used to predict *ACSL4* mRNA as a target of miRNAs-449. MiRWalk database combines miRNA binding sites within the complete gene sequence and it also compares the results from 12 different miRNA–gene interaction prediction programs (miRWalk, Microt4, miRanda, mirbridge, miRDB, miRMap, miRNAMap, Pictar2, PITA, RNA22, RNAhybrid and, Targetscan)[283]. If software predicts an interaction is scored as 1, otherwise is scored as 0.

3.12.3 MirPath analysis

DIANA TOOLS- mirPath v.3 (http://www.microrna.gr/miRPathv3) biological database was used to study cancer pathways affected by miRNAs-449 family (miRNA-449a, miRNA-449b-5p, and miRNA-449c-5p) while predicting possible targets. TarBase v7.0 was selected for miRNAs-449 targets analyses, and pathways union was selected for regulated KEGG pathways analysis. Pathways union derives a fused *p-value* for each pathway by combining the previously calculated significance levels between each miRNA and each pathway, using Fisher's Exact Test statistical analysis method[284]. The *p-value* threshold was 0.05.

3.13 Patient samples

Formalin-fixed and paraffin-embedded samples (FFPE) tissues were obtained from patients undergoing primary biopsies at Biomedical Research Institute INCLIVA (Spain) and were subsequently treated following standard guidelines. All samples were analyzed by an expert pathologist to ensure >30% tumor infiltration, and HR and HER2 status were evaluated by IHC and/or FISH in the latter case. MiRNAs-449 and *ACSL4* expression was analyzed by RT-qPCR in a discovery cohort of TNBC (*n*=55 for miRNAs-449 and *n*=33 for ACSL4) versus healthy tissues (*n*=23) before treatment. Clinicopathological characteristics are described in **table S1 and S2**, respectively. *ACSL4* expression was also analyzed in primary biopsies of non-relapse (*n*=12) and relapse (*n*=20) patients after receiving (neo)adjuvant-containing chemotherapy treatment. The data collection of the patients was carried out in a period between 21 and 105 months. Clinicopathological characteristics are described in **table S3**. Briefly, total RNA was isolated from FFPE tissue blocks using the RecoverAll Total Nucleic Acid Kit (Ambion, Austin, USA) and 1µg was retro-transcribed with specific

primers using TaqMan™ MicroRNA Reverse Transcription Kit (Applied Biosystems, Waltham, USA) following manufacturer's instructions. RT-qPCR was then performed with TaqMan® Universal Master Mix (Applied Biosystems, Waltham, USA) and TaqMan® 20× assays (Applied Biosystems, Waltham, USA) on 9700HT Fast Real-Time PCR system (Applied Biosystems, Waltham, USA). Expression of housekeeping *GAPDH* mRNA or miRNA-16 was used as an internal control. All the participants in the study signed written informed consent. The study was approved on the 25th of June of 2015 (ethical approval number 2014/178) and all patients signed the written informed consent.

3.14 Statistical analyses

All statistical analyses were performed in GraphPad Prism version 8.0.1 software (La Jolla, USA). All data were presented as mean ± standard deviation (SD), except for quantification of intracellular DOX uptake which is presented as mean ± standard error of the mean (SEM). IC_{50} values were calculated using a variable slope (four parameters) curve. Mean comparisons were performed using a two-tailed Student's *T*-test for normal distribution and a Mann-Whitney U-test for abnormal distribution.

A value of $p<0.05$ was defined as statistically significant. Assays were performed in biological and technical triplicate.

CHAPTER 4

Results

4.1 MiRNA-449 family is repressed in TNBC through epigenetic mechanisms

4.1.1 MiRNA-449 family is downregulated in TNBC patients and cell lines and its expression is associated with worst OS

To elucidate the miRNA-449 family's (miRNA-449a, miRNA-449b-5p, and miRNA-449c-5p) role in BC, basal levels were first evaluated by RT-qPCR in TNBC cell lines (MDA-MB-231 and MDA-MB-436) and one non-tumoral immortalized cell line (MCF10A). The results showed a significantly lower expression of miRNAs-449 in both BC cell lines (MDA-MB-231 and MDA-MB-436) compared to the MCF10A cell line (p=0.0047 and p=0.0025 for miRNA-449a, p<0.0001 and p=0.0015 for miRNA-449b-5p, p=0.0221 and p=0.0302 for miRNA-449c-5p, respectively) (**Figure 19A**). Similarly, the expression of these miRNAs was also evaluated by RT-qPCR in a discovery cohort of primary biopsies from TNBC tissue samples (n=55) and healthy tissue samples (n=23). MiRNAs-449 family was also found significantly decreased in TNBC tissue samples compared to healthy tissue samples (p<0.0001 for the three miRNAs) (**Figure 19B**), thus confirming the underexpression of these miRNAs not only in cell lines but also in TNBC patient samples.

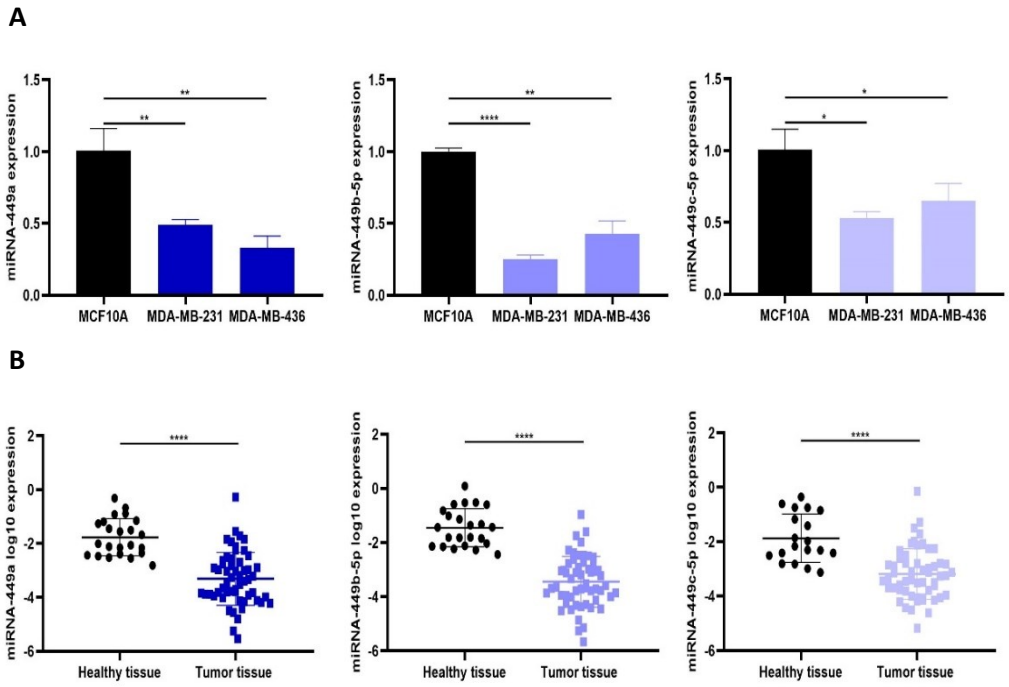

Figure 19: MiRNA-449 family is downregulated in TNBC patients and cell lines. (**A**) MiRNA-449 family (miRNA-449a, miRNA-449b-5p, and miRNA-449c-5p) expression was analyzed by RT-qPCR in TNBC cell lines (MDA-MB- 231 and MDA-MB-436), and the non-tumor immortalized line (MCF10A). (**B**). MiRNA-449 family expression was analyzed by RT-qPCR in a discovery cohort of TN (*n*=55) sample patients and healthy tissues (*n*=23) samples. Student T-test was used for statistical analysis for A. Mann-Whitney test was used for statistical analysis for B. **p*<0.05; ***p*<0.01, *****p*<0.0001.

Moreover, in order to study the clinical relevance, the prognostic value was evaluated based on miRNAs-449 expression in 97 TNBC patients from the TCGA group of Kaplan-Meier plotter, and a worst OS was found significantly associated with lower miRNAs-449 expression (HR=0.39, 95% Confidence Interval (CI)=0.15-1.04 *p*=0.05 for miRNA-449a, HR=0.16 CI=0.05-0.56 *p*=0.0011 for miRNA-449b-5p, HR=0.33 CI=0.11-0.95 *p*=0.03 for miRNA-449c-5p) (**Figure 20**).

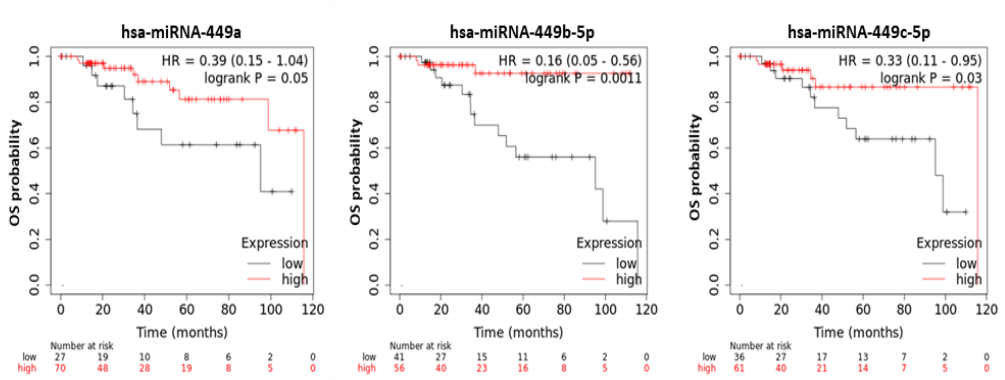

Figure 20: MiRNA-449 family lower expression is associated with worst OS. Representation of OS Kaplan Meier curves in TNBC samples (*n*=97) from TCGA group based on an optimal cut-off of miRNAs-449 for low (black) and high (red) expression (*p*=0.05 for miRNA-449a, *p*=0.0011 for miRNA-449b-5p, and *p*=0.03 for miRNA-449c-5p).

4.1.2 HDAC1 and SIRT1 are overexpressed in TNBC and inhibit miRNAs-449 expression by histone deacetylation

Based on pre-existing literature on the modulation of miRNAs-449 expression by different epigenetic mechanisms, we assessed the involvement of histone acetylation modulation in TNBC. In this sense, the two histones deacetylases HDAC1 and SIRT1 have been previously demonstrated as direct targets of miRNA-449 family[285,219], so the following experiments focused on the relationship between miRNA-449 family and, HDAC1 and SIRT1. For that, we first evaluated the basal expression of two histone deacetylases, HDAC1 and SIRT1, in both TNBC cell lines (MDA-MB-231 and MDA-MB-436) and the non-tumoral immortalized cell line MCF10A. The results showed a significantly higher mRNA expression in TNBC cell lines (MDA-MB-231 and MDA-MB-436) of *HDAC1* (*p*=0.002 and *p*=0.0002, respectively) and *SIRT1* (*p*=0.0006 and *p*=0.0011, respectively) compared to MFC10A

cell line (**Figure 21A, B**). This upregulation of HDAC1 and SIRT1 was also confirmed at the protein level (**Figure 21C**).

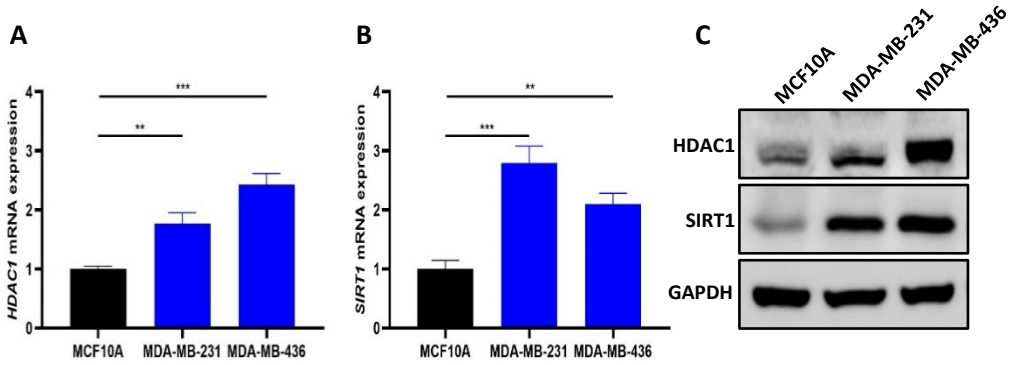

Figure 21: HDAC1 and SIRT1 are upregulated in TNBC cell lines. HDAC1 and SIRT1 expression were analyzed by (**A** and **B**, respectively) RT-qPCR and (**C**) Western blot in TNBC cell lines (MDA-MB-231 and MDA-MB-436) and the non-tumor immortalized line MCF10A. GAPDH was used as loading control for C. Student T-test was used for statistical analyses for A and B. ***p*<0.01, ****p*<0.001.

Given the histone deacetylase activity of HDAC1 and SIRT1, a possible implication of these two proteins in miRNAs-449 modulation was evaluated. *HDAC1* knockdown produced an induction of miRNAs-449 in MDA-MB-231 (*p*=0.0005 for miRNA-449a, *p*=0.0044 for miRNA-449b-5p, and *p*=0.0010 for miRNA-449c-5p) and MDA-MB-436 cell lines (*p*=0.0003 for miRNA-449a, *p*<0.0001 for miRNA-449b-5p, and *p*=0.0003 for miRNA-449c-5p) (**Figure 22A**). Similarly, *SIRT1* knockdown also produced same effect in MDA-MB-231 (*p*=0.0002 for miRNA-449a, *p*=0.0001 for miRNA-449b-5p, and *p*<0.0001 for miRNA-449c-5p) and MDA-MB-436 cell lines (*p*=0.0072 for miRNA-449a, *p*=0.0035 for miRNA-449b-5p, and *p*=0.0005 for miRNA-449c-5p) (**Figure 22B**).

Pharmacologic treatment with the histone deacetylase type I and II inhibitor (TSA) and SIRT1 inhibitor (NAM) was also performed. Both TSA and NAM treatment

produced an increment of acetyl-H3 expression compared to control in both TNBC cell lines (**Figure 22C, D**), thus verifying the action mechanism of these two drugs. Furthermore, TSA treatment produced a significant increase of miRNAs-449 expression in both MDA-MB-231 (p=0.0002 for miRNA-449a, p=0.0052 for miRNA-449b-5p, and p<0.0001 for miRNA-449c-5p) and MDA-MB-436 cell lines (p=0.0008 for miRNA-449a, p<0.0001 for miRNA-449b-5p, and p=0.0007 for miRNA-449c-5p) (**Figure 22E**). This upregulation for miRNA-449a (p=0.0121 for MDA-MB-231 and p=0.0020 for MDA-MB-436), miRNA-449b-5p (p=0.0191 for MDA-MB-231 and p=0.0010 for MDA-MB-436), and miRNA-449c-5p (p=0.0497 for MDA-MB-231 and p=0.0002 for MDA-MB-436) was also obtained after NAM treatment (**Figure 22F**). Therefore, these results reinforce the previous ones carried out with a specific siRNA for *HDAC1* and *SIRT1* and suggest a miRNAs-449 modulation by histone acetylation.

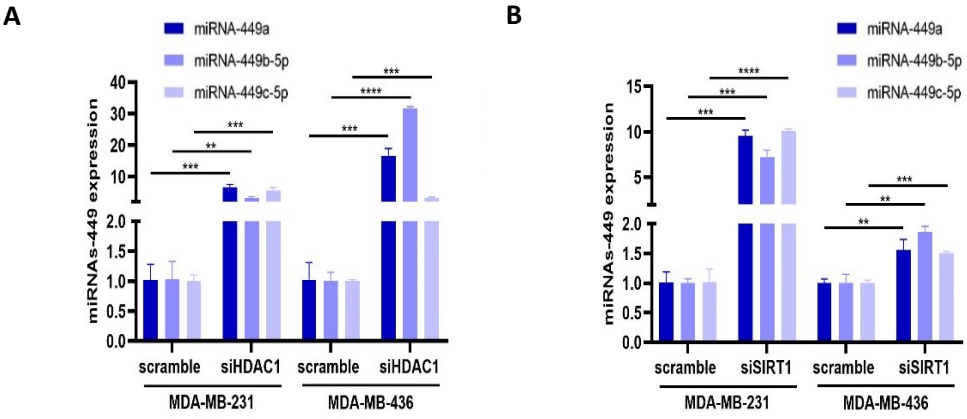

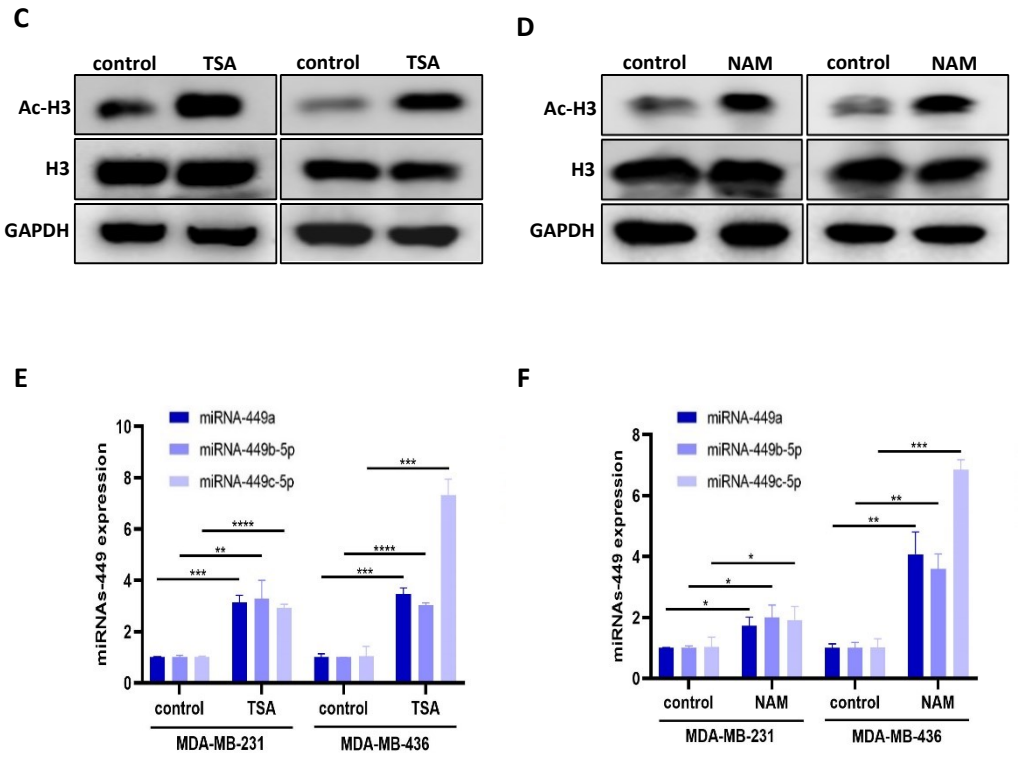

Figure 22: HDAC1 and SIRT1 inhibition by siRNA and pharmacologic treatment induce miRNA-449 family expression. MiRNA-449 family (miRNA-449a, miRNA-449b-5p, and miRNA-449c-5p) expression was analyzed by RT-qPCR in TNBC cell lines (MDA-MB- 231 and MDA-MB-436) after (**A**) *HDAC1* and (**B**) *SIRT1* siRNA transfection. Ac-H3 and H3 expression was analyzed by Western blot in TNBC cell lines after (**C**) TSA and (**D**) NAM treatment. MiRNA-449 family expression was analyzed by RT-qPCR in TNBC cell lines after (**E**) 10nM 24h of TSA and (**F**) 300µM 24h of NAM treatment. GAPDH was used as loading control for C and D. Student T-test was used for statistical analyses for A, B, E, and F.*p<0.05, **p<0.01, ***p<0.001, ****p<0.0001.

4.1.3 MiRNA-449 family downregulate HDAC1 and SIRT1 expression by a negative feedback loop

In order to assess if there is a homeostasis mechanism for the expression of miRNAs-449 in BC, the expression of HDAC1 and SIRT1 was evaluated after a miRNAs-449 mimic transfection. The results showed significant downregulation of *HDAC1* (p=0.0002 for MDA-MB-231 and p=0.0085 for MDA-MB-436) and *SIRT1* (p=0.0007 for MDA-MB-231 and p=0.0055 for MDA-MB-436) at mRNA level after miRNAs-449 overexpression (**Figure 23A, B**). This lower expression was also observed at the protein level (**Figure 23C**). HDAC1 and SIRT1 expression was also evaluated after miRNAs-449 mimics transfection separately. The results showed a significant downregulation of *HDAC1* after miRNA-449a (p=0.0057 for MDA-MB-231 and p=0.0016 for MDA-MB-436), miRNA-449b-5p (p=0.0004 for MDA-MB-231 and p<0.0001 for MDA-MB-436), and miRNA-449c-5p (p=0.0061 for MDA-MB-231 and p=0.0003 for MDA-MB-436) overexpression (**Figure 23D**). Similarly, miRNA-449a (p=0.0114 for MDA-MB-231 and p=0.0026 for MDA-MB-436), miRNA-449b-5p (p=0.0105 for MDA-MB-231 and p=0.0001 for MDA-MB-436), and miRNA-449c-5p (p=0.0061 for MDA-MB-231 and p<0.0001 for MDA-MB-436) mimic transfection separately produced a *SIRT1* downregulation (**Figure 23E**). This drop in expression was also observed at the protein level (**Figure 23F**). All together suggest the existence of a miRNAs-449/SIRT1-HDAC1 negative feedback loop.

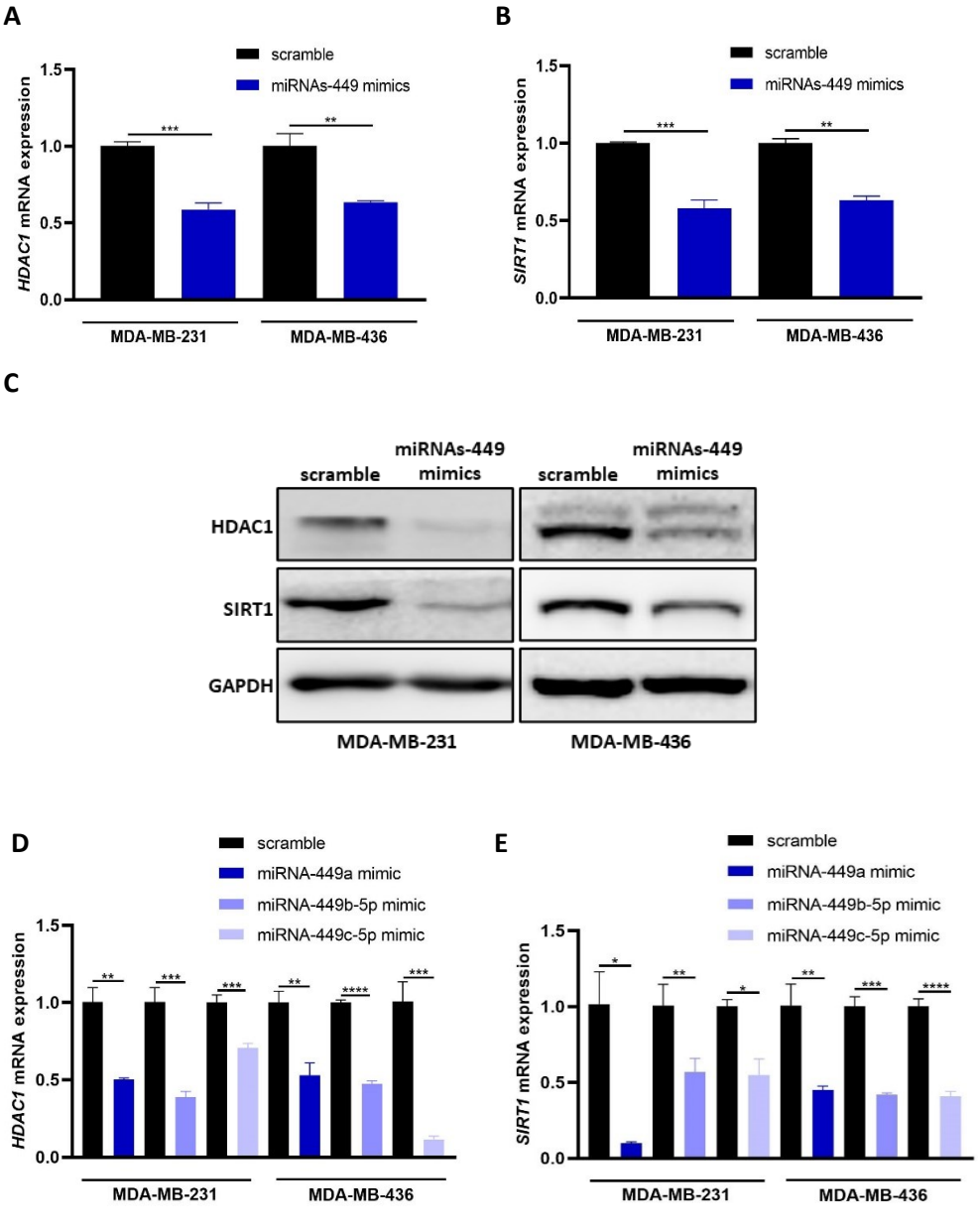
A
scramble
miRNAs-449 mimics
HDAC1 mRNA expression
1.5
1.0
0.5
0.0
***
**
MDA-MB-231
MDA-MB-436
B
scramble
miRNAs-449 mimics
SIRT1 mRNA expression
1.5
1.0
0.5
0.0
***
**
MDA-MB-231
MDA-MB-436
C
scramble
miRNAs-449 mimics
scramble
miRNAs-449 mimics
HDAC1
SIRT1
GAPDH
MDA-MB-231
MDA-MB-436
D
scramble
miRNA-449a mimic
miRNA-449b-5p mimic
miRNA-449c-5p mimic
HDAC1 mRNA expression
1.5
1.0
0.5
0.0
**
***
***
**
****
***
MDA-MB-231
MDA-MB-436
E
scramble
miRNA-449a mimic
miRNA-449b-5p mimic
miRNA-449c-5p mimic
SIRT1 mRNA expression
1.5
1.0
0.5
0.0
*
**
*
**
***
****
MDA-MB-231
MDA-MB-436

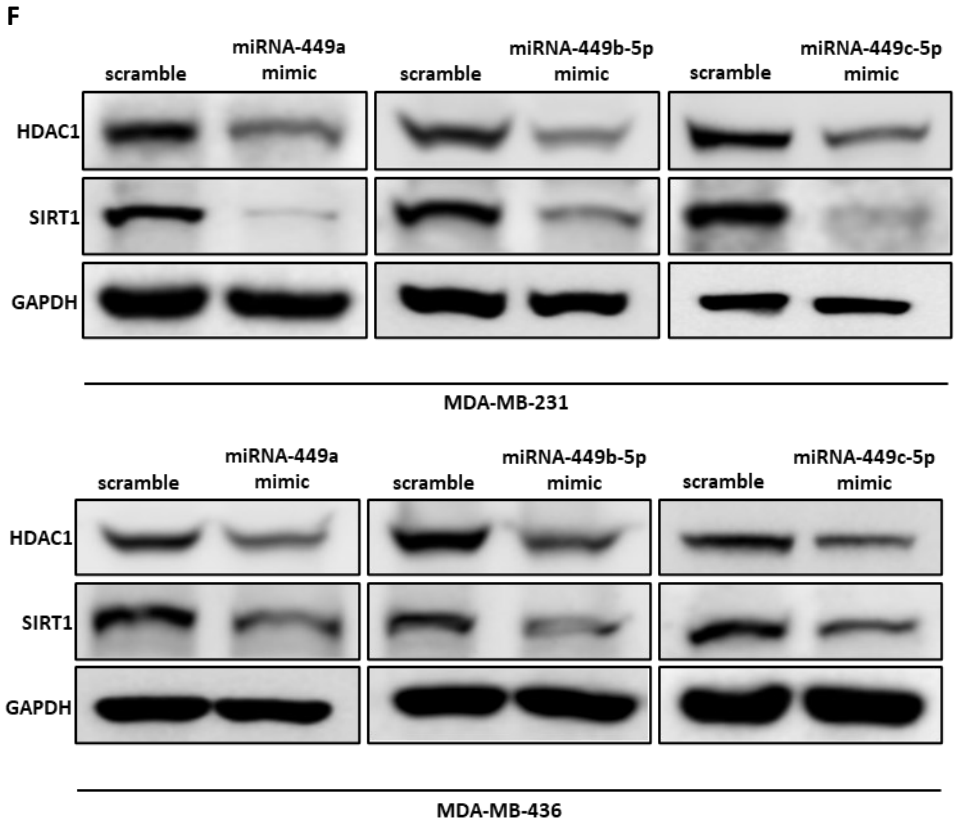

Figure 23: MiRNA-449 family overexpression downregulates HDAC1 and SIRT1 expression. MiRNAs-449 mimics transfection was performed in MDA-MB-231 and MDA-MB-436 cell lines. HDAC1 and SIRT1 expression were analyzed by (**A** and **B**, respectively) RT-qPCR and (**C**) Western blot. MiRNAs-449a, miRNA-449b-5p, and miRNA-449c-5p mimics transfection separately were performed in MDA-MB-231 and MDA-MB-436 cell lines. HDAC1 and SIRT1 expression was analyzed by (**D** and **E**, respectively) RT-qPCR and (**F**) Western blot. GAPDH was used as loading control for C and F. Student T-test was used for statistical analyses for A, B, D, and E. **p*<0.05, ***p*<0.01, ****p*<0.001, ****p<0.0001.

4.2 MiRNA-449 family modulates TNBC aggressiveness through ACSL4 targeting

4.2.1 MiRNA-449 family modulates fatty acid metabolism through ACSL4 direct targeting

Although various studies point out the role of miRNAs-449 as tumor suppressors, more deep research is needed to understand their mechanism of action. Hierarchical clustering of miRNAs-449 and cancer pathways using miRPath software predicted that there is a significant interaction between these miRNAs and central carbon metabolism (p<1.14e-8), fatty acid biosynthesis (p<1e-325), and fatty acid metabolism (p<1e-325) (**Figure 24A**), thus suggesting a fatty acid metabolism modulation by miRNA-449 family. The interaction of fatty acid biosynthesis and miRNAs-449 was predicted through 3 different genes by using TarBase v7.0: *FASN*, *Acyl-CoA synthetase long-chain family member 4* (*ACSL4*), and *Acetyl-CoA carboxylase alpha* (*ACACA*). Based on existing literature in TNBC, subsequent trials focused on the study of ACSL4.

Basal expression of ACSL4 was then analyzed in TNBC and MCF10A cell lines. The results showed a significantly higher expression of *ACSL4* in MDA-MB-231 (p<0.0001) and MDA-MB-436 (p=0.0001) cell lines compared to the MFC10A cell line (**Figure 24B**). The same results were obtained at the protein level (**Figure 24C**). Similarly, *ACSL4* was significantly higher expressed in TNBC patient's tissues compared to healthy tissues (p<0.0001) (**Figure 24D**). These results suggest an inverse correlation with miRNAs-449 expression in TNBC.

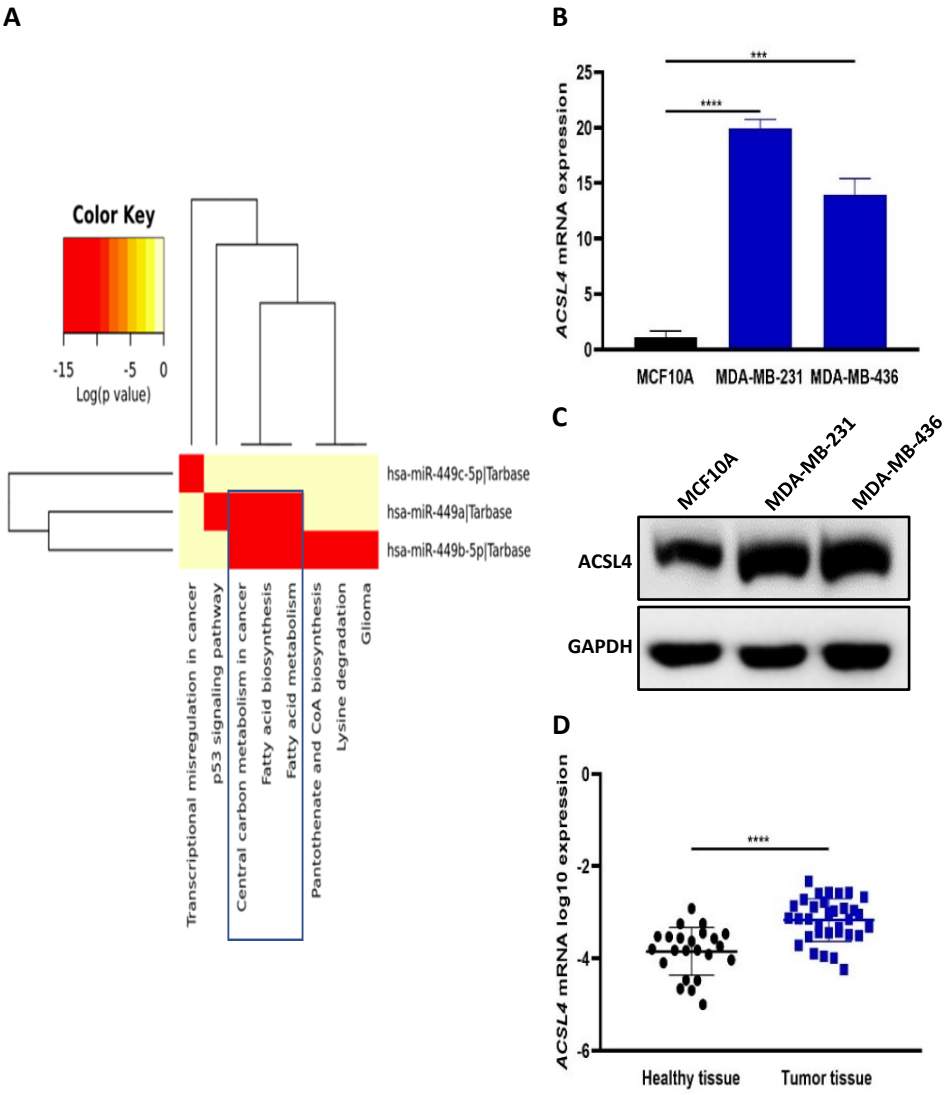

Figure 24: MiRNA-449 family is predicted to modulate fatty acid metabolism through ACSL4. (**A**) MiRpath software analysis of miRNAs-449 targeted pathways. The color indicates a logarithmic transformation of Fisher's Exact test-adjusted *p-values* (red for lower *p-values*). ACSL4 expression was analyzed by (**B**) RT-qPCR and (**C**) Western blot in TNBC cell lines (MDA-MB-231 and MDA-MB-436) and non-tumoral BC cell line (MCF10A). (**D**) *ACSL4* mRNA expression was analyzed by RT-qPCR in a discovery cohort of TNBC (*n*=33) sample patients and healthy tissue samples (*n*=23). Student T-test was used for statistical analyses for B. Mann-Whitney test was used for statistical analysis for D. Values are expressed as mean ± SD (n=3). GAPDH was used as loading control for C. ***p<0.001, ****p<0.0001.

To evaluate *ACSL4* as a potential target of miRNAs-449 in BC, we first used miRWalk online database, and 3'UTR of *ACSL4* mRNA was found to have predicted target sites for miRNA-449a (8 out of 12) and miRNA-449b-5p (8 out of 12) in the majority of miRNA–gene interaction prediction programs, while only 5 out of 12 prediction programs predicted for miRNA-449c-5p (**Table S4**). Furthermore, to determine if *ACSL4* is a direct target of miRNAs-449, we cloned the miRNAs-449 predicted target sequence of 3'UTR-*ACSL4* mRNA into pEZX-MT06 luciferase reporter vector. Co-transfection with miRNAs-449a and miRNA-449b-5p in the HEK-293T cell line significantly decreased luciferase activity compared to scramble control, in 3'UTR-*ACSL4* plasmid (p<0.0001 for miRNA-449a and p<0.001 for miRNA-449b-5p) but not in the empty one compared to scramble control, indicating that *ACSL4* mRNA is a direct target of miRNA-449a and miRNA-449b-5p. However, no differences were observed in miRNA-449c-5p co-transfection (**Figure 25A**).

MiRNAs-449 mimics were then transfected in TNBC cell lines and ACSL4 expression was evaluated in order to analyze ACSL4 modulation. MiRNAs-449 overexpression produced a significant downregulation of *ACSL4* in MDA-MB-231 (p=0.0045) and MDA-MB-436 (p=0.0006) cell lines compared to the scramble control (**Figure 25B**). This was also confirmed at the protein level (**Figure 25C**). To study the individual role of each one of miRNAs-449 in ACSL4 expression, TNBC cell lines were transfected separately with the corresponding miRNA-449 family member. The results showed a significant downregulation of *ACSL4* after overexpression of miRNA-449a (p=0.0019 for MDA-MB-231 and p=0.0001 for MDA-MB-436), miRNA-449b-5p (p=0.0002 for MDA-MB-231 and p=0.0042 for MDA-MB-436), and miRNA-449c-5p (p=0.0029 for MDA-MB-231 and p=0.0006 for MDA-MB-436) (**Figure 25D**). A drop in ACSL4 expression was also observed at the protein level (**Figure 25E**). These results

suggest an ACSL4 downregulation by miRNA-449a/b-5p direct and miRNA-449c-5p indirect targeting.

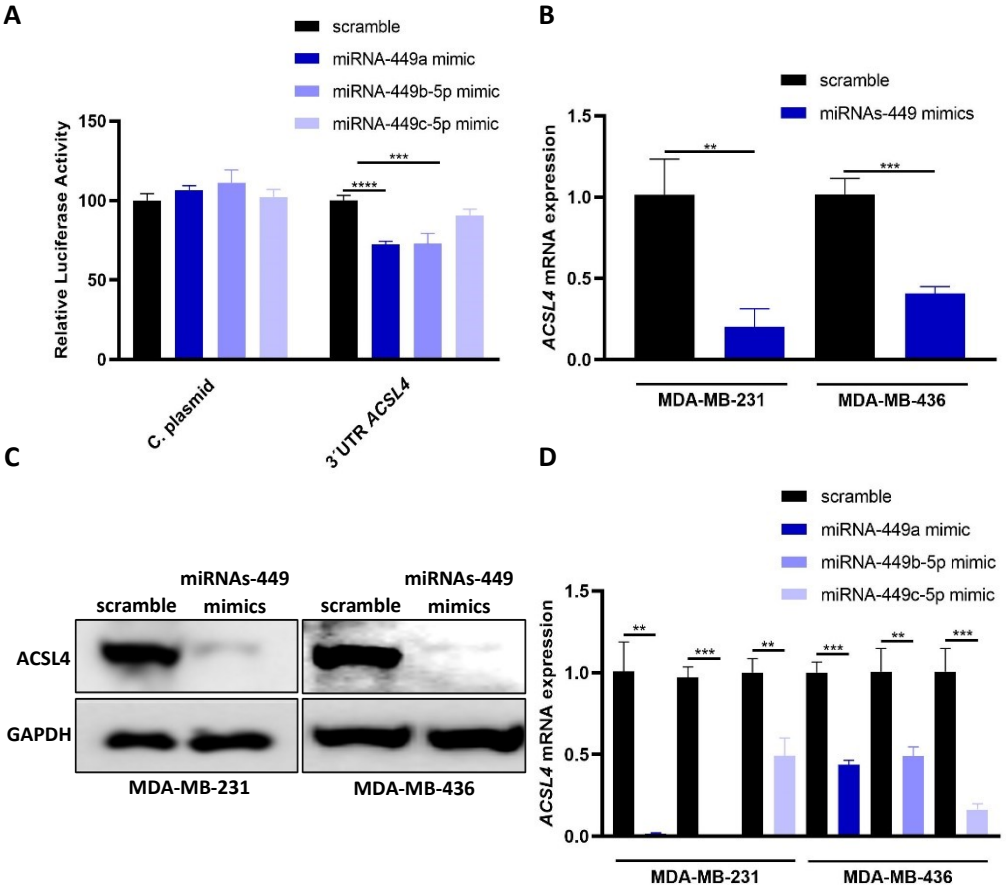

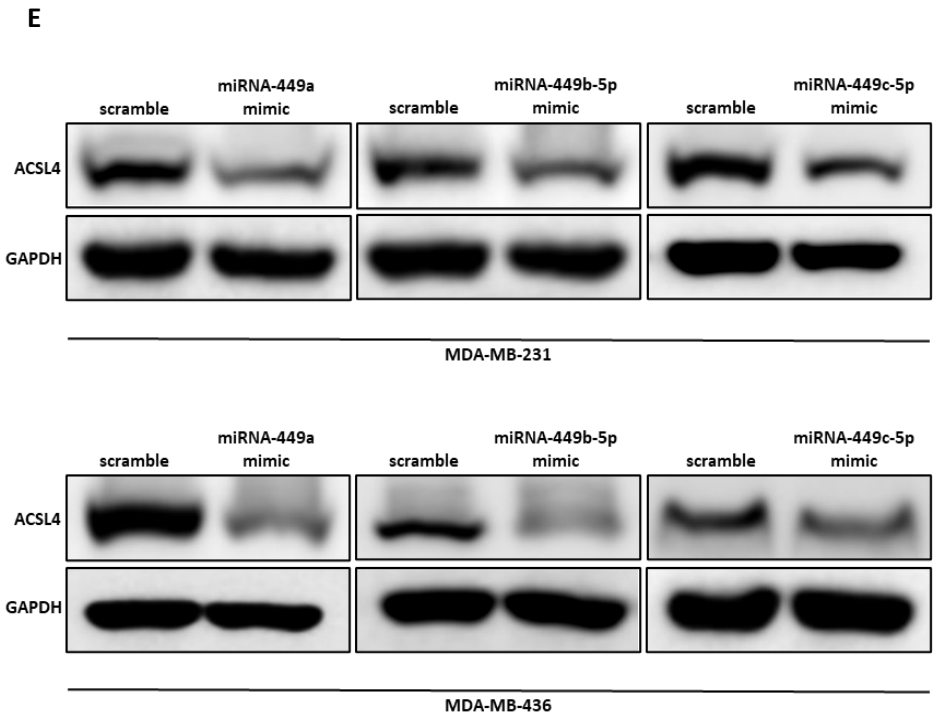

Figure 25: MiRNAs-449 downregulate ACSL4 expression by direct (miRNA-449a/b-5p) and indirect (miRNA-449c-5p) targeting. (**A**) Luciferase reporter assay was performed in HEK-293T cell line co-transfected with pEZX-MT06 (3'UTR *ACSL4* containing or empty vector) and miRNA-449a, miRNA-449b-5p, or miRNA-449c-5p mimics separately. ACSL4 expression was analyzed by (**B**) RT-qPCR and (**C**) Western blot after miRNA-449 family mimics transfection in MDA-MB-231 and MDA-MB-436 cell lines. ACSL4 expression was analyzed by (**D**) RT-qPCR and (**E**) Western-blot after miRNAs-449 mimics transfection separately in MDA-MB-231 and MDA-MB-436 cell lines. Student T-test was used for statistical analyses for A, B, and D. GAPDH was used as loading control for C and E. ** $p<0.01$, *** $p<0.001$, **** $p<0.0001$. C. plasmid: Control plasmid.

4.2.2 MiRNAs-449 overexpression inhibits proliferation, colony formation, migration and invasion through ACSL4 downregulation

Once an inverse correlation was observed between miRNAs-449 and ACSL4 expression, the role of these miRNAs through ACSL4 modulation in different cancer hallmarks was investigated in TNBC.

Both exogenous introduction of miRNAs-449 and *ACSL4* knockdown significantly decreased cell proliferation compared to scramble control in a time-dependent manner (**Figure 26A, B**).

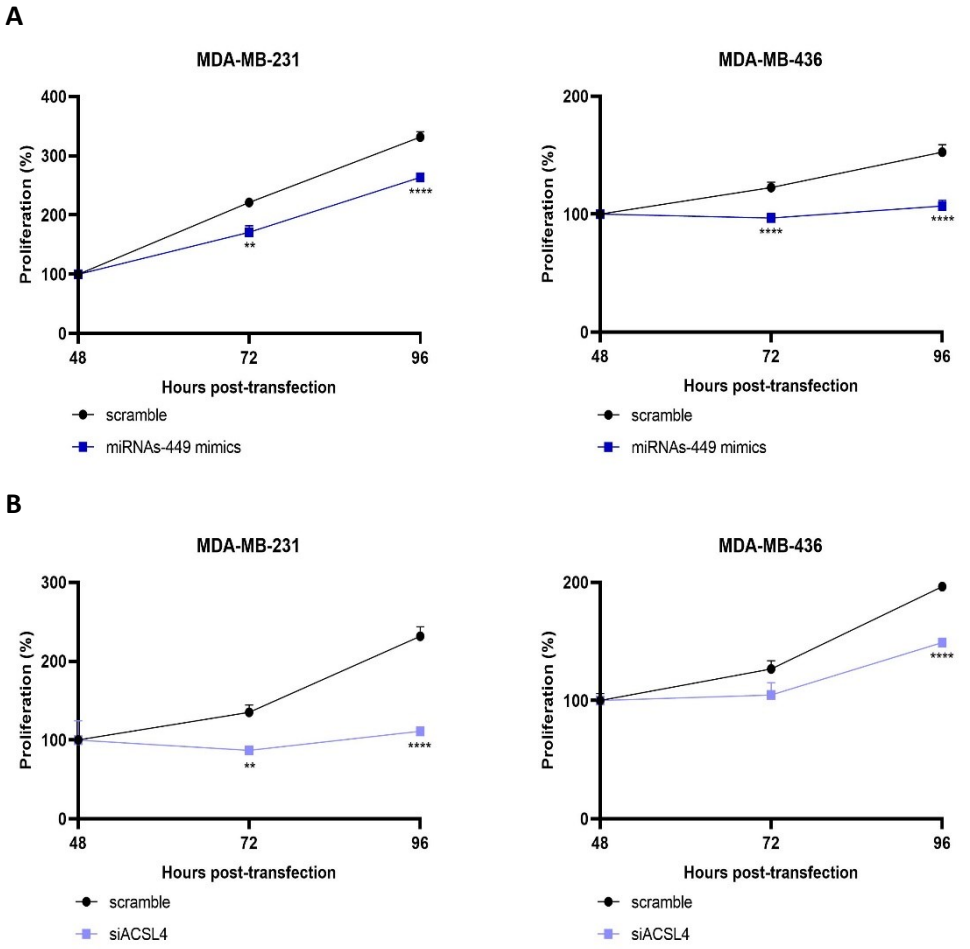

Figure 26: MiRNAs-449 decrease cell proliferation through ACSL4 downregulation in TNBC. Cell proliferation was analyzed by WST-1 at different times post-transfection for (**A**) miRNAs-449 mimics and (**B**) ACSL4 siRNA transfection in MDA-MB-231 and MDA-MB-436 cell lines. 48h post-transfection was set as 100% proliferation. Student T-test was used for statistical analyses at each time point. ***p*<0.01, *****p*<0.0001.

A migration assay was performed to evaluate the effect of miRNAs-449 in EMT. The results showed that miRNAs-449 overexpression significantly reduced the number of migrating cells by transwell migration assay in TNBC cell lines (*p*<0.0001 for MDA-

MB-231 and MDA-MB-436) compared to scramble control (**Figure 27A, B**). *ACSL4* knockdown also produced the same results (p<0.0001 for MDA-MB-231 and MDA-MB-436) (**Figure 27C, D**). In addition, the expression of epithelial (CDH1: E-cadherin) and mesenchymal markers (CDH2: N-cadherin, VIM: vimentin, FN1: fibronectin) were analyzed in TNBC cells. MiRNAs-449 overexpression and *ACSL4* knockdown upregulated the expression of CDH1 and downregulated the expression of CDH2, VIM and FN1, thus diminishing the ability to undergo the EMT process (**Figure 27E, F**).

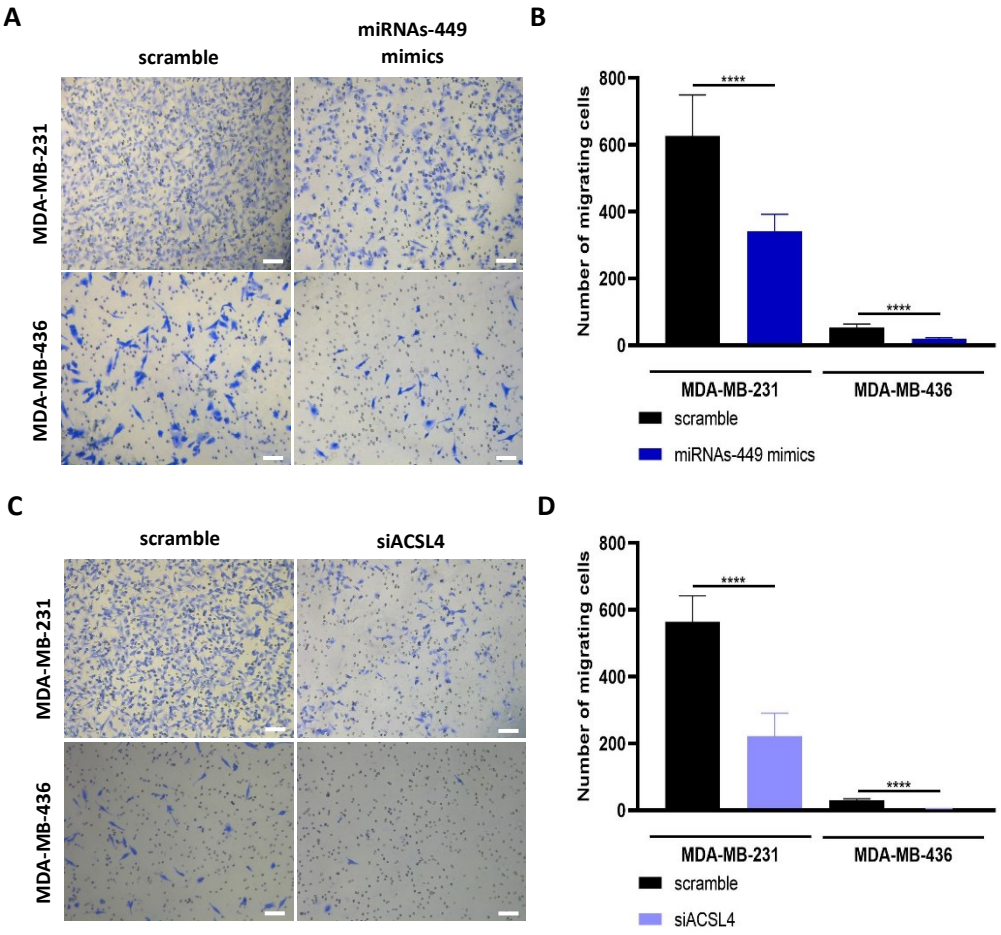

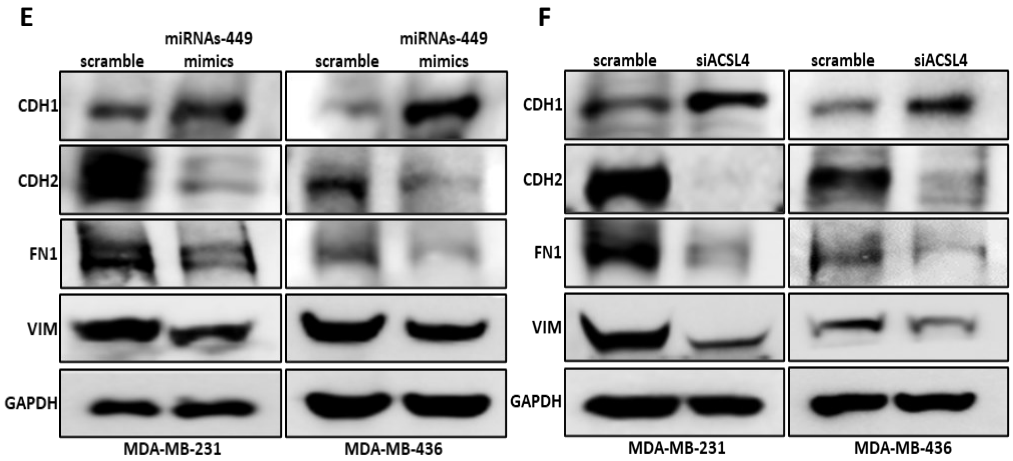

Figure 27: MiRNAs-449 inhibit migration by diminishing the ability of the EMT process through ACSL4 downregulation. TNBC cell lines (MDA-MB-231 and MDA-MB-436) were transfected with miRNAs-449 (miRNA-449a, miRNA-449b-5p, and miRNA-449c-5p) mimics or small-interfering (si*RNA*) targeting *ACSL4.* (**A**) Representative images of cell migration by transwell assay and (**B**) quantification of migrating cells after miRNAs-449 mimics transfection. (**C**) Representative images of cell migration by transwell assay and (**D**) quantification of migrating cells after *ACSL4* siRNA transfection. Expression of EMT markers (CDH1, CDH2, FN1 and VIM) was analyzed by Western blot after (**E**) miRNAs-449 and (**F**) *ACSL4* siRNA transfection. Scale bar: 100 µm for A and C. Student T-test was used for statistical analyses for B and D. GAPDH was used as loading control for E and F. ****p<0.0001.

Moreover, the clonogenic capacity of TNBC cells was analyzed through a colony formation assay. The overexpression of miRNAs-449 significantly reduced the number of colonies formed in MDA-MB-231 (p=0.0042) and MDA-MB-436 (p=0.0088) cell lines compared to scramble control (**Figure 28A, B**). Similarly, the same results were obtained after *ACSL4* knockdown (p=0.0114 for MDA-MB-231 and p=0.0080 for MDA-MB-436) (**Figure 28C, D**). For a deeper study of the ability to form tumors, the expression of stem-cell markers was also evaluated. A drop in SRY-Box

transcription factor 2 (SOX2), Nanog homeobox (Nanog), and Octamer-binding transcription factor 4 (OCT4) expression were observed after the transfections indicated above in both MDA-MB-231 and MDA-MB-436 cell lines (**Figure 28E, F**). These results suggest that miRNAs-449 overexpression diminishes the potential to form tumors through ACSL4 downregulation and thus producing a loss of stem-cell characteristics.

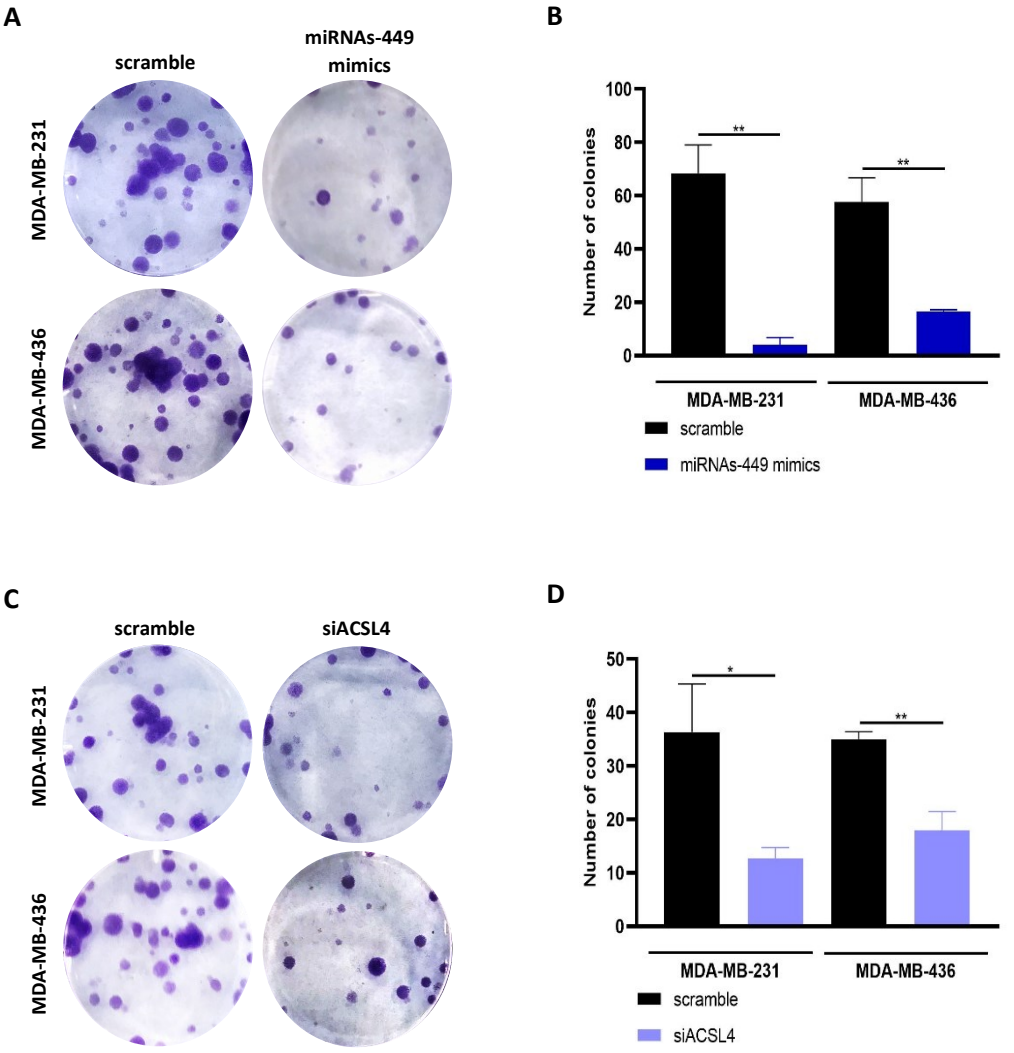

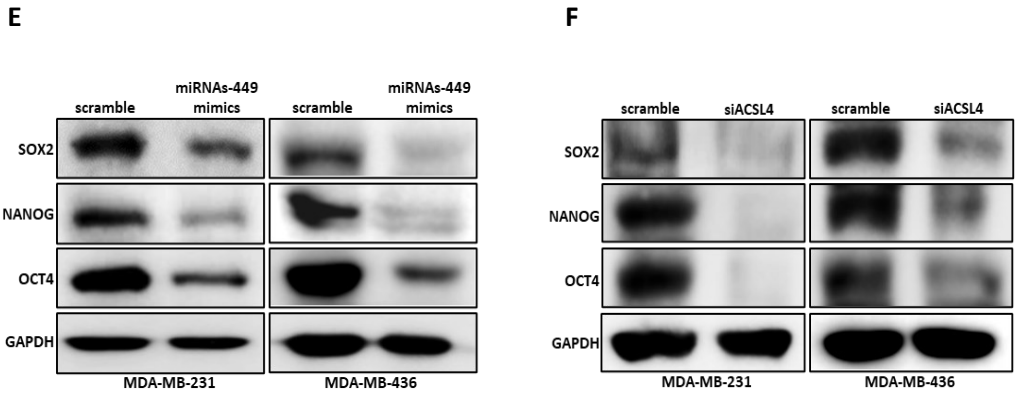

Figure 28: MiRNAs-449 diminish colony formation by loss of stem cell characteristics through ACSL4 downregulation. TNBC cell lines (MDA-MB-231 and MDA-MB-436) were transfected with miRNAs-449 (miRNA-449a, miRNA-449b-5p, and miRNA-449c-5p) mimics or small-interfering (si*RNA*) targeting *ACSL4.* (**A**) Representative images of colony formation assay and (**B**) quantification of the number of colonies after miRNAs-449 mimics transfection. (**C**) Representative images of colony formation assay and (**D**) quantification of the number of colonies after *ACSL4* siRNA transfection. Expression of stem-cell markers (SOX2, Nanog, OCT4) was analyzed by Western blot after (**E**) miRNAs-449 mimics and (**F**) *ACSL4* siRNA transfection. Student T-test was used for statistical analyses for B and D. GAPDH was used as loading control for E and F. **p*<0.05, ***p*<0.01.

4.3 MiRNAs-449 modulate DOX response through ACSL4/ ATP-binding cassette superfamily G member 2 (ABCG2) axis

4.3.1 ACSL4 higher expression is associated with chemotherapy resistance in DOX-resistant cell line and TNBC patients

Based on previous results of our group and literature [251,286], further experiments were performed to analyze the biological role of miRNAs-449 in DOX resistance through *ACSL4* modulation. For that, basal expression of miRNAs-449 and ACSL4 was

first analyzed in DOX-resistant (MDA-MB-231R) and DOX-sensitive cell lines (MDA-MB-231). The results showed a significantly lower expression of miRNAs-449 (p=0.0001 for miRNA-449a, p<0.0001 for miRNA-449b-5p, and p=0.0050 for miRNA-449c-5p) (**Figure 29A**) but higher expression of *ACSL4* (p<0.0001) (**Figure 29B**) in DOX-resistant compared to parental cell line. This latter was also confirmed at the protein level (**Figure 29C**).

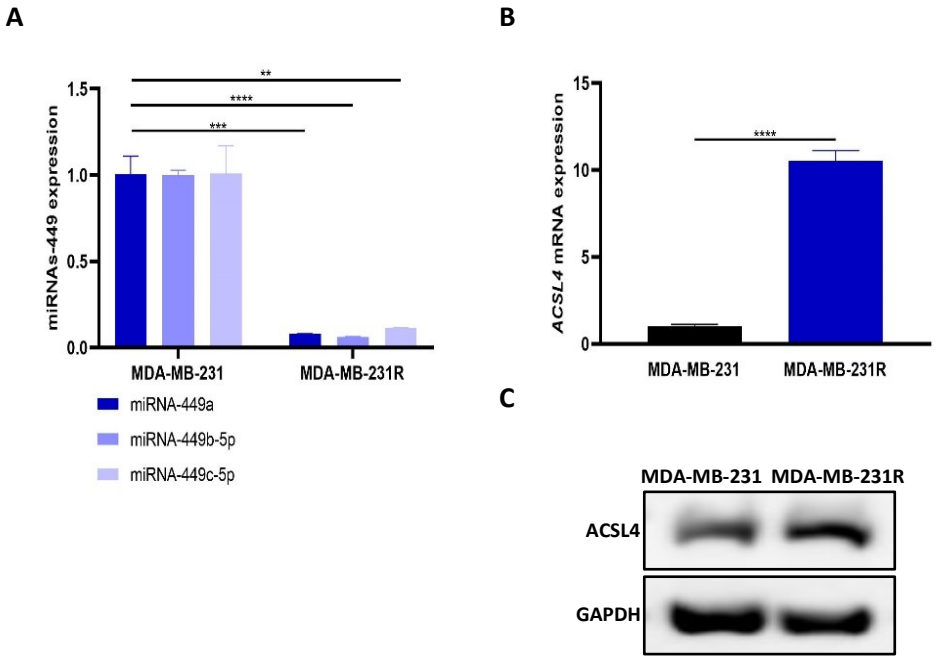

Figure 29: MiRNA-449 family and ACSL4 are lower and higher expressed, respectively, in DOX-resistant compared to the parental cell line. (**A**) MiRNA-449 family (miRNA-449a, miRNA-449b-5p, and miRNA-449c-5p) expression was analyzed by RT-qPCR in DOX-sensitive (MDA-MB-231) and DOX-resistant (MDA-MB-231) cell lines. ACSL4 expression was analyzed by (**B**) RT-qPCR and (**C**) Western blot in MDA-MB-231 and MDA-MB-231R cell lines. Student T-test was used for statistical analyses for A and B. GAPDH was used as a loading control. **p<0.01, ***p<0.001, ****p<0.0001.

To verify the modulation of the miRNA-449 family by epigenetic mechanisms in this DOX-resistant model, basal expression of HDAC1 and SIRT1 was also assessed. As expected, HDAC1 and SIRT1 were significantly higher expressed in DOX-resistant compared to the parental cell line, both at mRNA (p=0.0003 for *HDAC1* and p<0.0001 for *SIRT1*) (**Figure 30A**) and protein level (**Figure 30B**).

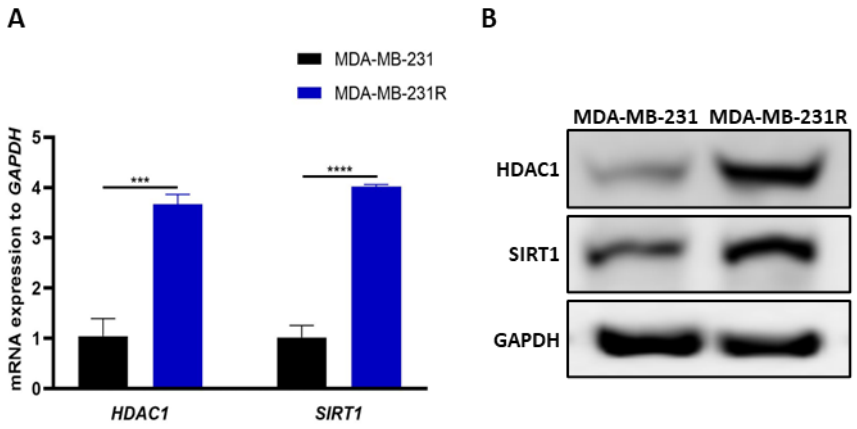

Figure 30: HDAC1 and SIRT1 are overexpressed in DOX-resistant compared to the parental cell line. HDAC1 and SIRT1 expression was analyzed by (**A**) RT-qPCR and (**B**) Western blot in DOX-resistant (MDA-MB-231R) and DOX-sensitive (MDA-MB-231) cell lines. Student T-test was used for statistical analyses for A. GAPDH was used as loading control for B. ***p<0.001, ****p<0.0001.

Furthermore, miRNAs-449 gain-of-function separately was also performed in the DOX-resistant model. The results showed a downregulation of HDAC1 (p=0.0061 for miRNA-449a, p<0.0001 for miRNA-449b-5p, and p=0.0259 for miRNA-449c-5p), SIRT1 (p=0.0202 for miRNA-449, p=0.0048 for miRNA-449b-5p, and p=0.0243 for miRNA-449c-5p) and ACSL4 (p=0.0060 for miRNA-449a, p=0.0263 for miRNA-449b-5p, and p=0.0066 for miRNA-449c-5p) both at mRNA (**Figure 31A, B, D**) and protein level (**Figure 31C, E**). These results suggest that our hypothesis is also fulfilled in the resistant model.

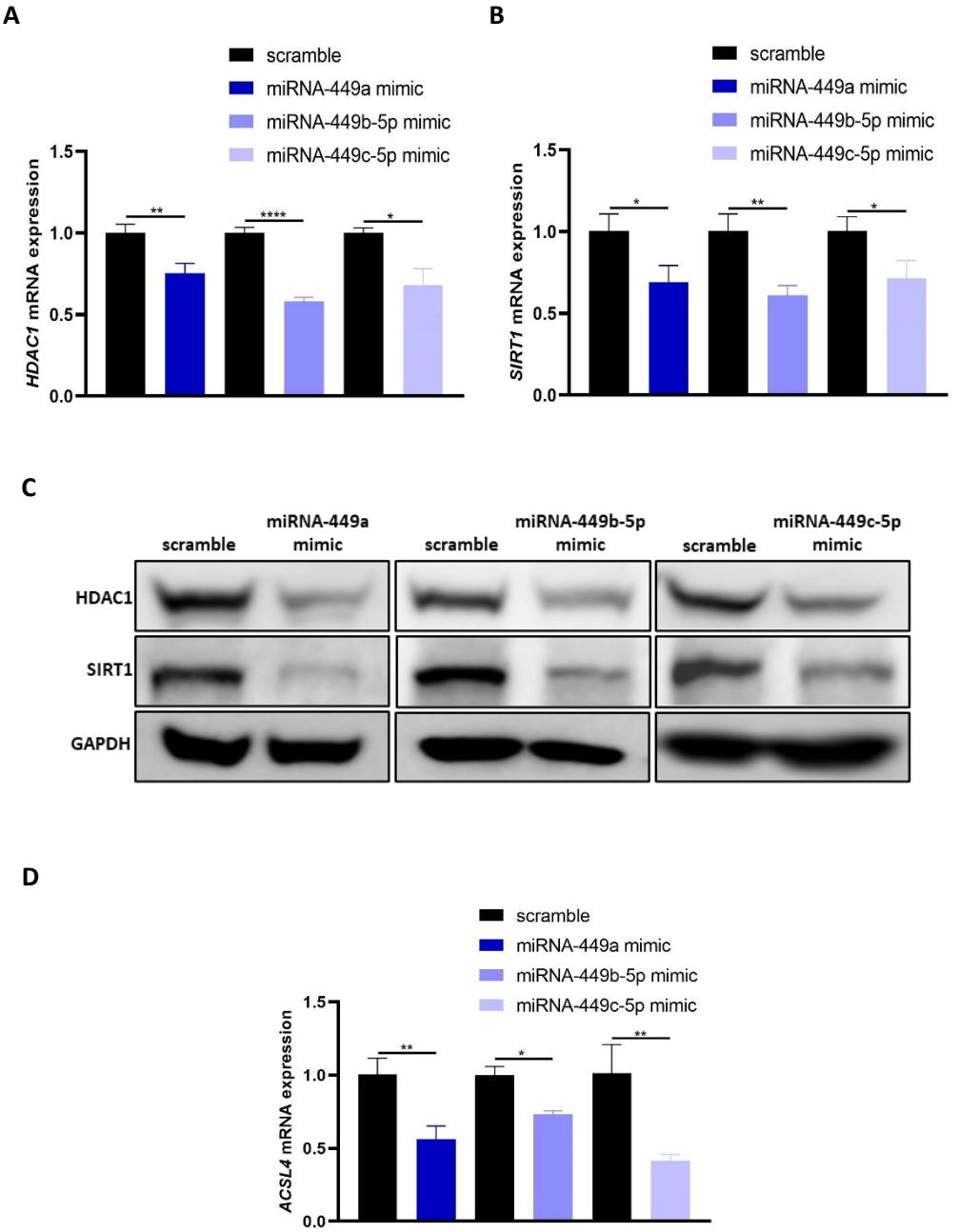
A
scramble
miRNA-449a mimic
miRNA-449b-5p mimic
miRNA-449c-5p mimic
HDAC1 mRNA expression
1.5
1.0
0.5
0.0
**
****
*
B
scramble
miRNA-449a mimic
miRNA-449b-5p mimic
miRNA-449c-5p mimic
SIRT1 mRNA expression
1.5
1.0
0.5
0.0
*
**
*
C
scramble
miRNA-449a mimic
scramble
miRNA-449b-5p mimic
scramble
miRNA-449c-5p mimic
HDAC1
SIRT1
GAPDH
D
scramble
miRNA-449a mimic
miRNA-449b-5p mimic
miRNA-449c-5p mimic
ACSL4 mRNA expression
1.5
1.0
0.5
0.0
**
*
**

E

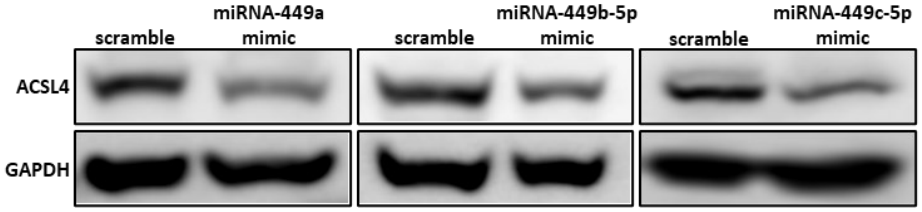

Figure 31: MiRNAs-449a, b-5p, and c-5p overexpression downregulates SIRT1, HDAC1, and ACSL4 expression in DOX-resistant cell line. HDAC1 and SIRT1 expression as analyzed by (**A**, **B**, respectively) RT-qPCR and (**C**) Western blot in DOX-resistant (MDA-MB-231R) cell line after miRNAs-449a, b-5p, and c-5p mimics transfection separately. ACSL4 expression was analyzed by (**D**) RT-qPCR and (**E**) Western blot in the MDA-MB-231R cell line after miRNAs-449a, b-5p, and c-5p mimics transfection separately. Student T-test was used for statistical analyses for A, B, and D. GAPDH was used as loading control for C and E. **p*<0.05, ***p*<0.01, *****p*<0.0001.

In order to assess the clinical relevance of ACSL4, we analyzed its expression in a discovery cohort of TNBC patients who relapse or not after chemotherapy treatment. A significantly higher expression of *ACSL4* was obtained in relapse compared to non-relapse TNBC tissue samples (*p*=0.0003) (**Figure 32A**). The prognostic value was also confirmed by *in silico* analysis. Kaplan-Meier curves showed a significantly lower DFS in TNBC patients (*n*=53) with high expression of *ACSL4* compared to those with lower *ACSL4* expression (HR=3.31, CI=0.93-11.73, *p*=0.05) (**Figure 32B**). These results suggest a possible implication of *ACSL4* in chemotherapy response.

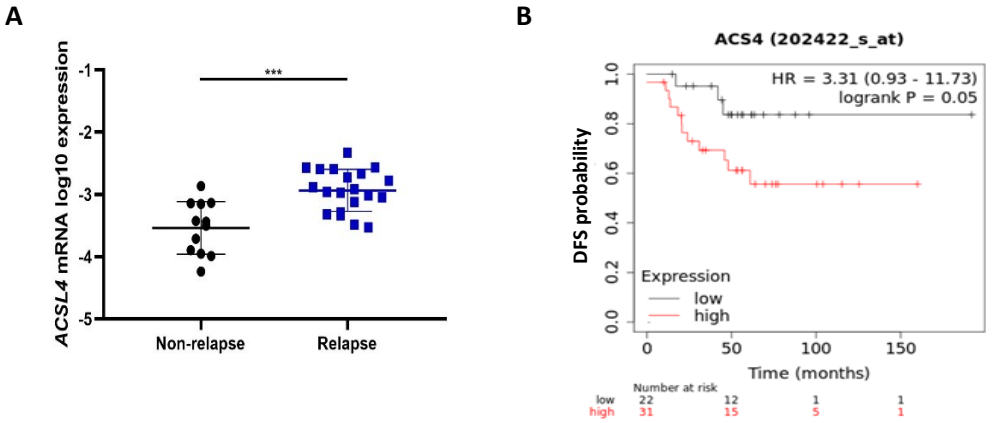

Figure 32: *ACSL4* higher expression is associated with relapse and lower DFS in TNBC. (**A**) *ACSL4* expression was analyzed by RT-qPCR in a discovery cohort of non-relapse (*n*=12) and relapse (*n*=20) TNBC sample patient tissues after chemotherapy treatment. (**B**) Representation of DFS Kaplan Meier curves in TNBC samples (*n*=53) based on an optimal cut-off of *ACSL4* for low (black) and high (red) expression (*p*=0.05). Mann-Whithney test was used for statistical analysis for A. ***$p<0.001$. ACS4: ACSL4.

4.3.2 MiRNAs-449 overexpression sensitizes TNBC cells to DOX through ACSL4 downregulation

A previous study carried out in our laboratory demonstrated that DOX treatment produces a significant induction of miRNAs-449 in DOX-sensitive (MDA-MB-231 and MDA-MB-436), but not in DOX-resistant cells (MDA-MB-231R)[251]. These results were also confirmed in this study (MDA-MB-231: $p=0.0022$ for miRNA-449a, $p<0.0001$ for miRNA-449b-5p, and $p<0.0001$ for miRNA-449c-5p; MDA-MB-436: $p<0.0001$ for miRNA-449a, $p<0.0001$ for miRNA-449b-5p, and $p<0.0001$ for miRNA-449c-5p) (**Figure 33A**). Furthermore, *ACSL4* expression after DOX treatment was also analyzed, and a significant downregulation was observed in DOX-sensitive ($p=0.0263$

for MDA-MB-231 and p=0.0015 for MDA-MB-436), but not in DOX-resistant cells (**Figure 33B**). The same results were obtained at the protein level (**Figure 33C**).

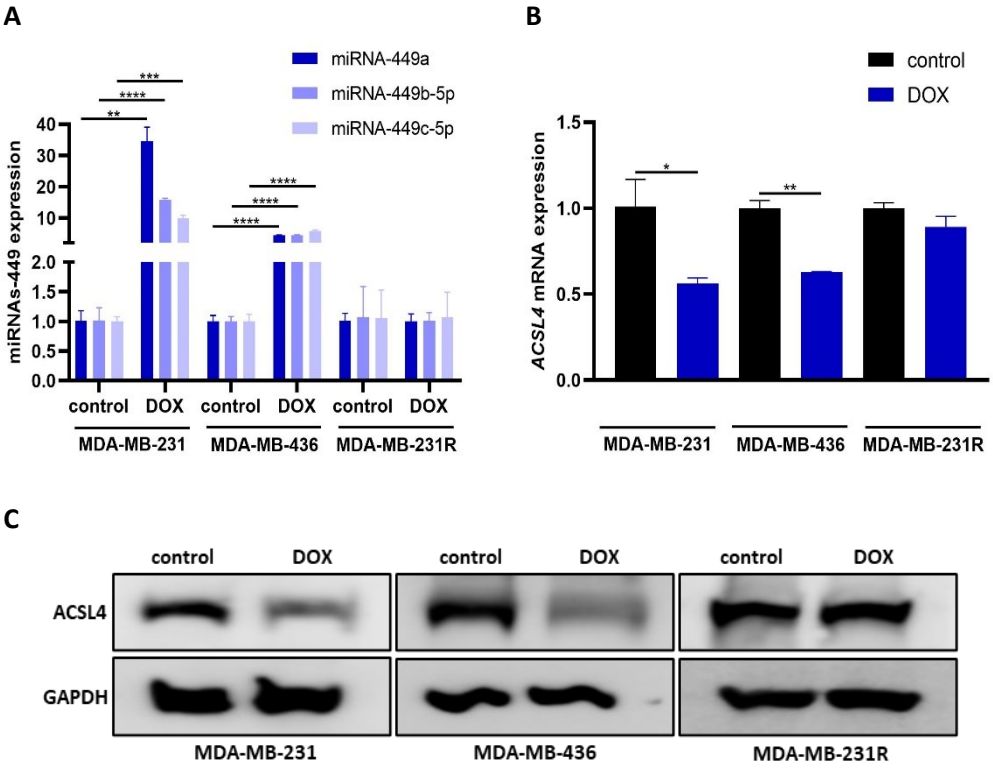

Figure 33: MiRNAs-449 and ACSL4 are up and downregulated, respectively, after DOX treatment in DOX-sensitive but not in DOX-resistant cells. (**A**) MiRNA-449 family (miRNA-449a, miRNA-449b-5p, and miRNA-449c-5p) expression was analyzed by RT-qPCR in DOX-sensitive (MDA-MB-231 and MDA-MB-436) and DOX-resistant (MDA-MB-231R) cell lines after 1 µM 48h of DOX treatment. ACSL4 expression was analyzed by (**B**) RT-qPCR and (**C**) Western blot in DOX-sensitive (MDA-MB-231 and MDA-MB-436) and DOX-resistant (MDA-MB-231R) cell lines after 1 µM 48h of DOX treatment. Student T-test was used for statistical analyses for A and B. GAPDH was used as loading control for C. *p<0.05, **p<0.01, ***p<0.001, ****p<0.0001.

To further explore the function of miRNAs-449 in the modulation of chemotherapy response, cell cytotoxicity was analyzed after miRNAs-449 overexpression or *ACSL4* knockdown and exposure to different doses of DOX. MiRNAs-449 overexpression decreased IC_{50} value from 1.20 µM to 0.75 µM for MDA-MB-231 (p=0.001), from 2.86 to 1.02 for MDA-MB-436 (p=0.0002), and from 8.23 µM to 0.048 µM for MDA-MB-231R (p<0.0001) (**Figure 34A**). Similar results were obtained after *ACSL4* knockdown, thus diminishing IC_{50} value from 1.75 µM to 0.97 µM from MDA-MB-231 (p<0.0001), from 2.35 to 0.13 for MDA-MB-436 (p<0.0001), and from 4.31 µM to 1.29 µM for MDA-MB-231R (p=0.0002) (**Figure 34B**). An apoptosis assay was also performed for the same conditions. Both miRNAs-449 overexpression and *ACSL4* knockdown alone induced apoptosis in MDA-MB-231 (miRNAs-449: p=0.0006, siACSL4: p<0.0001), MDA-MB-436 (miRNAs-449: p<0.0001, siACSL4: p=0.0001), and MDA-MB-231R (miRNAs-449: p<0.0001, siACSL4: p<0.0001) cells (**Figure 34C**). Besides, miRNAs-449 overexpression and *ACSL4* knockdown increased DOX-induced apoptosis in MDA-MB-231 (miRNAs-449: p=0.0033, siACSL4: p=0.0010), MDA-MB-436 (miRNAs-449: p=0.0009, siACSL4: p<0.0001), and MDA-MB-231R (miRNAs-449: p=0.0014, siACSL4: p<0.0001) cell lines (**Figure 34D**). These results suggest that the miRNA-449 family increases sensitivity to DOX through ASCL4 downregulation.

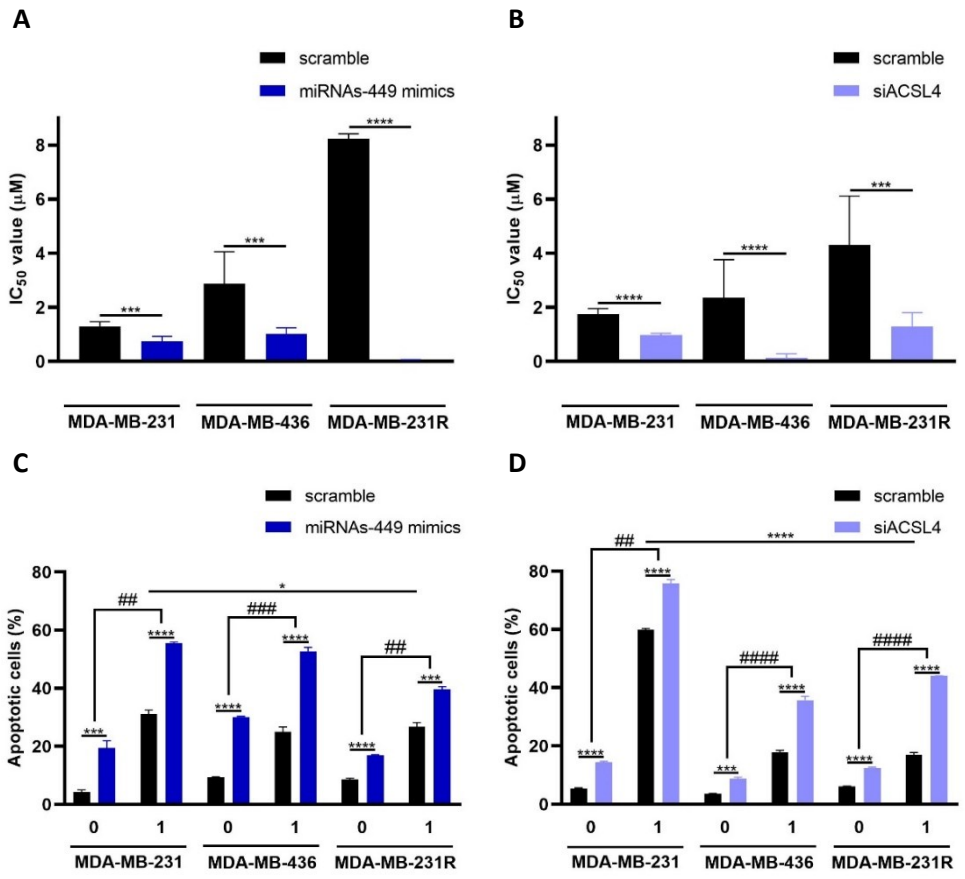

Figure 34: MiRNAs-449 overexpression and *ACSL4* knockdown increase sensitivity to DOX. Cell cytotoxicity was analyzed by WST-1 to determine IC_{50} value. MDA-MB-231, MDA-MB-436, and MDA-MB-231R cell lines were transfected with (**A**) miRNA-449 family (miRNA-449a, miRNA-449b-5p, and miRNA-449c-5p) mimics or (**B**) ACSL4 siRNA and treated or not with different doses of DOX for 48h. Cell apoptosis was evaluated by Annexin V-FITC staining. MDA-MB-231, MDA-MB-436, and MDA-MB-231R cell lines were transfected with (**C**) miRNA-449 family (miRNA-449a, miRNA-449b-5p, and miRNA-449c-5p) mimics or (**D**) ACSL4 siRNA and treated or not with 1 µM 48h of DOX. Student T-test was used for statistical analysis for C and D. **p*<0.05, ***p*<0.01, ****p*<0.001, *****p*<0.0001. # was used for different statistical analyses based on the difference in the percentage of apoptotic cells between scramble and miRNAs-449 mimics conditions, and DOX treatment. ## *p*<0.01, ## *p*<0.001, #### *p*<0.0001.

4.3.3 MiRNAs-449 overexpression increases intracellular DOX accumulation through ACSL4/ABCG2 axis

In order to elucidate the mechanism of action of miRNAs-449/ACSL4 axis modulation of DOX response, a cellular efflux mechanism was investigated. In this sense, the changes in ABCG2 expression were further explored. For this, ABCG2 expression was first analyzed in MDA-MB-231 and MDA-MB-231R cell lines, and *ABCG2* was found statistically upregulated in DOX-resistant compared to the parental cell line (p=0.0183) (**Figure 35A**). The same results were obtained at the protein level (**Figure 35B**). Additionally, to determine ABCG2 modulation by miRNAs-449, TNBC cell lines were transfected with miRNAs-449 mimics or *ACSL4*-specific silencer (siACSL4), and ABCG2 expression was analyzed. The results showed a downregulation of ABCG2 expression after miRNAs-449 overexpression (**Figure 35C**) and *ACSL4* knockdown (**Figure 35D**), thus suggesting a negative and positive regulation of ABCG2 by miRNAs-449 and ACSL4, respectively.

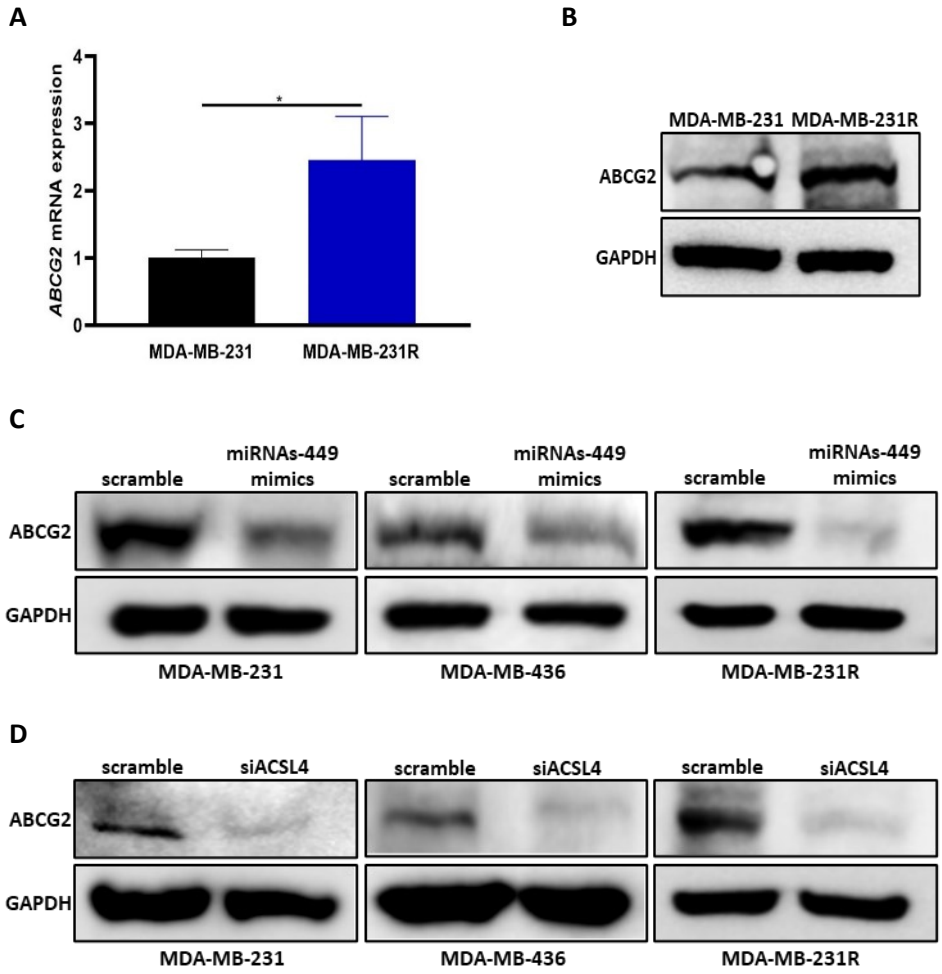

Figure 35: ABCG2 is upregulated in DOX-resistant cells and its expression is downregulated by miRNAs-449 overexpression and *ACSL4* knockdown. ABCG2 expression was analyzed by (**A**) RT-qPCR and (**B**) Western blot in MDA-MB-231 and MDA-MB-231R cell lines. ABCG2 expression was analyzed by Western blot in MDA-MB-231, MDA-MB-436, and MDA-MB-231R cell lines after (**C**) miRNA-449 family (miRNA-449a, miRNA-449b-5p, and miRNA-449c-5p) mimics and (**D**) ACSL4 siRNA transfection. Student T-test was used for statistical analysis for A. GAPDH was used as loading control for B, C, and D. *p<0.05.

Once ABCG2 modulation by miRNAs-449/ACSL4 axis was assessed, a functional assay was performed to evaluate this axis modulation in drug extrusion pumps. For this, intracellular DOX accumulation was analyzed after miRNAs-449 mimics and siACSL4 transfection in TNBC cell lines. Both miRNAs-449 overexpression (p<0.0001 for MDA-MB-231, p<0.0001 for MDA-MB-436, and p<0.0001 for MDA-MB-231R) (**Figure 36A, B**) and *ACSL4* knockdown (p<0.0001 for MDA-MB-231, p<0.0001 for MDA-MB-436, and p<0.0001 for MDA-MB-231R) (**Figure 36C, D**) significantly increased DOX accumulation in cells. These results suggest that overexpression of the miRNA-449 family decreases ABCG2 expression through ACSL4 downregulation, thus increasing the intracellular DOX accumulation due to the lower amount of extruded DOX by this pump.

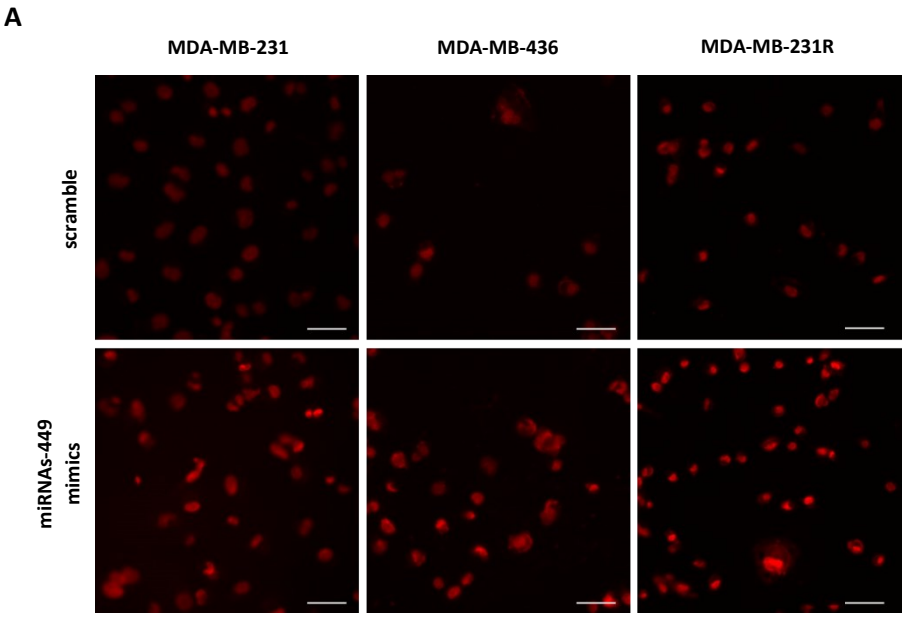

B

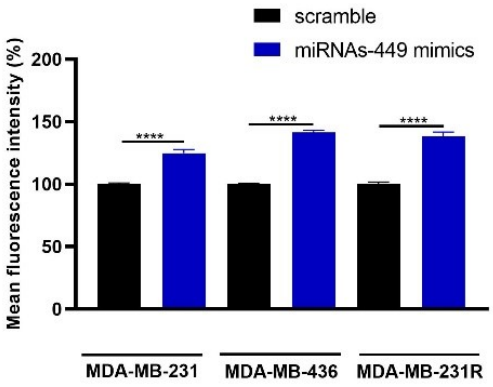
scramble
miRNAs-449 mimics
Mean fluorescence intensity (%)
200
150
100
50
0
****
****
****
MDA-MB-231
MDA-MB-436
MDA-MB-231R

C

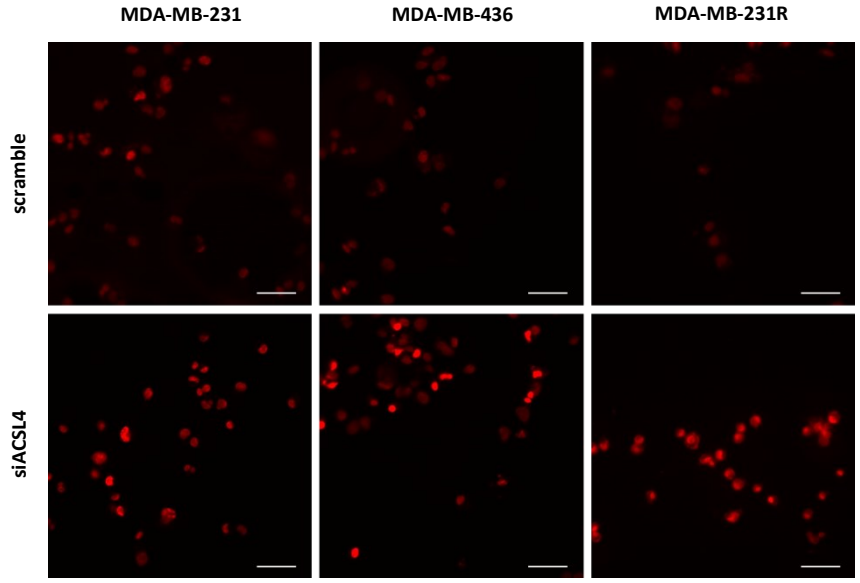
MDA-MB-231
MDA-MB-436
MDA-MB-231R
scramble
siACSL4

D

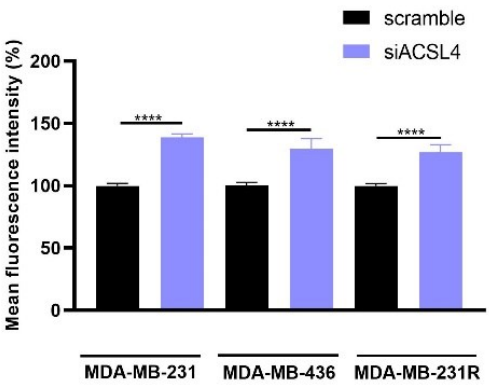

Figure 36: MiRNAs-449 overexpression and *ACSL4* knockdown increase intracellular DOX accumulation. Intracellular DOX accumulation was evaluated by fluorescence microscopy after 5µM 3h incubation of DOX (red) in MDA-MB-231, MDA-MB-436, and MDA-MB-231R cell lines transfected with miRNAs-449 mimics (miRNA-449a, miRNA-449b-5p, and miRNA-449c-5p) or ACSL4 siRNA. (**A**) Representative images (40X magnification) and (**B**) quantification of mean fluorescence intensity for miRNAs-449 mimics transfection. (**C**) Representative images (40X magnification) and (**D**) quantification of mean fluorescence intensity for ACSL4 siRNA transfection. Scale bar for A and C images: 50 µm. Student T-test was used for statistical analyses for B and D. ****p<0.0001.

CHAPTER 5

Discussion

BC prognosis and treatment are mostly based on the molecular markers' expression of each patient by multigenic analysis. Patients' treatment choice is based on the expression of HR and HER2, among other factors. Hormone blockers and inhibitors are used in patients with expression of ER and/or PR, while anti-HER2 drugs are administered to those patients with overexpression of HER2. These targeted therapies are commonly used in combination with chemotherapy. Nevertheless, TNBC is characterized by the lack of expression of these biomarkers, which makes chemotherapy almost the only treatment option in clinical practice[287]. After treatment, some TNBC patients relapse after receiving chemotherapy[288]. Therefore, the study of TNBC is crucial to decipher its molecular and genetic bases and to find new therapeutic tools that help to improve the efficacy of current treatments.

Gene expression studies point to the deregulation of miRNAs in cancer by different mechanisms such as amplifications or deletions of gene locations, transcriptional control changes, epigenetic alterations, and defects in miRNA biogenesis machinery[174,177,187,189]. Regarding its role in cancer, miRNAs can function as tumor suppressors or oncomirs depending on the posttranscriptional regulation of their target mRNAs[173]. Specifically, this study focuses on the role of the miRNA-449 family in TNBC in order to elucidate their involvement in cellular aggressiveness and modulation of DOX response.

In the present study, our results identified the miRNA-449 family to be downregulated in TNBC cell lines and patients compared to controls. In addition, lower miRNAs-449 expression was associated with a worse prognosis, thus suggesting a tumor suppressor role. In the same line, previous studies pointed out a miRNAs-449 downregulation in several cancer types[208,215,244,285], including TNBC[289–291]. Nevertheless, studies in BC are inconclusive and none of them evaluate the expression of miRNA-449c-5p, being our study the first to analyze it.

The miRNA-449 family downregulation can be partially explained by epigenetic alteration of its promoter region. Concretely, our results showed an overexpression of the histone deacetylases HDAC1 and SIRT1, thus explaining lower miRNAs-449 expression levels in TNBC. This histone deacetylation increases ionic interactions between DNA and histones, thus compacting chromatin and preventing transcriptional activation[292–294]. Due to the absence of DNA-binding domain, HDAC1 and SIRT1 promote histone deacetylation by forming repressor complexes with transcription factors such as E2F1[295,296], which is a well-known miRNA-449 family activator [235]. It has been previously described a miRNA-449a upregulation by HDAC1 and SIRT1 knockdown in colorectal cancer, as well as HDAC1 knockdown in hepatocellular carcinoma[215,226]. In this sense, HDACs chemical inhibition is also suggested to induce overexpression of miRNA-449a, miRNA-449b-5p, and miRNA-449c-5p in hepatocellular carcinoma[241,297], and only miRNA-449a in BC and skeletal muscle cells[184,186]. Consistent with the genetic knockdown, our results showed that inhibition of HDAC1 by TSA and SIRT1 by NAM increased miRNAs-449 expression in TNBC cell lines.

Moreover, HDAC1 and SIRT1 are known to be directly regulated by miRNA-449a and miRNA-449b-5p[285,219]. Additionally, our results pointed out an HDAC1 and SIRT1 downregulation by miRNA-449c-5p. Altogether this study provides evidence of a negative feedback loop modulation between the miRNAs-449 and HDAC1/SIRT1, thus contributing to the homeostasis in cells or tumor phenotype. In non-tumoral cells, miRNAs-449 are higher expressed and downregulate HDAC1 and SIRT1, which in turn permits these higher miRNAs expression. In contrast, higher expression of these epigenetic molecules inhibits miRNAs-449 expression by histone deacetylation, thus contributing to the tumoral phenotype.

Taking into account the existence of this negative feedback, artificial expression of this miRNAs family can be suggested as a possible approach to revert the tumor phenotype. Different studies suggest that miRNAs-449 act as tumor suppressors in different cancer types[235,243,298] including BC[289,299], but its mechanism of action is still controversial, and very little is known about its involvement in treatment resistance in the context of BC. In addition, most studies focus on the role of miRNA-449a, but miRNA-449b-5p or miRNA-449c-5p must be further studied. In this sense, we focus on the study of all three.

In order to elucidate which cancer pathways are modulated by miRNAs-449, bioinformatic analyses were performed and fatty acid metabolism was predicted to be regulated by this family of miRNAs. This is consistent with the fact that cancer cells have an altered lipid metabolism based on a high rate of synthesis and oxidation of fatty acids, to generate energy and increase the macromolecular biosynthesis necessary to support tumorigenesis and cancer progression[300]. Several studies pointed out that increased lipogenesis in cancer is due to a higher activity of enzymes involved in fatty acid activation, which is a prerequisite for the use of fatty acids in lipid metabolic pathways[301]. In this sense, bioinformatic analyses predicted that fatty acid metabolism interaction was through *FASN, ACACA,* and *ACSL4* genes. FASN and ACACA are known to be positively correlated with HER2-overexpressing tumors[302–304], while ACSL4 has been highly expressed in ER, PR, HER2, and androgen receptor-negative tumors. It is known that the promoter region of *ACSL4* contains a binding region for ERα and androgen receptor, although the reason for this inverse correlation between ACSL4 and HR/HER2 expression is poorly understood[305–307]. Based on this data, further experiments of this thesis focused on the relationship of miRNAs-449 and ACSL4 in TNBC.

ACSL4 is an enzyme that catalyzes the activation of long-chain fatty acids by esterification with coenzyme A, with arachidonic acid and eicosapentaenoic acid as substrate preferences[308]. Previous studies confirmed its association with aggressiveness in BC [305,309–311]. However, the interaction between ACSL4 and miRNAs-449 has not been studied before.

Our results showed an inverse correlation between miRNAs-449 and ACSL4 expression in TNBC cell lines and patients, and proved for the first time that miRNA-449a and miRNA-449b-5p inhibit ACSL4 expression through direct interaction with *ACSL4* 3'UTR. Despite there being no direct interaction between miRNA-449c-5p and *ACSL4* 3'UTR, we confirmed that the overexpression of the miRNA inhibits ACSL4 expression in TNBC cells, which is attributable to an indirect mechanism mediated by secondary molecules. Our results are in agreement with other studies that revealed different binding specificities between miRNA-449a, miRNA-449b-5p, and miRNA-449c-5p[241].

Our study showed a lower OS associated with lower miRNA-449 family expression in TNBC. In the same trend, lower miRNA-449a expression has been previously correlated with worse prognosis, advanced stages and lymph node metastasis in non-small cell lung cancer, colorectal cancer and BC, among others[244,312,313]. Besides, the miRNA-449 family is known to inhibit cell proliferation, migration, invasion, and to induce cell cycle arrest and apoptosis through multiple gene modulation in several cancer types[203,205,209,212,214,216,219,220]. In this study, we intend to elucidate miRNAs-449 implication in cancer progression through *ACSL4* targeting. In line with this, our results showed a higher *ACSL4* expression in TNBC cell lines and patients when compared to controls, and its expression was associated with lower DFS. However, the prognostic role of ACSL4 in previous literature is controversial. On the one hand, some studies support our results, as higher *ACSL4* expression has been related to

lower OS, DFS, and advanced stages of hepatocellular carcinoma. Furthermore, higher proliferation rates, migration capacity, and colony formation, have been observed upon *ACSL4* overexpression in hepatocellular carcinoma and BC[314,315]. On the other hand, other studies correlate higher *ACSL4* expression with better OS, RFS, and DFS, in lung adenocarcinoma, renal cell carcinoma, and colorectal cancer, among others[316–319], so a tumor-specific dual role is hypothesized. Based on our results, this study suggests an oncogenic role for ACSL4 in TNBC.

In the present study, both *ACSL4* knockdown and miRNAs-449 overexpression inhibited cell proliferation, migration by diminishing the ability to undergo the EMT process, and colony formation. These results support the previous ones and emphasize the role of miRNAs-449 as tumor suppressors, and the oncogenic role of ACSL4. Different mechanisms of action have been proposed for aggressiveness modulation by ACSL4. It is known that once arachidonic acid is activated, it is released into the mitochondria and processed by 5-lipooxygenase to form lipoxygenase metabolites. These metabolites are known to be implicated in cyclooxygenase-2 upregulation, which produces prostaglandin E2[309,320]. Conversely, the lipoxygenase metabolites also activate mTORC2, which activates AKT pathway [311]. Both pathways (prostaglandins and AKT) are well established as positive cancer aggressiveness modulators[321–325]. In addition, ACSL4 overexpression is suggested to promote cancer aggressiveness through c-myc stabilization in hepatocellular carcinoma[314]. Altogether our results suggest that miRNAs-449 inhibit BC progression through *ACSL4* downregulation in TNBC.

Despite the importance of studying the microRNAs implication in cancer progression, it is also essential to understand their implication in treatment response. Nevertheless, all previous studies focus only on miRNA-449a. MiRNA-449a overexpression is known to sensitize to ionizing radiation in prostate and lung

cancer, cisplatin in ovarian cancer, and tamoxifen and olaparib in BC[217,225,236,239,250]. Previous work carried out by our group evidenced that miRNA-449 family overexpression sensitizes to DOX through modulation of cell cycle factors in TNBC[251]. Given their multiple targets and their relationship with proliferative processes, this study deeps into the knowledge of the role of miRNAs-449 in modulating DOX response through *ACSL4* targeting. Regarding ACSL4, its knockdown has been associated with cisplatin, paclitaxel and DOX sensitivity in TNBC, and docetaxel sensitivity in prostate cancer[286,315,326]. In addition, *ACSL4* overexpression in the MCF7 cell line increased etoposide and tamoxifen resistance, while *ACSL4* overexpression in the SKBR3 cell line increased lapatinib resistance[305]. In contrast to this, *ACSL4* knockdown expression increased sorafenib resistance in hepatocellular carcinoma[327].

In this study, we observed that DOX treatment increased miRNA-449 family and decreased ACSL4 expression in DOX-sensitive, but not in DOX-resistant cell lines. E2F1 and P53 are two well-known transcription factors that are activated upon DNA-damage response as produced by DOX treatment[328–330]. MiRNA-34a is known to be upregulated upon P53 activation, and due to its higher structural similarity with the miRNA-449 family, we hypothesized that the same effect could be observed in miRNAs-449. However, our results evidenced an upregulation of miRNAs-449 after DOX treatment in DOX-sensitive cells, both in P53 wild-type and P53-deficient cell line, thus suggesting a miRNAs-449 overexpression in a P53-independent but E2F1-responsive manner, as suggested by other studies[235,219,]. In the case of DOX-resistant cells, E2F1 activation is not induced[251], which explains the lack of changes in the expression of the miRNA-449 family.

In addition, miRNAs-449 were also less expressed in DOX-resistant than in parental cells. Inversely, ACSL4 was overexpressed in DOX-resistant cells and patients who

relapsed after DOX-containing chemotherapy treatment, and its high expression was associated with worse prognosis. Both miRNAs-449 overexpression and *ACSL4* knockdown decreased DOX IC_{50} value and increased DOX-induced apoptosis. These results suggest that overexpression of miRNAs-449 sensitize TNBC cells to DOX through *ACSL4* downregulation.

The role of ACSL4 and its relationship with fatty acid metabolism has been extensively studied, although its role in chemotherapy resistance is not as evident. Therefore, we aim to elucidate this mechanism of action. In this context, ACSL4 overexpression is suggested to positively regulate mTORC/ABCG2 axis in BC[286]. ABCG2 physiological function is to maintain homeostasis of different endogenous molecules by mediating its efflux. However, its expression has been increased in different pathophysiological situations such as cancer, being implicated in cancer progression and drug resistance[331]. ABCG2 is one of the most well-known molecules involved in drug resistance, as it mediates efflux of several drugs including DOX[332,333]. Our results pointed out for the first time a drug extrusion pump modulation by miRNAs-449. Concretely, we observed that miRNAs-449 overexpression negatively modulated ABCG2 expression through ACSL4 downregulation, thus increasing DOX accumulation inside the cells and giving sensitivity to DOX.

In conclusion, this study evidences an epigenetic repression of miRNAs-449 by HDAC1 and SIRT1 histone deacetylation of its promoter region, and suggests a BC aggressiveness and DOX sensitivity upon miRNAs-449 overexpression through ACSL4 targeting in TNBC (**figure 37**). Thus, miRNAs-449 are suggested to be promising candidates for future therapeutic approaches. As miRNAs administered alone have limitations of bioavailability, intracellular activity, and side effects, future therapeutic approaches in combination with viral and non-viral vectors can be proposed[269]. Combination therapy with miRNAs-449 mimics and/or ACSL4 inhibitors

could be also studied, as ACSL4 inhibitor PRGL493 is demonstrated to block tumor growth in both prostate and BC animal models and has emerged as a potential molecule for clinical practice[315]. Further studies are needed to confirm these miRNAs-449 therapeutic potential.

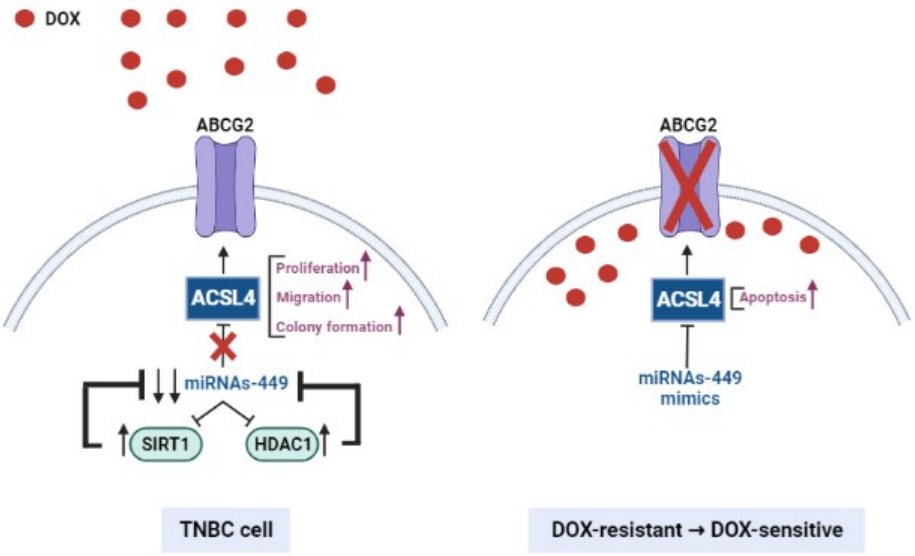

Figure 37: Proposed model of miRNAs-449 implication in TNBC aggressiveness and DOX response. MiRNAs-449 are downregulated in TNBC through a negative feedback loop with SIRT1 and HDAC1, leading to ACSL4 overexpression that promotes cell proliferation, migration and colony formation. Moreover, ACSL4 increases ABCG2 expression, thus diminishing intracellular DOX concentration and promoting DOX resistance. MiRNAs-449 overexpression downregulates the ACSL4/ABCG2 axis and sensitize DOX-resistant cells to DOX. Created with BioRender. TNBC: triple-negative breast cancer; DOX: doxorubicin; SIRT1: Sirtuin 1; HDAC1: Histone deacetylase 1; ACSL4: Acyl-CoA Synthetase Long-Chain Family Member 4; ABCG2: ATP-binding cassette superfamily G member 2.

CHAPTER 6 |

Conclusions

Based on the results presented, the conclusions of this study are as follows:

1. MiRNA-449 family is downregulated in TNBC cell lines and patients, and its lower expression is associated with lower OS.
2. The miRNA-449 family maintains a negative feedback loop modulation with HDAC1 and SIRT1. These histone deacetylases are overexpressed in TNBC and inhibit the miRNAs-449 expression by histone deacetylation of its promoter region.
3. *In silico* analyses predict a higher interaction of miRNAs-449 with fatty acid metabolism pathways through *ACSL4* targeting. ACSL4 is inversely correlated with miRNAs-449 in TNBC cell lines and patients, and is evidenced as a novel direct target of miRNA-449a and miRNA-449b-5p, but indirect target of miRNA-449c-5p by gene interaction studies.
4. MiRNAs-449 overexpression produces an ACSL4 downregulation and inhibits TNBC aggressiveness through diminishing cell proliferation, migration, and colony formation.
5. MiRNAs-449 overexpression sensitizes TNBC cell lines to DOX through ACSL4/ABCG2 axis downregulation, which in turn increases the intracellular DOX accumulation and produces cell apoptosis.

CHAPTER 7 |

Bibliography

1. Sung, H. *et al.* Global Cancer Statistics 2020: GLOBOCAN Estimates of Incidence and Mortality Worldwide for 36 Cancers in 185 Countries. *CA. Cancer J. Clin.* **71**, 209–249 (2021).

2. Siegel, R. L., Miller, K. D., Wagle, N. S. & Jemal, A. Cancer statistics, 2023. *CA. Cancer J. Clin.* **73**, 17–48 (2023).

3. Rycaj, Kiera and Tang, D. Cell-of-Origin of Cancer versus Cancer Stem Cells: Assays and Interpretation. *Cancer Res.* **75**, 4003–4011 (2015).

4. Hanahan, D. Hallmarks of Cancer: New Dimensions. *Cancer Discov.* **12**, 31–46 (2022).

5. Miao, H. *et al.* Incidence and outcome of male breast cancer: An international population-based study. *J. Clin. Oncol.* **29**, 4381–4386 (2011).

6. Momenimovahed, Z. & Salehiniya, H. Epidemiological characteristics of and risk factors for breast cancer in the world. *Breast Cancer Targets Ther.* **11**, 151–164 (2019).

7. Siegel, R. L., Miller, K. D., Fuchs, H. E. & Jemal, A. Cancer statistics, 2022. *CA. Cancer J. Clin.* **72**, 7–33 (2022).

8. Soerjomataram, I. & Bray, F. Planning for tomorrow: global cancer incidence and the role of prevention 2020–2070. *Nat. Rev. Clin. Oncol.* **18**, 663–672 (2021).

9. Youlden, D. R., Cramb, S. M., Yip, C. H. & Baade, P. D. Incidence and mortality of female breast cancer in the Asia-Pacific region. *Cancer Biol. Med.* **11**, 101–115 (2014).

10. Huang, J. *et al.* Global incidence and mortality of breast cancer: a trend analysis. *Aging (Albany. NY).* **13**, 5748–5803 (2021).

11. Balmaña, J., Díez, O., Rubio, I. T. & Cardoso, F. BRCA in breast cancer: ESMO clinical practice guidelines. *Ann. Oncol.* **22**, 31–34 (2011).

12. Chang-Claude, J. *et al.* Age at menarche and menopause and breast cancer risk in the International BRCA1/2 Carrier Cohort Study. *Cancer Epidemiol. Biomarkers Prev.* **16**, 740–746 (2007).

13. Nattinger, A. B. & Mitchell, J. L. Breast cancer screening and prevention. *Ann. Intern. Med.* **164**, ITC81–ITC94 (2016).

14. Zhu, Y. *et al.* BRCA mutations and survival in breast cancer: an updated

systematic review and meta-analysis. *Oncotarget* **7**, 70113–70127 (2016).

15. Liu, M., Xie, F., Liu, M., Zhang, Y. & Wang, S. Association between BRCA mutational status and survival in patients with breast cancer: a systematic review and meta-analysis. *Breast Cancer Res. Treat.* **186**, 591–605 (2021).

16. Miller, K. D. *et al.* Cancer statistics for adolescents and young adults, 2020. *CA. Cancer J. Clin.* **70**, 443–459 (2020).

17. Murphy, B. L., Day, C. N., Hoskin, T. L., Habermann, E. B. & Boughey, J. C. Adolescents and Young Adults with Breast Cancer have More Aggressive Disease and Treatment Than Patients in Their Forties. *Ann. Surg. Oncol.* **26**, 3920–3930 (2019).

18. Cathcart-Rake, E. J., Ruddy, K. J., Bleyer, A. & Johnson, R. H. Breast Cancer in Adolescent and Young Adult Women Under the Age of 40 Years. *JCO Oncol. Pract.* **17**, 305–313 (2021).

19. Flaherty, D. C., Bawa, R., Burton, C. & Goldfarb, M. Breast Cancer in Male Adolescents and Young Adults. *Ann. Surg. Oncol.* **24**, 84–90 (2017).

20. Andersen, S. W. *et al.* Reproductive windows, genetic loci, and breast cancer risk. *Ann. Epidemiol.* **24**, 376–382 (2014).

21. Hamajima, N. *et al.* Menarche, menopause, and breast cancer risk: Individual participant meta-analysis, including 118 964 women with breast cancer from 117 epidemiological studies. *Lancet Oncol.* **13**, 1141–1151 (2012).

22. Wang, A. T., Vachon, C. M., Brandt, K. R. & Ghosh, K. Breast density and breast cancer risk: A practical review. *Mayo Clin. Proc.* **89**, 548–557 (2014).

23. Advani, S. M. *et al.* Association of Breast Density with Breast Cancer Risk among Women Aged 65 Years or Older by Age Group and Body Mass Index. *JAMA Netw. Open* **4**, e2122810 (2021).

24. Beral, V., Bull, D., Doll, R., Peto, R. & Reeves, G. Breast cancer and breastfeeding: Collaborative reanalysis of individual data from 47 epidemiological studies in 30 countries, including 50 302 women with breast cancer and 96 973 women without the disease. *Lancet* **360**, 187–195 (2002).

25. Husby, A., Wohlfahrt, J., Øyen, N. & Melbye, M. Pregnancy duration and breast cancer risk. *Nat. Commun.* **9**, 4255 (2018).

26. Unar-Munguía, M., Torres-Mejía, G., Colchero, M. A. & González De Cosío, T.

Breastfeeding Mode and Risk of Breast Cancer: A Dose-Response Meta-Analysis. *J. Hum. Lact.* **33**, 422–434 (2017).

27. Zhou, Y. *et al.* Association between breastfeeding and breast cancer risk: Evidence from a meta-analysis. *Breastfeed. Med.* **10**, 175–182 (2015).

28. Chlebowski, R. T. *et al.* Association of Menopausal Hormone Therapy with Breast Cancer Incidence and Mortality during Long-term Follow-up of the Women's Health Initiative Randomized Clinical Trials. *JAMA - J. Am. Med. Assoc.* **324**, 369–380 (2020).

29. Winters, S., Martin, C., Murphy, D. & Shokar, N. K. *Breast Cancer Epidemiology, Prevention, and Screening*. *Progress in Molecular Biology and Translational Science* vol. 151 (Elsevier Inc., 2017).

30. Santen, R. J. *et al.* Underlying breast cancer risk and menopausal hormone therapy. *J. Clin. Endocrinol. Metab.* **105**, dgaa073 (2020).

31. Mørch, L. S. *et al.* Contemporary Hormonal Contraception and the Risk of Breast Cancer. *N. Engl. J. Med.* **377**, 2228–2239 (2017).

32. Lin, F. R., Niparko, J. K. & Ferrucci, and L. Recent oral contraceptive use by formulation and breast cancer risk among women 20–49 years of age. *Cancer Res.* **23**, 4078–89 (2014).

33. Lovett, J. L. *et al.* Oral contraceptives cause evolutionarily novel increases in hormone exposure. *Evol. Med. Public Heal.* **2017**, 97–108 (2017).

34. Calle, E. E. *et al.* Breast cancer and hormonal contraceptives: Collaborative reanalysis of individual data on 53 297 women with breast cancer and 100 239 women without breast cancer from 54 epidemiological studies. *Lancet* **347**, 1713–1727 (1996).

35. Chan, D. S. M. *et al.* Body mass index and survival in women with breast cancer—systematic literature review and meta-analysis of 82 follow-up studies. *Ann. Oncol.* **25**, 1901–1914 (2014).

36. Bergstrom, A., Pisani, P., Tenet, V., Wolk, A. & Adami, H. O. Erratum: Overweight as an avoidable cause of cancer in Europe (International Journal of Cancer (2001) 91 (421-430)). *Int. J. Cancer* **91**, 421–430 (2001).

37. Gravena, A. A. F. *et al.* The obesity and the risk of breast cancer among pre and postmenopausal women. *Asian Pacific J. Cancer Prev.* **19**, 2429–2436 (2018).

38. Iyengar, N. M. *et al.* Association of Body Fat and Risk of Breast Cancer in Postmenopausal Women with Normal Body Mass Index: A Secondary Analysis of a Randomized Clinical Trial and Observational Study. *JAMA Oncol.* **5**, 155–163 (2019).

39. Bagnardi, V. *et al.* Alcohol consumption and site-specific cancer risk: A comprehensive dose-response meta-analysis. *Br. J. Cancer* **112**, 580–593 (2015).

40. Choi, Y. J., Myung, S. K. & Lee, J. H. Light alcohol drinking and risk of cancer: A meta-analysis of cohort studies. *Cancer Res. Treat.* **50**, 474–487 (2018).

41. Bérubé, S., Lemieux, J., Moore, L., Maunsell, E. & Brisson, J. Smoking at time of diagnosis and breast cancer-specific survival: New findings and systematic review with meta-analysis. *Breast Cancer Res.* **16**, R42 (2014).

42. Shield, K. D., Soerjomataram, I. & Rehm, J. Alcohol Use and Breast Cancer: A Critical Review. *Alcohol. Clin. Exp. Res.* **40**, 1166–1181 (2016).

43. Duan, W., Li, S., Meng, X., Sun, Y. & Jia, C. Smoking and survival of breast cancer patients: A meta-analysis of cohort studies. *The Breast* **33**, 117–124 (2017).

44. Kazemi, A. *et al.* Intake of various food groups and risk of breast cancer: A systematic review and dose-response meta-analysis of prospective studies. *Adv. Nutr.* **12**, 809–849 (2021).

45. Schwingshackl, L., Schwedhelm, C., Galbete, C. & Hoffmann, G. Adherence to mediterranean diet and risk of cancer: An updated systematic review and meta-analysis. *Nutrients* **9**, 1063 (2017).

46. Kyu, H. H. *et al.* Physical activity and risk of breast cancer, colon cancer, diabetes, ischemic heart disease, and ischemic stroke events: Systematic review and dose-response meta-analysis for the Global Burden of Disease Study 2013. *BMJ* **354**, i3857 (2016).

47. Pizot, C. *et al.* Physical activity, hormone replacement therapy and breast cancer risk: A meta-analysis of prospective studies. *Eur. J. Cancer* **52**, 138–154 (2016).

48. DeSantis, C. E. *et al.* Breast cancer statistics, 2019. *CA. Cancer J. Clin.* **69**, 438–451 (2019).

49. Myers, E. R. *et al.* Benefits and harms of breast cancer screening: A systematic

review. *JAMA - J. Am. Med. Assoc.* **314**, 1615–1634 (2015).

50. Park, H. L. *et al.* Mammography screening and mortality by risk status in the California teachers study. *BMC Cancer* **21**, 1341 (2021).

51. Autier, P., Koechlin, A., Smans, M., Vatten, L. & Boniol, M. Mammography screening and breast cancer mortality in Sweden. *J. Natl. Cancer Inst.* **104**, 1080–1093 (2012).

52. Hubbard, R. et. a. Cumulative probability of false-positive recall or biopsy recommendation after 10 years of screening mammography. *Ann. Intern. Med.* **155**, 481–492 (2011).

53. Bulliard, J. L. *et al.* Breast cancer screening and overdiagnosis. *Int. J. Cancer* **149**, 846–853 (2021).

54. Canelo-Aybar, C. *et al.* Benefits and harms of breast cancer mammography screening for women at average risk of breast cancer: A systematic review for the European Commission Initiative on Breast Cancer. *J. Med. Screen.* **28**, 389–404 (2021).

55. Jørgensen, K. J. & Gøtzsche, P. C. Overdiagnosis in publicly organised mammography screening programmes: Systematic review of incidence trends. *BMJ* **339**, 206–209 (2009).

56. Mascara, M. & Constantinou, C. Global Perceptions of Women on Breast Cancer and Barriers to Screening. *Curr. Oncol. Rep.* **23**, 74 (2021).

57. Sardanelli, F. et. a. Multicenter Surveillance of Women at High Genetic Breast Cancer Risk Using Mammography, Ultrasonography, and Contrast-Enhanced Magnetic Resonance Imaging (the High Breast Cancer Risk Italian 1 Study). *Invest Radiol* **46**, 94–105 (2011).

58. Cardoso, F. *et al.* Early breast cancer: ESMO Clinical Practice Guidelines for diagnosis, treatment and follow-up. *Ann. Oncol.* **30**, 1194–1220 (2019).

59. Monticciolo, D. L. *et al.* Breast Cancer Screening in Women at Higher-Than-Average Risk: Recommendations From the ACR. *J. Am. Coll. Radiol.* **15**, 408–414 (2018).

60. Ginsburg, O. *et al.* Breast cancer early detection: a phased approach to implementation. *Cancer* **126**, 2379–2393 (2020).

61. Makki, J. Diversity of breast carcinoma: Histological subtypes and clinical

relevance. *Clin. Med. Insights Pathol.* **8**, 23–31 (2015).

62. Nascimento, R. G. do & Otoni, K. M. Histological and molecular classification of breast cancer: what do we know? *Mastology* **30**, e20200024 (2020).

63. Malhotra, G. K., Zhao, X., Band, H. & Band, V. Histological, molecular and functional subtypes of breast cancers. *Cancer Biol. Ther.* **10**, 955–960 (2010).

64. Eheman, C. R. *et al.* The changing incidence of in situ and invasive ductal and lobular breast carcinomas: United States, 1999-2004. *Cancer Epidemiol. Biomarkers Prev.* **18**, 1763–1769 (2009).

65. Forae, G., Nwachokor, F. & Igbe, A. Histopathological profile of breast cancer in an African population. *Ann. Med. Health Sci. Res.* **4**, 369–373 (2014).

66. Tadros, A. B., Wen, H. Y. & Morrow, M. Breast Cancers of Special Histologic Subtypes Are Biologically Diverse. *Ann. Surg. Oncol.* **25**, 3158–3164 (2018).

67. Kurundkar, A. *et al.* Comparison of AJCC Anatomic and Clinical Prognostic Stage Groups in Breast Cancer: Analysis of 3322 Cases From a Single Institution. *Clin. Breast Cancer* **18**, e1347–e1352 (2018).

68. Park, Y. H. *et al.* Clinical relevance of TNM staging system according to breast cancer subtypes. *Ann. Oncol.* **22**, 1554–1560 (2011).

69. Giuliano, A. E. et. a. Breast Cancer—Major Changes in the American Joint Committee on Cancer Eighth Edition Cancer Staging Manual. *CA CANCER J CLIN* **67**, 290–303 (2017).

70. Hortobagyi, G. N., Edge, S. B. & Giuliano, A. New and Important Changes in the TNM Staging System for Breast Cancer. *Am. Soc. Clin. Oncol. Educ. B.* 457–467 (2018) doi:10.1200/edbk_201313.

71. Nicolini, A., Ferrari, P. & Duffy, M. J. Prognostic and predictive biomarkers in breast cancer: Past, present and future. *Semin. Cancer Biol.* **52**, 56–73 (2018).

72. Santos, M. *et al.* Value of the nottingham histological grading parameters and nottingham prognostic index in canine mammary carcinoma. *Anticancer Res.* **35**, 4219–4228 (2015).

73. Weiss, A. *et al.* Validation study of the American joint committee on cancer eighth edition prognostic stage compared with the anatomic stage in breast cancer. *JAMA Oncol.* **4**, 203–209 (2018).

74. Mittendorf, E. A. et. a. Bioscore: A staging system for breast cancer patients

that reflects the prognostic significance of underlying tumor biology. *Ann Surg Oncol* **24**, 3502–3509 (2017).

75. Shi, J. *et al.* Prognostic and Predictive Value of the American Joint Committee on Cancer Pathological Prognostic Staging System in Nodal Micrometastatic Breast Cancer. *Front. Oncol.* **10**, 570175 (2020).

76. Goldhirsch, A. *et al.* Strategies for subtypes-dealing with the diversity of breast cancer: Highlights of the St Gallen international expert consensus on the primary therapy of early breast cancer 2011. *Ann. Oncol.* **22**, 1736–1747 (2011).

77. Rakha, E. A. & Green, A. R. Molecular classification of breast cancer: what the pathologist needs to know. *Pathology* **49**, 111–119 (2017).

78. Goldhirsch, A. *et al.* Personalizing the treatment of women with early breast cancer: Highlights of the st gallen international expert consensus on the primary therapy of early breast Cancer 2013. *Ann. Oncol.* **24**, 2206–2223 (2013).

79. Hashmi, A. A. *et al.* Ki67 index in intrinsic breast cancer subtypes and its association with prognostic parameters. *BMC Res. Notes* **12**, 605 (2019).

80. Liang, Q., Ma, D., Gao, R. F. & Yu, K. Da. Effect of Ki-67 Expression Levels and Histological Grade on Breast Cancer Early Relapse in Patients with Different Immunohistochemical-based Subtypes. *Sci. Rep.* **10**, 7648 (2020).

81. Perou, C. M. *et al.* Molecular portraits of human breast tumours. *Nature* **406**, 747–752 (2000).

82. Bernard, P. S. *et al.* Supervised risk predictor of breast cancer based on intrinsic subtypes. *J. Clin. Oncol.* **27**, 1160–1167 (2009).

83. Sorlie, T. et. a. Gene expression patterns of breast carcinomas distinguish tumor subclasses with clinical implications. *PNAS* **98**, 10869–10874 (2001).

84. Herschkowitz, J. I. *et al.* Identification of conserved gene expression features between murine mammary carcinoma models and human breast tumors. *Genome Biol.* **8**, R76 (2007).

85. Prat, A. *et al.* Phenotypic and molecular characterization of the claudin-low intrinsic subtype of breast cancer. *Breast Cancer Res.* **12**, R68 (2010).

86. Yersal, O. & Barutca, S. Biological subtypes of breast cancer: Prognostic and

therapeutic implications. *World J. Clin. Oncol.* **5**, 412–424 (2014).

87. Kennecke, H. *et al.* Metastatic behavior of breast cancer subtypes. *J. Clin. Oncol.* **28**, 3271–3277 (2010).

88. Rouzier, R. *et al.* Breast cancer molecular subtypes respond differently to preoperative chemotherapy. *Clin. Cancer Res.* **11**, 5678–5685 (2005).

89. Prat, A. *et al.* Clinical implications of the intrinsic molecular subtypes of breast cancer. *The Breast* **24**, S26–S35 (2015).

90. Prat, A. & Perou, C. M. Deconstructing the molecular portraits of breast cancer. *Mol. Oncol.* **5**, 5–23 (2011).

91. Rakha, E. A., Reis-Filho, J. S. & Ellis, I. O. Basal-like breast cancer: A critical review. *J. Clin. Oncol.* **26**, 2568–2581 (2008).

92. Naito, Y. & Urasaki, T. Precision medicine in breast cancer. *Chinese Clin. Oncol.* **7**, 29 (2018).

93. Lænkholm, A. V. *et al.* PAM50 risk of recurrence score predicts 10-year distant recurrence in a comprehensive danish cohort of postmenopausal women allocated to 5 years of endocrine therapy for hormone receptor-positive early breast cancer. *J. Clin. Oncol.* **36**, 735–740 (2018).

94. Lænkholm, A. V. *et al.* Population-based Study of Prosigna-PAM50 and Outcome Among Postmenopausal Women With Estrogen Receptor-positive and HER2-negative Operable Invasive Lobular or Ductal Breast Cancer. *Clin. Breast Cancer* **20**, e423–e432 (2020).

95. Yin, L., Duan, J. J., Bian, X. W. & Yu, S. C. Triple-negative breast cancer molecular subtyping and treatment progress. *Breast Cancer Res.* **22**, 61 (2020).

96. Fisusi, F. A. & Akala, E. O. Drug Combinations in Breast Cancer Therapy. *Pharm. Nanotechnol.* **7**, 3–23 (2019).

97. Senkus, E. *et al.* Primary breast cancer: ESMO Clinical Practice Guidelines for diagnosis, treatment and follow-up. *Ann. Oncol.* **26**, v8–v30 (2015).

98. Rapiti, E. *et al.* Complete excision of primary breast tumor improves survival of patients with metastatic breast cancer at diagnosis. *J. Clin. Oncol.* **24**, 2743–2749 (2006).

99. Marks, C. E. *et al.* Metastatic breast cancer: Who benefits from surgery? *Am.*

J. Surg. **223**, 81–93 (2022).

100. Wapnir, I. L. *et al.* Long-term outcomes of invasive ipsilateral breast tumor recurrences after lumpectomy in NSABP B-17 and B-24 randomized clinical trials for DCIS. *J. Natl. Cancer Inst.* **103**, 478–488 (2011).

101. Narod, S. A., Iqbal, J., Giannakeas, V., Sopik, V. & Sun, P. Breast cancer mortality after a diagnosis of ductal carcinoma in situ. *JAMA Oncol.* **1**, 888–896 (2015).

102. Darby, S. *et al.* Effect of radiotherapy after breast-conserving surgery on 10-year recurrence and 15-year breast cancer death: Meta-analysis of individual patient data for 10 801 women in 17 randomised trials. *Lancet* **378**, 1707–1716 (2011).

103. Bartelink, H. *et al.* Whole-breast irradiation with or without a boost for patients treated with breast-conserving surgery for early breast cancer: 20-year follow-up of a randomised phase 3 trial. *Lancet Oncol.* **16**, 47–56 (2015).

104. Houssami, N., MacAskill, P., Von Minckwitz, G., Marinovich, M. L. & Mamounas, E. Meta-analysis of the association of breast cancer subtype and pathologic complete response to neoadjuvant chemotherapy. *Eur. J. Cancer* **48**, 3342–3354 (2012).

105. Audeh, W., Blumencranz, L., Kling, H., Trivedi, H. & Srkalovic, G. Prospective Validation of a Genomic Assay in Breast Cancer: The 70-gene MammaPrint Assay and the MINDACT Trial. *Acta Med. Acad.* **48**, 18–34 (2019).

106. Thibodeau, S. & Voutsadakis, I. A. Prediction of Oncotype Dx recurrence score using clinical parameters: A comparison of available tools and a simple predictor based on grade and progesterone receptor. *Hematol. Oncol. Stem Cell Ther.* **12**, 89–96 (2019).

107. Mansour, E. G. *et al.* Survival advantage of adjuvant chemotherapy in high-risk node-negative breast cancer: Ten-year analysis - An intergroup study. *J. Clin. Oncol.* **16**, 3486–3492 (1998).

108. Zarcos-Pedrinaci, I. *et al.* Impact of adjuvant chemotherapy on the survival of patients with breast cancer diagnosed by screening. *Cancer Med.* **8**, 6662–6670 (2019).

109. Won, K. A. & Spruck, C. Triple-negative breast cancer therapy: Current and future perspectives. *Int. J. Oncol.* **57**, 1245–1261 (2020).

110. Ruddy, K. J. & Ganz, P. A. Treatment of Nonmetastatic Breast Cancer. *JAMA - J. Am. Med. Assoc.* **321**, 1716–1717 (2019).

111. De Laurentiis, M. *et al.* Taxane-based combinations as adjuvant chemotherapy of early breast cancer: A meta-analysis of randomized trials. *J. Clin. Oncol.* **26**, 44–53 (2008).

112. Masuda, N. *et al.* Adjuvant Capecitabine for Breast Cancer after Preoperative Chemotherapy. *N. Engl. J. Med.* **376**, 2147–2159 (2017).

113. Tutt, A. *et al.* Europe PMC Funders Group Europe PMC Funders Author Manuscripts Europe PMC Funders Author Manuscripts A randomised phase III trial of carboplatin compared with docetaxel in BRCA1 / 2 mutated and pre-specified triple negative breast cancer " BRCAness " subg. *Nat Med* **24**, 628–637 (2018).

114. Von Minckwitz, G. *et al.* Neoadjuvant carboplatin in patients with triple-negative and HER2-positive early breast cancer (GeparSixto; GBG 66): A randomised phase 2 trial. *Lancet Oncol.* **15**, 747–756 (2014).

115. Hilton, H. N., Clarke, C. L. & Graham, J. D. Estrogen and progesterone signalling in the normal breast and its implications for cancer development. *Mol. Cell. Endocrinol.* **466**, 2–14 (2018).

116. Davies, C. *et al.* Long-term effects of continuing adjuvant tamoxifen to 10 years versus stopping at 5 years after diagnosis of oestrogen receptor-positive breast cancer: ATLAS, a randomised trial. *Lancet* **381**, 805–816 (2013).

117. Yang, G., Nowsheen, S., Aziz, K. & Georgakilas, A. G. Toxicity and adverse effects of Tamoxifen and other anti-estrogen drugs. *Pharmacol. Ther.* **139**, 392–404 (2013).

118. Cianfrocca, M. E. & Gradishar, W. J. Results of the ATAC (Arimidex, Tamoxifen, Alone or in Combination) Trial After Completion of 5 Years' Adjuvant Treatment for Breast Cancer. *Breast Dis.* **17**, 188 (2006).

119. Oh, D. Y. & Bang, Y. J. HER2-targeted therapies — a role beyond breast cancer. *Nat. Rev. Clin. Oncol.* **17**, 33–48 (2020).

120. Krishnamurti, U. & Silverman, J. F. HER2 in breast cancer: A review and update. *Adv. Anat. Pathol.* **21**, 100–107 (2014).

121. Derakhshani, A. *et al.* Overcoming trastuzumab resistance in HER2-positive

breast cancer using combination therapy. *J. Cell. Physiol.* **235**, 3142–3156 (2020).

122. Bradley, R. *et al.* Trastuzumab for early-stage, HER2-positive breast cancer: a meta-analysis of 13 864 women in seven randomised trials. *Lancet Oncol.* **22**, 1139–1150 (2021).

123. Romond, E. H. *et al.* Trastuzumab plus Adjuvant Chemotherapy for Operable HER2-Positive Breast Cancer. *N. Engl. J. Med.* **353**, 1673–1684 (2005).

124. Piccart-Gebhart, M. J. et. a. Trastuzumab after Adjuvant Chemotherapy in HER2-Positive Breast Cancer Martine. *N. Engl. J. Med.* **353**, 1659–1672 (2005).

125. Perez, E. A. *et al.* Trastuzumab plus adjuvant chemotherapy for human epidermal growth factor receptor 2 - Positive breast cancer: Planned joint analysis of overall survival from NSABP B-31 and NCCTG N9831. *J. Clin. Oncol.* **32**, 3744–3752 (2014).

126. Eiger, D., Pondé, N. F. & De Azambuja, E. Pertuzumab in HER2-positive early breast cancer: Current use and perspectives. *Futur. Oncol.* **15**, 1823–1843 (2019).

127. Díaz-Redondo, T. *et al.* Different Pathological Complete Response Rates According to PAM50 Subtype in HER2+ Breast Cancer Patients Treated With Neoadjuvant Pertuzumab/Trastuzumab vs. Trastuzumab Plus Standard Chemotherapy: An Analysis of Real-World Data. *Front. Oncol.* **9**, 1178 (2019).

128. Geyer CE, Forster J, Lindquist D, Chan S, R. C. & Al, E. Lapatinib plus capecitabine for HER2-positive advanced breast cancer. *N Engl J Med* **355**, 2733–2743 (2006).

129. Chan, A. *et al.* Neratinib after trastuzumab-based adjuvant therapy in patients with HER2-positive breast cancer (ExteNET): A multicentre, randomised, double-blind, placebo-controlled, phase 3 trial. *Lancet Oncol.* **17**, 367–377 (2016).

130. Murthy, R. K. *et al.* Tucatinib, Trastuzumab, and Capecitabine for HER2-Positive Metastatic Breast Cancer. *N. Engl. J. Med.* **382**, 597–609 (2020).

131. Verma, S. *et al.* Trastuzumab Emtansine for HER2-Positive Advanced Breast Cancer. *N. Engl. J. Med.* **367**, 1783–1791 (2012).

132. Modi, S. *et al.* Trastuzumab Deruxtecan in Previously Treated HER2-Positive Breast Cancer. *N. Engl. J. Med.* **382**, 610–621 (2020).

133. Fusco, N. *et al.* PIK3CA Mutations as a Molecular Target for Hormone Receptor-Positive, HER2-Negative Metastatic Breast Cancer. *Front. Oncol.* **11**, 644737 (2021).

134. Mosele, F. *et al.* Outcome and molecular landscape of patients with PIK3CA-mutated metastatic breast cancer. *Ann. Oncol.* **31**, 377–386 (2020).

135. Samuels, Y and Waldman, T. Oncogenic Mutations of PIK3CA in Human Cancers Yardena. *Curr Top Microbiol Immunol* **347**, 21–41 (2010).

136. André, F. *et al.* Alpelisib for PIK3CA -Mutated, Hormone Receptor–Positive Advanced Breast Cancer . *N. Engl. J. Med.* **380**, 1929–1940 (2019).

137. Tutt, A. N. J. *et al.* Adjuvant Olaparib for Patients with BRCA1 - or BRCA2 - Mutated Breast Cancer . *N. Engl. J. Med.* **384**, 2394–2405 (2021).

138. Robson, M. *et al.* Olaparib for Metastatic Breast Cancer in Patients with a Germline BRCA Mutation . *N. Engl. J. Med.* **377**, 523–533 (2017).

139. Litton, J. K. *et al.* Talazoparib in Patients with Advanced Breast Cancer and a Germline BRCA Mutation . *N. Engl. J. Med.* **379**, 753–763 (2018).

140. Ahlin, C. *et al.* High expression of cyclin D1 is associated to high proliferation rate and increased risk of mortality in women with ER-positive but not in ER-negative breast cancers. *Breast Cancer Res. Treat.* **164**, 667–678 (2017).

141. Stendahl, M. *et al.* Cyclin D1 overexpression is a negative predictive factor for tamoxifen response in postmenopausal breast cancer patients. *Br. J. Cancer* **90**, 1942–1948 (2004).

142. Finn, R. S. *et al.* Palbociclib and Letrozole in Advanced Breast Cancer. *N. Engl. J. Med.* **375**, 1925–1936 (2016).

143. Turner, N. C. *et al.* Overall Survival with Palbociclib and Fulvestrant in Advanced Breast Cancer. *N. Engl. J. Med.* **379**, 1926–1936 (2018).

144. Im, S.-A. *et al.* Overall Survival with Ribociclib plus Endocrine Therapy in Breast Cancer. *N. Engl. J. Med.* **381**, 307–316 (2019).

145. Johnston, S. *et al.* Abemaciclib as initial therapy for advanced breast cancer: MONARCH 3 updated results in prognostic subgroups. *npj Breast Cancer* **7**, 3638 (2021).

146. Johnston, S. R. D. *et al.* Abemaciclib combined with endocrine therapy for the adjuvant treatment of HR1, HER22, node-positive, high-risk, early breast

cancer (monarchE). *J. Clin. Oncol.* **38**, 3987–3998 (2020).

147. Hare, S. H. & Harvey, A. J. mTOR function and therapeutic targeting in breast cancer. *Am. J. Cancer Res.* **7**, 383–404 (2017).

148. Pritchard, K. I. *et al.* Everolimus in Postmenopausal Hormone- Receptor–Positive Advanced Breast Cancer. *N Engl J Med* **366**, 520–529 (2012).

149. Gou, Q. *et al.* PD-L1 degradation pathway and immunotherapy for cancer. *Cell Death Dis.* **11**, 955 (2020).

150. Cortes, J. *et al.* Pembrolizumab plus chemotherapy versus placebo plus chemotherapy for previously untreated locally recurrent inoperable or metastatic triple-negative breast cancer (KEYNOTE-355): a randomised, placebo-controlled, double-blind, phase 3 clinical trial. *Lancet* **396**, 1817–1828 (2020).

151. Kim, Charissa; Gao, Ruli; Sei, Emi; Brandt, Rachel; Crosetto, Nicola; Foukakis, Theodoros; Navin, N. Chemoresistance Evolution in Triple-Negative Breast Cancer Delineated by Single Cell Sequencing. *Cell* **173**, 879–893 (2018).

152. Saliminejad, K., Khorram Khorshid, H. R., Soleymani Fard, S. & Ghaffari, S. H. An overview of microRNAs: Biology, functions, therapeutics, and analysis methods. *J. Cell. Physiol.* **234**, 5451–5465 (2019).

153. Park, J. H. & Kho, C. Micrornas and calcium signaling in heart disease. *Int. J. Mol. Sci.* **22**, 10582 (2021).

154. Iranzad, R. *et al.* Roles of microRNAs in renal disorders related to primary podocyte dysfunction. *Life Sci.* **277**, 119463 (2021).

155. Bohosova, J. *et al.* MicroRNAs in the development of resistance to antiseizure drugs and their potential as biomarkers in pharmacoresistant epilepsy. *Epilepsia* **62**, 2573–2588 (2021).

156. Abuelezz, N. Z., Nasr, F. E., AbdulKader, M. A., Bassiouny, A. R. & Zaky, A. MicroRNAs as Potential Orchestrators of Alzheimer's Disease-Related Pathologies: Insights on Current Status and Future Possibilities. *Front. Aging Neurosci.* **13**, 743573 (2021).

157. Conti, I. *et al.* Micrornas patterns as potential tools for diagnostic and prognostic follow-up in cancer survivorship. *Cells* **10**, 2069 (2021).

158. Feinbaum, R., Ambros, V. & Lee, R. The C. elegans Heterochronic Gene lin-4

Encodes Small RNAs with Antisense Complementarity to lin-14. *Cell* **116**, 843–854 (2004).

159. Pasquinelli, A. E. *et al.* Conservation of the sequence and temporal expression of let-7 heterochronic regulatory RNA. *Nature* **408**, 86–89 (2000).

160. Schanen, B. C. & Li, X. Transcriptional regulation of mammalian miRNA genes. *Genomics* **97**, 1–6 (2011).

161. Ha, M. & Kim, V. N. Regulation of microRNA biogenesis. *Nat. Rev. Mol. Cell Biol.* **15**, 509–524 (2014).

162. O'Brien, J., Hayder, H., Zayed, Y. & Peng, C. Overview of microRNA biogenesis, mechanisms of actions, and circulation. *Front. Endocrinol. (Lausanne).* **9**, 402 (2018).

163. Winter, J., Jung, S., Keller, S., Gregory, R. I. & Diederichs, S. Many roads to maturity: MicroRNA biogenesis pathways and their regulation. *Nat. Cell Biol.* **11**, 228–234 (2009).

164. Annese, T., Tamma, R., De Giorgis, M. & Ribatti, D. microRNAs Biogenesis, Functions and Role in Tumor Angiogenesis. *Front. Oncol.* **10**, 581007 (2020).

165. Pasquinelli, A. E. MicroRNAs and their targets: Recognition, regulation and an emerging reciprocal relationship. *Nat. Rev. Genet.* **13**, 271–282 (2012).

166. Huntzinger, E. & Izaurralde, E. Gene silencing by microRNAs: Contributions of translational repression and mRNA decay. *Nat. Rev. Genet.* **12**, 99–110 (2011).

167. Chipman, L. B. & Pasquinelli, A. E. miRNA Targeting: Growing beyond the Seed. *Trends Genet.* **35**, 215–222 (2019).

168. Kiriakidou, M. *et al.* An mRNA m7G Cap Binding-like Motif within Human Ago2 Represses Translation. *Cell* **129**, 1141–1151 (2007).

169. Xu, P. *et al.* A Systematic Way to Infer the Regulation Relations of miRNAs on Target Genes and Critical miRNAs in Cancers. *Front. Genet.* **11**, 278 (2020).

170. He, S. *et al.* MicroRNAs activate natural killer cells through Toll-like receptor signaling. *Blood* **121**, 4663–4671 (2013).

171. Fabbri, M. *et al.* MicroRNAs bind to Toll-like receptors to induce prometastatic inflammatory response. *PNAS* **109**, 110–116 (2012).

172. Calin, G. A. *et al.* Frequent deletions and down-regulation of micro-RNA genes miR15 and miR16 at 13q14 in chronic lymphocytic leukemia. *PNAS* **99**, 15524–15529 (2002).

173. Peng, Y. & Croce, C. M. The role of microRNAs in human cancer. *Signal Transduct. Target. Ther.* **1**, 15004 (2016).

174. Zhang, L. *et al.* microRNAs exhibit high frequency genomic alterations in human cancer. *Proc. Natl. Acad. Sci. U. S. A.* **103**, 9136–9141 (2006).

175. Mendell, J. miRiad roles for the miR-17-92 cluster in development and disease. *Cell* **133**, 217–222 (2008).

176. Saki, N., Abroun, S., Hajizamani, S., Rahim, F. & Shahjahani, M. Association of chromosomal translocation and MiRNA expression with the pathogenesis of multiple myeloma. *Cell J.* **16**, 99–110 (2014).

177. Moore, L. D., Le, T. & Fan, G. DNA methylation and its basic function. *Neuropsychopharmacology* **38**, 23–38 (2013).

178. Jin, C., Li, M., Ouyang, Y., Tan, Z. & Jiang, Y. MiR-424 functions as a tumor suppressor in glioma cells and is down-regulated by DNA methylation. *J. Neurooncol.* **133**, 247–255 (2017).

179. Supic, G. *et al.* Prognostic impact of miR-34b/c DNA methylation, gene expression, and promoter polymorphism in HPV-negative oral squamous cell carcinomas. *Sci. Rep.* **12**, 1296 (2022).

180. Long, X. R., He, Y., Huang, C. & Li, J. MicroRNA-148a is silenced by hypermethylation and interacts with DNA methyltransferase 1 in hepatocellular carcinogenesis. *Int. J. Oncol.* **45**, 1915–1922 (2014).

181. Rahman, M. M., Brane, A. C. & Tollefsbol, T. O. Micrornas and epigenetics strategies to reverse breast cancer. *Cells* **8**, 1214 (2019).

182. Scott, G. K., Mattie, M. D., Berger, C. E., Benz, S. C. & Benz, C. C. Rapid alteration of microRNA levels by histone deacetylase inhibition. *Cancer Res.* **66**, 1277–1281 (2006).

183. Buurman, R. *et al.* Histone deacetylases activate hepatocyte growth factor signaling by repressing microRNA-449 in hepatocellular carcinoma cells. *Gastroenterology* **143**, 811-820.e15 (2012).

184. Poddar, S., Kesharwani, D. & Datta, M. Histone deacetylase inhibition

regulates miR-449a levels in skeletal muscle cells. *Epigenetics* **11**, 579–587 (2016).

185. Vajen, B. et. a. MicroRNA-192-5p inhibits migration of triple negative breast cancer cells and directly regulates Rho GTPase activating protein 19. *Gens Chromosom. Cancer* **60**, 733–742 (2021).

186. Yang, X., Feng, M., Jiang, X., Wu, Z., Li, Z., Aau, M.& Yu, Q. miR-449a and miR-449b are direct transcriptional targets of E2F1 and negatively regulate pRb–E2F1 activity through a feedback loop by targeting CDK6 and CDC25A. *GENES Dev.* **23**, 2388–2393 (2009).

187. Gabay, Meital, Yulin Li, and D. F. MYC Activation Is a Hallmark of Cancer Initiation and Maintenance Meital. *Cold Spring Harb. Perspect. Med.* **36**, 186–194 (2009).

188. Feng, Z., Zhang, C., Wu, R. & Hu, W. Tumor suppressor p53 meets microRNAs. *J. Mol. Cell Biol.* **3**, 44–50 (2011).

189. Torrezan, G. T. *et al.* Recurrent somatic mutation in DROSHA induces microRNA profile changes in Wilms tumour. *Nat. Commun.* **5**, 4039 (2014).

190. Lee, S. S. *et al.* Dysregulation of the miRNA biogenesis components DICER1, DROSHA, DGCR8 and AGO2 in clear cell renal cell carcinoma in both a Korean cohort and the cancer genome atlas kidney clear cell carcinoma cohort. *Oncol. Lett.* **18**, 4337–4345 (2019).

191. Lin, R. J. *et al.* microRNA signature and expression of Dicer and Drosha can predict prognosis and delineate risk groups in neuroblastoma. *Cancer Res.* **70**, 7841–7850 (2010).

192. Merritt, W. et. a. Dicer, Drosha, and Outcomes in Patients with Ovarian Cancer William. *N Engl J Med* **359**, 2541–2650 (2008).

193. Karube, Y. *et al.* Reduced expression of Dicer associated with poor prognosis in lung cancer patients. *Cancer Sci.* **96**, 111–115 (2005).

194. Grelier, G. *et al.* Prognostic value of Dicer expression in human breast cancers and association with the mesenchymal phenotype. *Br. J. Cancer* **101**, 673–683 (2009).

195. Lu, J. *et al.* MicroRNA expression profiles classify human cancers. *Nature* **435**, 834–838 (2005).

196. Melo, S. A. *et al.* A genetic defect in exportin-5 traps precursor MicroRNAs in the nucleus of cancer cells. *Cancer Cell* **18**, 303–315 (2010).

197. Sun, H. L. *et al.* ERK Activation Globally Downregulates miRNAs through Phosphorylating Exportin-5. *Cancer Cell* **30**, 723–736 (2016).

198. Higuchi, T. *et al.* Suppression of MicroRNA-7 (miR-7) biogenesis by nuclear factor 90-nuclear factor 45 complex (NF90-NF45) controls cell proliferation in hepatocellular carcinoma. *J. Biol. Chem.* **291**, 21074–21084 (2016).

199. Yong-Ming, H. *et al.* MiR-449a: A potential therapeutic agent for cancer. *Anticancer. Drugs* **28**, 1067–1078 (2017).

200. Glubb, D. M. *et al.* Fine-scale mapping of the 5q11.2 breast cancer locus reveals at least three independent risk variants regulating MAP3K1. *Am. J. Hum. Genet.* **96**, 5–20 (2015).

201. Loukas, I. *et al.* Fine-tuning multiciliated cell differentiation at the post-transcriptional level: contribution of miR-34/449 family members. *Biol. Rev.* **96**, 2321–2332 (2021).

202. Wu, J. *et al.* Two miRNA clusters, miR-34b/c and miR-449, are essential for normal brain development, motile ciliogenesis, and spermatogenesis. *PNAS* **111**, 2851–2857 (2014).

203. Yu, J. *et al.* LINC00667/miR-449b-5p/YY1 axis promotes cell proliferation and migration in colorectal cancer. *Cancer Cell Int.* **20**, 322 (2020).

204. Jiang, J. *et al. MicroRNA-449b-5p suppresses the growth and invasion of breast cancer cells via inhibiting CREPT-mediated Wnt/β-catenin signaling*. *Chemico-Biological Interactions* vol. 302 (Elsevier B.V., 2019).

205. Chen, H. *et al.* MicroRNA-449a acts as a tumor suppressor in human bladder cancer through the regulation of pocket proteins. *Cancer Lett.* **320**, 40–47 (2012).

206. Ren, X. S. *et al.* Tumor-suppressive microRNA-449a induces growth arrest and senescence by targeting E2F3 in human lung cancer cells. *Cancer Lett.* **344**, 195–203 (2014).

207. Ye, W. *et al.* MiR-449a functions as a tumor suppressor in endometrial cancer by targeting CDC25A. *Oncol. Rep.* **32**, 1193–1199 (2014).

208. Chen, S. peng *et al.* MiR-449a suppresses the epithelial-mesenchymal

transition and metastasis of hepatocellular carcinoma by multiple targets. *BMC Cancer* **15**, 706 (2015).

209. Hu, S. *et al.* MicroRNA-449a delays lung cancer development through inhibiting KDM3A/HIF-1α axis. *J. Transl. Med.* **19**, 224 (2021).

210. Shekhar, R. *et al.* The microRNAs miR-449a and miR-424 suppress osteosarcoma by targeting cyclin A2 expression. *J. Biol. Chem.* **294**, 4381–4400 (2019).

211. Li, F., Liang, J. & Bai, L. MicroRNA-449a functions as a tumor suppressor in pancreatic cancer by the epigenetic regulation of ATDC expression. *Biomed. Pharmacother.* **103**, 782–789 (2018).

212. Liu, Y. *et al.* MiR-449a promotes liver cancer cell apoptosis by down-regulation of Calpain6 and POU2F1. *Oncotarget* **7**, 13491–13501 (2016).

213. Yao, Y. *et al.* MiR-449a exerts tumor-suppressive functions in human glioblastoma by targeting Myc-associated zinc-finger protein. *Mol. Oncol.* **9**, 640–656 (2015).

214. Li, X., Li, H., Zhang, R., Liu, J. & Liu, J. MicroRNA-449a inhibits proliferation and induces apoptosis by directly repressing E2F3 in gastric cancer. *Cell. Physiol. Biochem.* **35**, 2033–2042 (2015).

215. Sun, X. *et al.* miR-449a inhibits colorectal cancer progression by targeting. *Oncotarget* **8**, 100975–100988 (2017).

216. Li, J., Zheng, Z., Zhang, J., Tang, Y. & Wan, X. miR-449a regulates biological functions of hepatocellular carcinoma cells by targeting SATB1. *J. B.U.ON.* **25**, 1375–1382 (2020).

217. Mao, A. *et al.* MicroRNA-449a enhances radiosensitivity by downregulation of c-Myc in prostate cancer cells. *Sci. Rep.* **6**, 27346 (2016).

218. Huang, G. *et al.* MicroRNA-449a inhibits cell proliferation and migration by regulating mutant p53 in MDA-MB-468 cells. *Exp. Ther. Med.* **22**, 1020 (2021).

219. Kheir, T. B. *et al.* miR-449 inhibits cell proliferation and is down-regulated in gastric cancer. *Mol. Cancer* **10**, 1–12 (2011).

220. Chen, Q. *et al.* Tumor suppressor miR-449a inhibits the development of gastric cancer: Via down-regulation of SGPL1. *RSC Adv.* **8**, 26020–26028 (2018).

221. Wu, A. Y. *et al.* Suppressive effect of microRNA-449a on the NDRG1/PTEN/AKT axis regulates endometrial cancer growth and metastasis. *Exp. Cell Res.* **382**, 111468 (2019).

222. Chen, W., Liu, Y., Chen, H., Ning, H. & Ding, K. Loss of miR-449a-caused PrLZ overexpression promotes prostate cancer metastasis. *Int. J. Oncol.* **51**, 435–444 (2017).

223. Duan, A. *et al.* Star-PAP regulates tumor protein D52 through modulating miR-449a/34a in breast cancer. *Biol. Open* **8**, bio045914 (2019).

224. Meng, L., Yuan, S., Zhu, L., Shangguan, Z. & Zhao, R. Ultrasound-microbubbles-mediated microRNA-449a inhibits lung cancer cell growth via the regulation of notch1. *Onco. Targets. Ther.* **12**, 7437–7450 (2019).

225. Zhou, Y., Chen, Q., Qin, R., Zhang, K. & Li, H. MicroRNA-449a reduces cell survival and enhances cisplatin-induced cytotoxicity via downregulation of NOTCH1 in ovarian cancer cells. *Tumor Biol.* **35**, 12369–12378 (2014).

226. Buurman, R. *et al.* Histone deacetylases activate hepatocyte growth factor signaling by repressing microRNA-449 in hepatocellular carcinoma cells. *Gastroenterology* **143**, 811–820 (2012).

227. Gao, X., Yu, L., Zhang, J. & Xue, P. Silencing of long non-coding RNA LINC01106 suppresses the proliferation, migration and invasion of endometrial cancer cells through regulating the miR-449a/MET axis. *Onco. Targets. Ther.* **13**, 9643–9655 (2020).

228. Zhang, H. *et al.* MicroRNA-449 suppresses proliferation of hepatoma cell lines through blockade lipid metabolic pathway related to SIRT1. *Int. J. Oncol.* **45**, 2143–2152 (2014).

229. Fang, Y., Gu, X., Li, Z., Xiang, J. & Chen, Z. miR-449b inhibits the proliferation of SW1116 colon cancer stem cells through downregulation of CCND1 and E2F3 expression. *Oncol. Rep.* **30**, 399–406 (2013).

230. Jiang, J. *et al.* MicroRNA-449b-5p suppresses the growth and invasion of breast cancer cells via inhibiting CREPT-mediated Wnt/β-catenin signaling. *Chem. Biol. Interact.* **302**, 74–82 (2019).

231. Yang, D., Li, J. song, Xu, Q. yu, Xia, T. & Xia, J. hong. Inhibitory Effect of MiR-449b on Cancer Cell Growth and Invasion through LGR4 in Non-Small-Cell Lung Carcinoma. *Curr. Med. Sci.* **38**, 582–589 (2018).

232. Wu, Z., Wang, H., Fang, S. & Xu, C. MiR-449c inhibits gastric carcinoma growth. *Life Sci.* **137**, 14–19 (2015).

233. Zhao, Z. *et al.* microRNA-449a functions as a tumor suppressor in neuroblastoma through inducing cell differentiation and cell cycle arrest. *RNA Biol.* **12**, 538–554 (2015).

234. Noonan, E. J., Place, R. F., Basak, S., Pookot, D. & Li, L. C. miR-449a causes Rb-dependent cell cycle arrest and senescence in prostate cancer cells. *Oncotarget* **1**, 349–358 (2010).

235. Lizé, M., Pilarski, S. & Dobbelstein, M. E2F1-inducible microRNA 449a/b suppresses cell proliferation and promotes apoptosis. *Cell Death Differ.* **17**, 452–458 (2010).

236. Mao, A. *et al.* miR-449a enhances radiosensitivity through modulating pRb/E2F1 in prostate cancer cells. *Tumor Biol.* **37**, 4831–4840 (2016).

237. Chen, J. *et al.* miRNA-449a is downregulated in osteosarcoma and promotes cell apoptosis by targeting BCL2. *Tumor Biol.* **36**, 8221–8229 (2015).

238. Zhang, N. *et al.* MiR-449a attenuates autophagy of T-cell lymphoma cells by downregulating ATG4B expression. *BMB Rep.* **53**, 254–259 (2020).

239. Li, L. *et al.* MiR-449a suppresses LDHA-mediated glycolysis to enhance the sensitivity of non-small cell lung cancer cells to ionizing radiation. *Oncol. Res.* **26**, 547–556 (2018).

240. Chen, W., Liu, Y., Chen, H., Ning, H. & Ding, K. Loss of miR-449a-caused PrLZ overexpression promotes prostate cancer metastasis. *Int. J. Oncol.* **51**, 435–444 (2017).

241. Sandbothe, M. *et al.* The microRNA-449 family inhibits TGF-β-mediated liver cancer cell migration by targeting SOX4. *J. Hepatol.* **66**, 1012–1021 (2017).

242. Xu, B., Zhang, X., Wang, S. & Shi, B. MiR-449a suppresses cell migration and invasion by targeting PLAGL2 in breast cancer. *Pathol. Res. Pract.* **214**, 790–795 (2018).

243. Yun, M. R. *et al.* Enhancer remodeling and MicroRNA alterations are associated with acquired resistance to ALK inhibitors. *Cancer Res.* **78**, 3350–3362 (2018).

244. Luo, W. *et al.* MicroRNA-449a Is Downregulated in Non-Small Cell Lung

Cancer and Inhibits Migration and Invasion by Targeting c-Met. *PLoS One* **8**, e64759 (2013).

245. Chen, X., Wang, A. & Yue, X. miR-449c inhibits migration and invasion of gastric cancer cells by targeting PFKFB3. *Oncol. Lett.* **16**, 417–424 (2018).

246. You, J. *et al.* MiR-449a suppresses cell invasion by inhibiting MAP2K1 in non-small cell lung cancer. *Am. J. Cancer Res.* **5**, 2730–2744 (2015).

247. Kumar, P. *et al.* Loss of miR-449a in ERG-associated prostate cancer promotes the invasive phenotype by inducing SIRT1. *Oncotarget* **7**, 22791–22806 (2016).

248. Meng, H. *et al.* MiR-449a regulates the cell migration and invasion of human non-small cell lung carcinoma by targeting ADAM10. *Onco. Targets. Ther.* **12**, 3829–3838 (2019).

249. Li, Q., Peng, J., Li, X., Leng, A. & Liu, T. miR-449a targets Flot2 and inhibits gastric cancer invasion by inhibiting TGF-β-mediated EMT. *Diagn. Pathol.* **10**, 202 (2015).

250. Vajen, B. *et al.* MicroRNA-449a Inhibits Triple Negative Breast Cancer by Disturbing DNA Repair and Chromatid Separation. *Int. J. Mol. Sci.* **23**, 5131 (2022).

251. Tormo, E. *et al.* The miRNA-449 family mediates doxorubicin resistance in triple-negative breast cancer by regulating cell cycle factors. *Sci. Rep.* **9**, 5316 (2019).

252. Condrat, C. E. *et al.* miRNAs as Biomarkers in Disease: Latest Findings Regarding Their Role in Diagnosis and Prognosis. *Cells* **9**, 276 (2020).

253. Cui, C. & Cui, Q. The relationship of human tissue microRNAs with those from body fluids. *Sci. Rep.* **10**, 5644 (2020).

254. Gilad, S. *et al.* Serum microRNAs are promising novel biomarkers. *PLoS One* **3**, e3148 (2008).

255. Chen, X. *et al.* Characterization of microRNAs in serum: A novel class of biomarkers for diagnosis of cancer and other diseases. *Cell Res.* **18**, 997–1006 (2008).

256. Cortez, M. A. *et al.* MicroRNAs in body fluids-the mix of hormones and biomarkers. *Nat. Rev. Clin. Oncol.* **8**, 467–477 (2011).

257. Ortiz-Quintero, B. Cell-free microRNAs in blood and other body fluids, as cancer biomarkers. *Cell Prolif.* **49**, 281–303 (2016).

258. Redova, M., Sana, J. & Slaby, O. Circulating miRNAs as new blood-based biomarkers for solid cancers. *Futur. Oncol.* **9**, 387–402 (2013).

259. Chen, X., Liang, H., Zhang, J., Zen, K. & Zhang, C. Y. Secreted microRNAs: A new form of intercellular communication. *Trends Cell Biol.* **22**, 125–132 (2012).

260. Lawrie, C. H. *et al.* Detection of elevated levels of tumour-associated microRNAs in serum of patients with diffuse large B-cell lymphoma. *Br. J. Haematol.* **141**, 672–675 (2008).

261. Adam-Artigues, A. *et al.* Identification of a two-microrna signature in plasma as a novel biomarker for very early diagnosis of breast cancer. *Cancers (Basel).* **13**, 2848 (2021).

262. Sun, Y. *et al.* Serum MicroRNA-155 as a Potential Biomarker to Track Disease in Breast Cancer. *PLoS One* **7**, e47003 (2012).

263. Ishikawa, D. *et al.* Expression level of MicroRNA-449a predicts the prognosis of patients with gastric cancer. *Anticancer Res.* **40**, 239–244 (2020).

264. Fu, D., Chen, Y. & Xu, D. Circulating miR-449a predicts survival outcome for colorectal cancer following curative resection: An observational study. *Medicine (Baltimore).* **100**, e25022 (2021).

265. Fu, Y., Chen, J. & Huang, Z. Recent progress in microrna-based delivery systems for the treatment of human disease. *ExRNA* **1**, 24 (2019).

266. del C, P., Monroig-Bosque., Chen, L., Zhang, S., Calin, G. . Small Molecule Compounds Targeting miRNAs for Cancer Therapy. *Adv Drug Deliv Rev* **81**, 104–116 (2015).

267. Gumireddy, K., Young, D.D., Xiong, X., Hogenesh.J.B., Huang, Q., Deiters, A. Small Molecule Inhibitors of MicroRNA miR-21 Function. *Angew Chem Int Engl* **47**, 7482–7484 (2008).

268. Chen, Yunghing; Gao, Dong-Yu; Huang, L. In vivo delivery of miRNAs for cancer therapy: Challenges and strategies. *Adv Drug Deliv Rev* **81**, 128–141 (2015).

269. Merhautova, J., Demlova, R. & Slaby, O. MicroRNA-based therapy in animal

models of selected gastrointestinal cancers. *Front. Pharmacol.* **7**, 329 (2016).

270. Baumann, V and Winkler, J. miRNA-based therapies: Strategies and delivery platforms for oligonucleotide and non-oligonucleotide agents V. *Futur. Med Chem* **6**, 1967–1984 (2014).

271. Rupaimoole, R. & Slack, F. J. MicroRNA therapeutics: Towards a new era for the management of cancer and other diseases. *Nat. Rev. Drug Discov.* **16**, 203–221 (2017).

272. Hosseinahli, N., Aghapour, M., Duijf, P. H. G. & Baradaran, B. Treating cancer with microRNA replacement therapy: A literature review. *J. Cell. Physiol.* **233**, 5574–5588 (2018).

273. Lee, S. W. L. *et al.* MicroRNA delivery through nanoparticles. *Biol. Med* **12**, 643–653 (2016).

274. Ganju, A., Khan, S., Hafaez, B.B., Behrman, S.W., Yallapu, M.M., Chauhan S.C., Jaggi, M. miRNA nanotherapeutics for cancer Aditya. *Drug Discov Today* **22**, 424–432 (2017).

275. Hu, F. *et al.* The exogenous delivery of microRNA-449b-5p using spermidine-PLGA nanoparticles efficiently decreases hepatic injury. *RSC Adv.* **9**, 35135–35144 (2019).

276. Zhou, W., Xu, M., Wang, Z. & Yang, M. Engineered exosomes loaded with miR-449a selectively inhibit the growth of homologous non-small cell lung cancer. *Cancer Cell Int.* **21**, 485 (2021).

277. Hong, D. S. *et al.* Phase 1 study of MRX34, a liposomal miR-34a mimic, in patients with advanced solid tumours. *Br. J. Cancer* **122**, 1630–1637 (2020).

278. van Zandwijk, N. *et al.* Safety and activity of microRNA-loaded minicells in patients with recurrent malignant pleural mesothelioma: a first-in-man, phase 1, open-label, dose-escalation study. *Lancet Oncol.* **18**, 1386–1396 (2017).

279. Chang, J. *et al.* Differential response of cancer cells to HDAC inhibitors trichostatin A and depsipeptide. *Br. J. Cancer* **106**, 116–125 (2012).

280. Avalos, J. L., Bever, K. M. & Wolberger, C. Mechanism of sirtuin nhibition by nicotinamide: Altering the NAD + cosubstrate specificity of a Sir2 enzyme. *Mol. Cell* **17**, 855–868 (2005).

281. Tacar, O., Sriamornsak, P. & Dass, C. R. Doxorubicin: An update on anticancer molecular action, toxicity and novel drug delivery systems. *J. Pharm. Pharmacol.* **65**, 157–170 (2013).

282. Rich, J. T. *et al.* A practical guide to understanding Kaplan-Meier curves. *Otolaryngol. - Head Neck Surg.* **143**, 331–336 (2010).

283. Dweep, H. & Gretz, N. MiRWalk2.0: A comprehensive atlas of microRNA-target interactions. *Nat. Methods* **12**, 697 (2015).

284. Vlachos, I. S. *et al.* DIANA-miRPath v3.0: Deciphering microRNA function with experimental support. *Nucleic Acids Res.* **43**, W460–W466 (2015).

285. Noonan, E. J. *et al.* miR-449a targets HDAC-1 and induces growth arrest in prostate cancer. *Oncogene* **28**, 1714–1724 (2009).

286. Orlando, U. D. *et al.* Acyl-CoA synthetase-4 is implicated in drug resistance in breast cancer cell lines involving the regulation of energy-dependent transporter expression. *Biochem. Pharmacol.* **159**, 52–63 (2019).

287. Waks, A. G. & Winer, E. P. Breast Cancer Treatment: A Review. *JAMA - J. Am. Med. Assoc.* **321**, 288–300 (2019).

288. Kim, C. *et al.* Chemoresistance Evolution in Triple-Negative Breast Cancer Delineated by Single-Cell Sequencing. *Cell* **173**, 879–893 (2018).

289. Jiang, J. *et al.* MicroRNA-449b-5p suppresses the growth and invasion of breast cancer cells via inhibiting CREPT-mediated Wnt/β-catenin signaling. *Chem. Biol. Interact.* **302**, 74–82 (2019).

290. Shi, W. *et al.* MiR-449a promotes breast cancer progression by targeting CRIP2. *Oncotarget* **7**, 18906–18918 (2016).

291. Zhang, Z. *et al.* Downregulation of MicroRNA-449 promotes migration and invasion of breast cancer cells by targeting tumor protein D52 (TPD52). *Oncol. Res.* **25**, 753–761 (2017).

292. Li, Y. & Seto, E. HDACs and HDAC inhibitors in cancer development and therapy. *Cold Spring Harb. Perspect. Med.* **6**, a026831 (2016).

293. Singh, A. K., Bishayee, A. & Pandey, A. K. Targeting histone deacetylases with natural and synthetic agents: An emerging anticancer strategy. *Nutrients* **10**, 731 (2018).

294. Ropero, S. & Esteller, M. The role of histone deacetylases (HDACs) in human

cancer. *Mol. Oncol.* **1**, 19–25 (2007).

295. Wang, C. *et al.* Interactions between E2F1 and SirT1 regulate apoptotic response to DNA damage. *Nat. Cell Biol.* **8**, 1025–1031 (2006).

296. Robertson, K. D. *et al.* DNMT1 forms a complex with RB, E2F1 and HDAC1 and represses transcription from E2F-responsive promoters. *Nat. Genet.* **25**, 338–342 (2000).

297. Zhang, X. *et al.* Epigenetically regulated miR-449a enhances hepatitis B virus replication by targeting cAMP-responsive element binding protein 5 and modulating hepatocytes phenotype. *Sci. Rep.* **6**, 25389 (2016).

298. Li, Q. *et al.* DNA methylation mediated downregulation of miR-449c controls osteosarcoma cell cycle progression by directly targeting oncogene c-Myc. *Int. J. Biol. Sci.* **13**, 1038–1050 (2017).

299. Chikh, A. *et al.* Class II phosphoinositide 3-kinase C2β regulates a novel signaling pathway involved in breast cancer progression. *Oncotarget* **7**, 18325–18345 (2016).

300. Germain, N. *et al.* Lipid metabolism and resistance to anticancer treatment. *Biology (Basel).* **9**, 474 (2020).

301. Radif, Y. *et al.* The endogenous subcellular localisations of the long chain fatty acid-activating enzymes ACSL3 and ACSL4 in sarcoma and breast cancer cells. *Mol. Cell. Biochem.* **448**, 275–286 (2018).

302. Yoon, S. *et al.* Up-regulation of acetyl-CoA carboxylase α and fatty acid synthase by human epidermal growth factor receptor 2 at the translational level in breast cancer cells. *J. Biol. Chem.* **282**, 26122–26131 (2007).

303. Ferraro, G. B. *et al.* Fatty acid synthesis is required for breast cancer brain metastasis. *Nat. Cancer* **2**, 414–428 (2021).

304. Menendez, J. A. & Lupu, R. Fatty acid synthase (FASN) as a therapeutic target in breast cancer. *Expert Opin. Ther. Targets* **21**, 1001–1016 (2017).

305. Wu, X. *et al.* Long Chain Fatty Acyl-CoA Synthetase 4 Is a Biomarker for and Mediator of Hormone Resistance in Human Breast Cancer. *PLoS One* **8**, e77060 (2013).

306. Dattilo, M. A. *et al.* Regulatory mechanisms leading to differential Acyl-CoA synthetase 4 expression in breast cancer cells. *Sci. Rep.* **9**, 10324 (2019).

307. Ma, Y. *et al.* Long-Chain Acyl-CoA synthetase 4–mediated fatty acid metabolism sustains androgen receptor pathway–independent prostate cancer. *Mol. Cancer Res.* **19**, 124–135 (2021).

308. Monaco, M. E. Fatty acid metabolism in breast cancer subtypes. *Oncotarget* **8**, 29487–29500 (2017).

309. Maloberti, P. M. *et al.* Functional interaction between acyl-coa synthetase 4, lipooxygenases and cyclooxygenase-2 in the aggressive phenotype of breast cancer cells. *PLoS One* **5**, e15540 (2010).

310. Monaco, M. E. *et al.* Expression of long-chain fatty Acyl-CoA synthetase 4 in breast and prostate cancers is associated with sex steroid hormone receptor negativity. *Transl. Oncol.* **3**, 91–98 (2010).

311. Orlando, U. D. *et al.* Acyl-CoA synthetase-4, a new regulator of mTOR and a potential therapeutic target for enhanced estrogen receptor function in receptor-positive and -negative breast cancer. *Oncotarget* **6**, 42632–42650 (2015).

312. Wei, K. L. *et al.* Downregulation of miRNA-449a expression associated with advanced stages and lymph node metastasis of breast cancer. *Int. J. Clin. Exp. Pathol.* **9**, 7370–7380 (2016).

313. Ishikawa, D. *et al.* The Significance of MicroRNA-449a and Its Potential Target HDAC1 in Patients with Colorectal Cancer. *Anticancer Res.* **39**, 2855–2860 (2019).

314. Chen, J. *et al.* ACSL4 promotes hepatocellular carcinoma progression via c-Myc stability mediated by ERK/FBW7/c-Myc axis. *Oncogenesis* **9**, 42 (2020).

315. Castillo, A. F. *et al.* New inhibitor targeting Acyl-CoA synthetase 4 reduces breast and prostate tumor growth, therapeutic resistance and steroidogenesis. *Cell. Mol. Life Sci.* **78**, 2893–2910 (2021).

316. Zhang, Y., Li, S., Li, F., Lv, C. & Yang, Q. kai. High-fat diet impairs ferroptosis and promotes cancer invasiveness via downregulating tumor suppressor ACSL4 in lung adenocarcinoma. *Biol. Direct* **16**, 10 (2021).

317. Lv, Y. *et al.* Low ferroptosis score predicts chemotherapy responsiveness and immune-activation in colorectal cancer. *Cancer Med.* 2033–2045 (2022) doi:10.1002/cam4.4956.

318. Yu, Y., Sun, X., Chen, F. & Liu, M. Genetic Alteration, Prognostic and

Immunological Role of Acyl-CoA Synthetase Long-Chain Family Member 4 in a Pan-Cancer Analysis. *Front. Genet.* **13**, 812674 (2022).

319. Guo, N. Identification of ACSL4 as a biomarker and contributor of ferroptosis in clear cell renal cell carcinoma. *Transl. Cancer Res.* **11**, 2688–2699 (2022).

320. Orlando, U. D. *et al.* The functional interaction between acyl-coa synthetase 4, 5-lipooxygenase and cyclooxygenase-2 controls tumor growth: A novel therapeutic target. *PLoS One* **7**, e40794 (2012).

321. Chang, S. H. *et al.* Role of prostaglandin E2-dependent angiogenic switch in cyclooxygenase 2-induced breast cancer progression. *Proc. Natl. Acad. Sci. U. S. A.* **101**, 591–596 (2004).

322. Xu, H. *et al.* CXCR2 promotes breast cancer metastasis and chemoresistance via suppression of AKT1 and activation of COX2. *Cancer Lett.* **412**, 69–80 (2018).

323. Miao, J. *et al.* Prostaglandin E2 and PD-1 mediated inhibition of antitumor CTL responses in the human tumor microenvironment. *Oncotarget* **8**, 89802–89810 (2017).

324. Tiemann, K. *et al.* Loss of ER retention motif of AGR2 can impact mTORC signaling and promote cancer metastasis. *Oncogene* **38**, 3003–3018 (2020).

325. Kim, J. & Guan, K. L. mTOR as a central hub of nutrient signalling and cell growth. *Nat. Cell Biol.* **21**, 63–71 (2019).

326. Jiang, X. *et al.* LncRNA NEAT1 promotes docetaxel resistance in prostate cancer by regulating ACSL4 via sponging miR-34a-5p and miR-204-5p. *Cell. Signal.* **65**, 109422 (2020).

327. Feng, J. *et al.* ACSL4 is a predictive biomarker of sorafenib sensitivity in hepatocellular carcinoma. *Acta Pharmacol. Sin.* **42**, 160–170 (2021).

328. Yang, W. *et al.* AMP-activated protein kinase α2 and E2F1 transcription factor mediate doxorubicin-induced cytotoxicity by forming a positive signal loop in mouse embryonic fibroblasts and non-carcinoma cells. *J. Biol. Chem.* **289**, 4839–4852 (2014).

329. Zhang, X. P., Liu, F. & Wang, W. Coordination between cell cycle progression and cell fate decision by the p53 and E2F1 pathways in response to DNA damage. *J. Biol. Chem.* **285**, 31571–31580 (2010).

330. Johnson, D. G. & Vélez-Cruz, R. E2f1 and p53 transcription factors as accessory factors for nucleotide excision repair. *Int. J. Mol. Sci.* **13**, 13554–13568 (2012).

331. Kukal, S. *et al. Multidrug efflux transporter ABCG2: expression and regulation*. *Cellular and Molecular Life Sciences* vol. 78 (Springer International Publishing, 2021).

332. Xiao, H., Zheng, Y., Ma, L., Tian, L. & Sun, Q. Clinically-Relevant ABC Transporter for Anti-Cancer Drug Resistance. *Front. Pharmacol.* **12**, 648407 (2021).

333. Shu, H. *et al.* High expression of ABCG2 is associated with chemotherapy resistance of osteosarcoma. *J. Orthop. Surg. Res.* **16**, 85 (2021).

Appendix

Supplementary figures

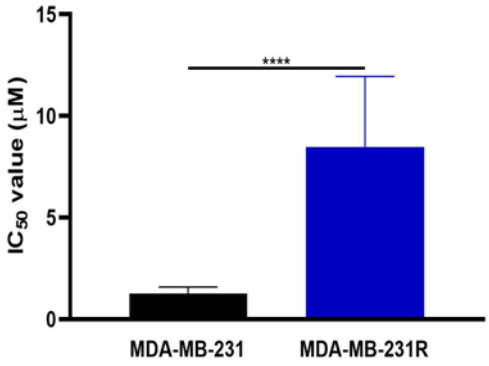

Figure S1: DOX-resistant cell line presents a higher IC_{50} value compared to the parental cell line. The IC_{50} value was determined by WST-1 after different doses of DOX treatment in DOX-resistant (MDA-MB-231R) (8.48 ± 3.46 μM) and DOX-sensitive (MDA-MB-231) (1.26 ± 0.32 μM) cell lines. **** $p<0.0001$.

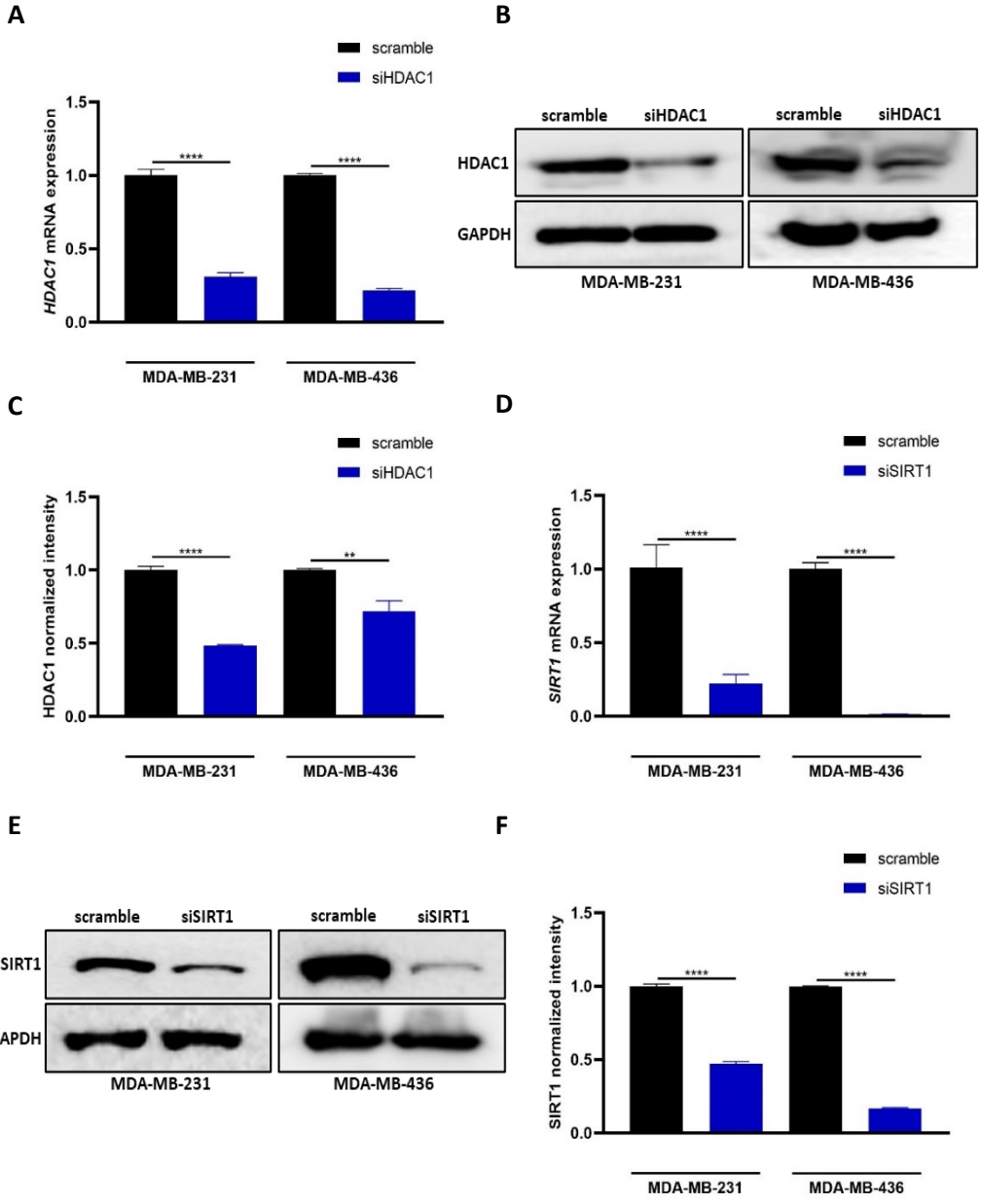
A
scramble
siHDAC1
HDAC1 mRNA expression
1.5
1.0
0.5
0.0
****
****
MDA-MB-231
MDA-MB-436
B
scramble
siHDAC1
scramble
siHDAC1
HDAC1
GAPDH
MDA-MB-231
MDA-MB-436
C
scramble
siHDAC1
HDAC1 normalized intensity
1.5
1.0
0.5
0.0
****
**
MDA-MB-231
MDA-MB-436
D
scramble
siSIRT1
SIRT1 mRNA expression
1.5
1.0
0.5
0.0
****
****
MDA-MB-231
MDA-MB-436
E
scramble
siSIRT1
scramble
siSIRT1
SIRT1
GAPDH
MDA-MB-231
MDA-MB-436
F
scramble
siSIRT1
SIRT1 normalized intensity
1.5
1.0
0.5
0.0
****
****
MDA-MB-231
MDA-MB-436

G

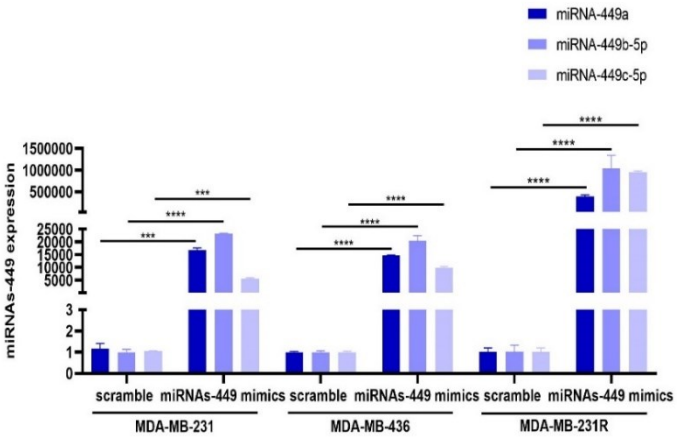
miRNA-449a
miRNA-449b-5p
miRNA-449c-5p
miRNAs-449 expression
scramble
miRNAs-449 mimics
MDA-MB-231
MDA-MB-436
MDA-MB-231R

H

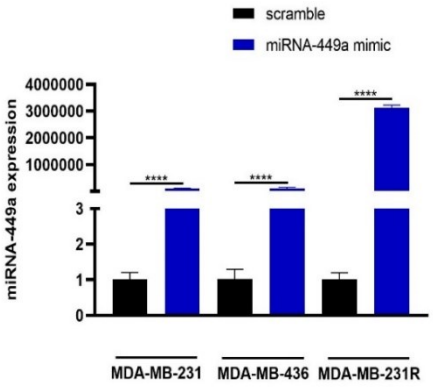
scramble
miRNA-449a mimic
miRNA-449a expression
MDA-MB-231
MDA-MB-436
MDA-MB-231R

I

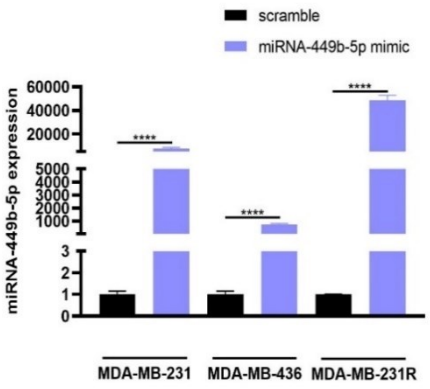
scramble
miRNA-449b-5p mimic
miRNA-449b-5p expression
MDA-MB-231
MDA-MB-436
MDA-MB-231R

J

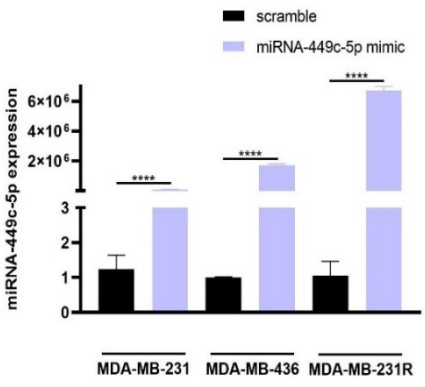
scramble
miRNA-449c-5p mimic
miRNA-449c-5p expression
MDA-MB-231
MDA-MB-436
MDA-MB-231R

K

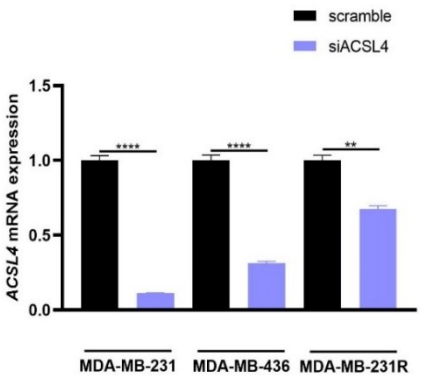
scramble
siACSL4
ACSL4 mRNA expression
MDA-MB-231
MDA-MB-436
MDA-MB-231R

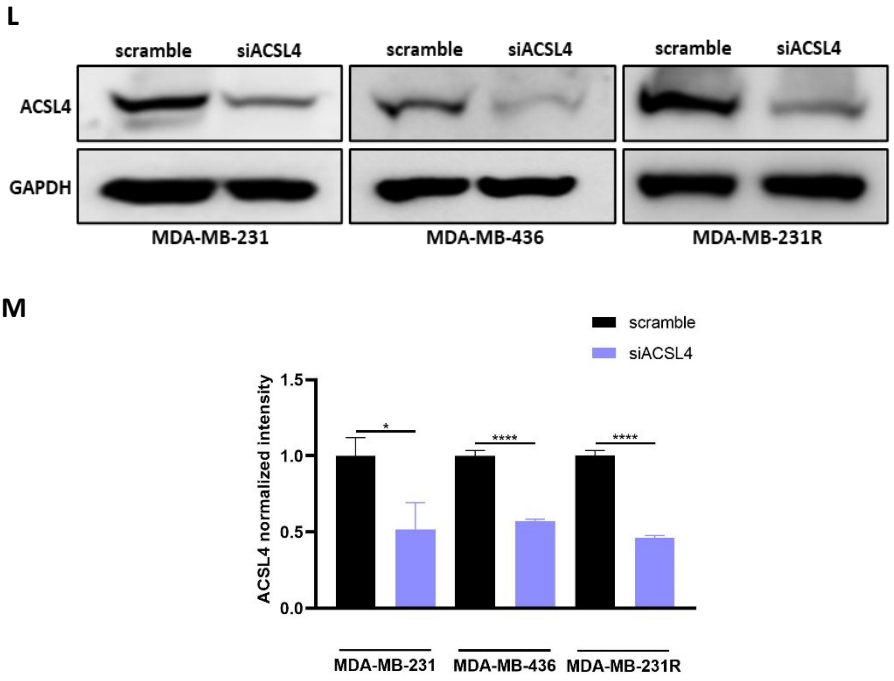

Figure S2: Verification of TNBC cell lines transfection. HDAC1 expression was analyzed by (**A**) RT-qPCR and (**B**) Western blot in MDA-MB-231 and MDA-MB-436 cell lines after siHDAC1 transfection. (**C**) Band densitometry of Western blots for HDAC1 were also performed and normalized to GAPDH. SIRT1 expression was analyzed by (**D**) RT-qPCR and (**E**) Western blot in MDA-MB-231 and MDA-MB-436 cell lines after siSIRT1 transfection. (**F**) Band densitometry of Western blots for SIRT1 were also performed and normalized to GAPDH. (**G**) miRNAs-449 expression were analyzed by RT-qPCR in MDA-MB-231, MDA-MB-436 and MDA-MB-231R cell lines after miRNAs-449 mimic transfection. (**H**) miRNA-449a, (**I**) miRNA-449b-5p and (**J**) miRNA-449c-5p expression were analyzed by RT-qPCR after in MDA-MB-231, MDA-MB-436 and MDA-MB-231R cell lines after miRNA-449a, miRNA-449b-4p and miRNA-449c-5p mimics transfection separately, respectively. ACSL4 expression was analyzed by (**K**) RT-qPCR and (**L**) Western blot in MDA-MB-231, MDA-MB-436 and MDA-MB-231R cell lines after siACSL4 transfection. (**M**) Band densitometry of Western blots for ACSL4 were also performed and normalized to GAPDH. Student T-test was used for statistical analyses for A, C, D, F, G, H, I, J, K and M. GAPDH was used as loading control for B, E and L.*p<0.05, **p<0.01, ***p<0.001, ****p<0.0001.

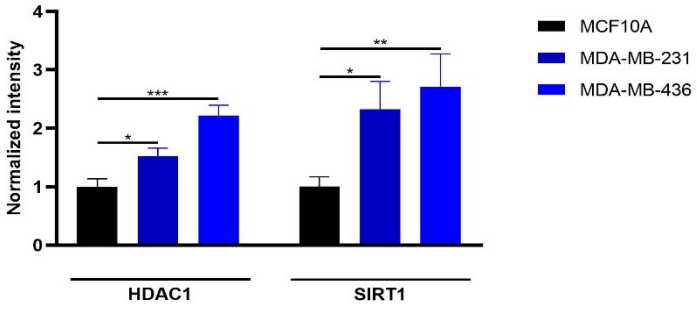

Figure S3: Bands densitometry for Western blot in figure 21C. Densitometry scores were normalized to GAPDH. Student T-test was used for statistical analyses. *p<0.05, **p<0.01, ***p<0.001.

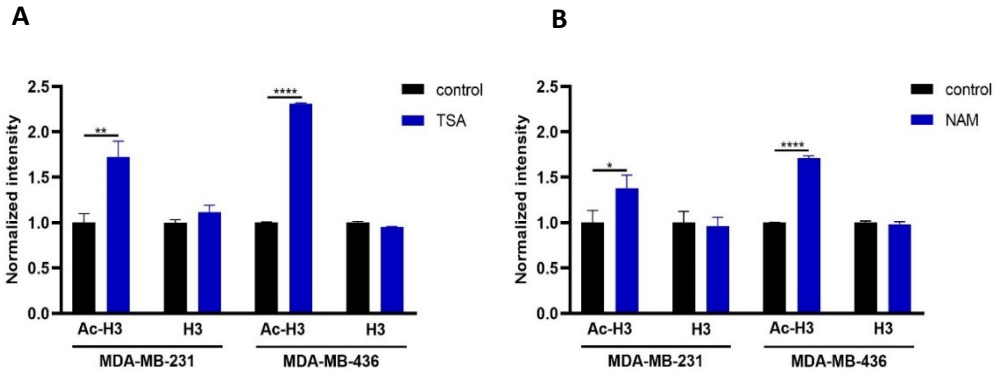

Figure S4: Bands densitometry for Western blot in figure 22. Band densitometry for figure (**A**) 22C and (**B**) 22D. Densitometry scores were normalized to GAPDH. Student T-test was used for statistical analyses. *p<0.05, **p<0.01, ****p<0.0001.

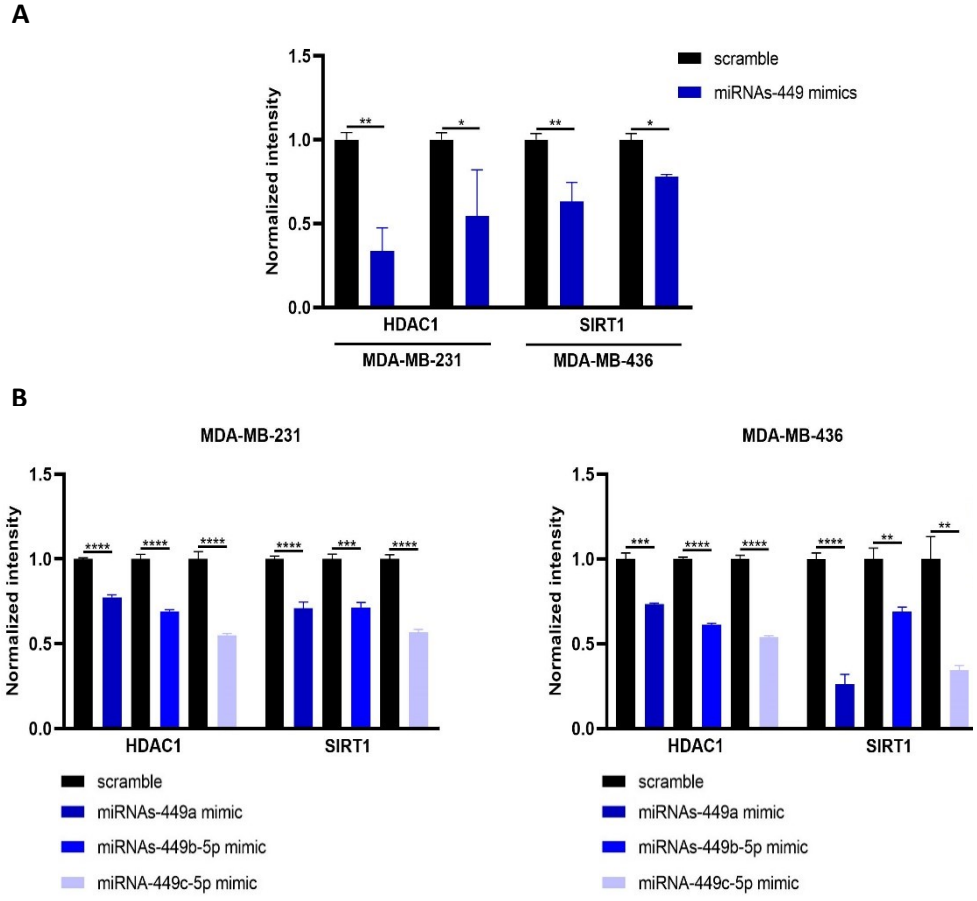

Figure S5: Bands densitometry for Western blot in figure 23. Band densitometry for figure (**A**) 23C and (**B**) 23F. Densitometry scores were normalized to GAPDH. Student T-test was used for statistical analyses. *p<0.05, **p<0.01, ***p<001, ****p<0.0001.

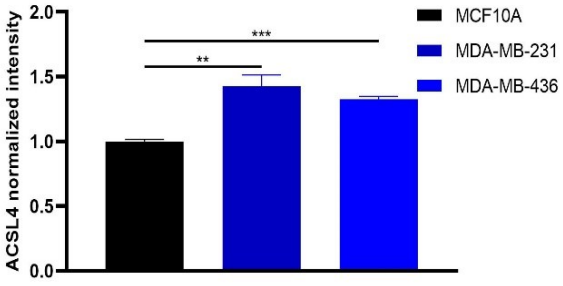

Figure S6: **Bands densitometry for Western blot in figure 24C.** Densitometry scores were normalized to GAPDH. Student T-test was used for statistical analyses. ***p*<0.01, ****p*<001.

A

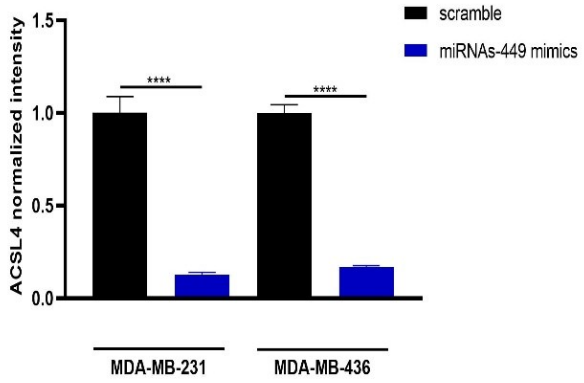

B

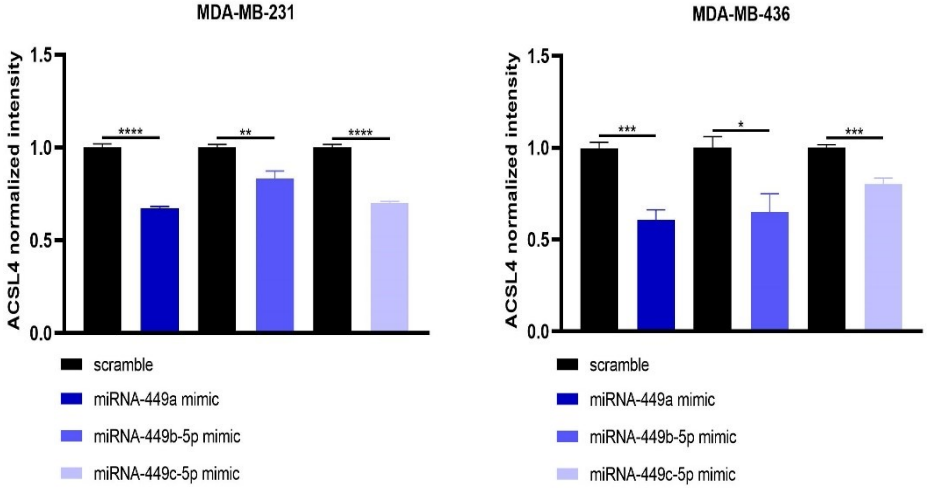

Figure S7: Bands densitometry for Western blot in figure 25. Band densitometry for figure (**A**) 25C and (**B**) 25E. Densitometry scores were normalized to GAPDH. Student T-test was used for statistical analyses. **p*<0.05, ***p*<0.01, ****p*<001, *****p*<0.0001.

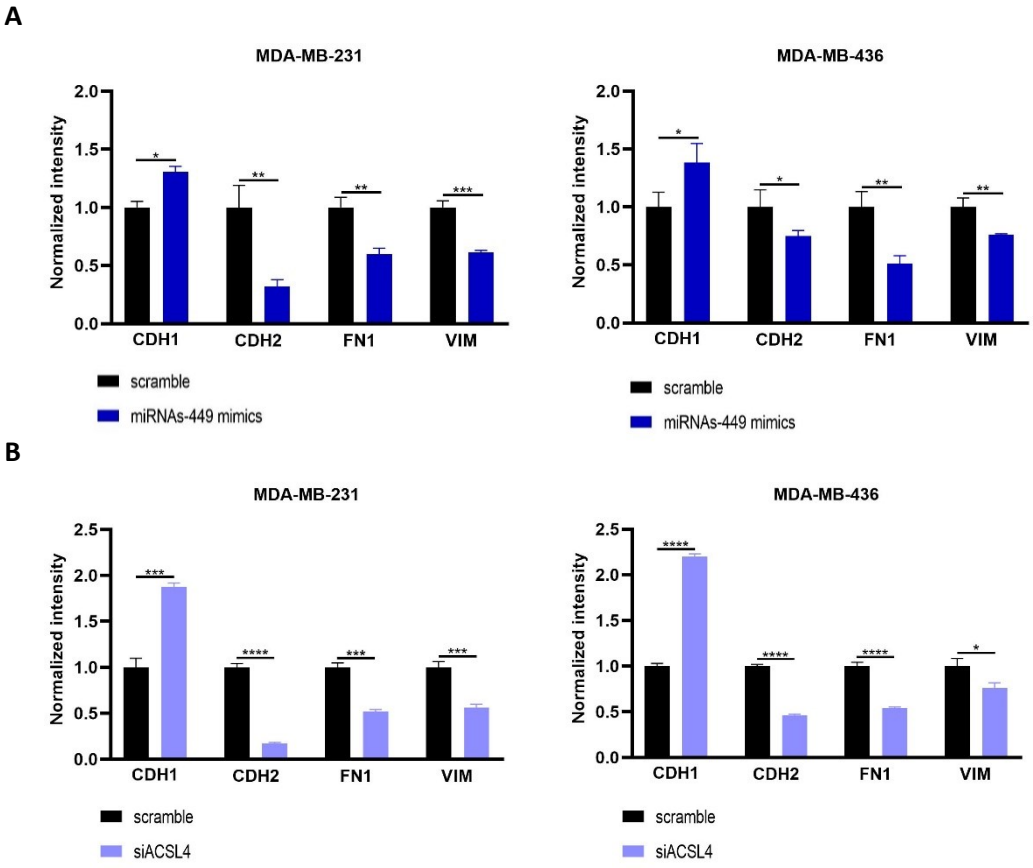

Figure S8: Bands densitometry for Western blot in figure 27. Band densitometry for figure (**A**) 27E and (**B**) 27F. Densitometry scores were normalized to GAPDH. Student T-test was used for statistical analyses. *p<0.05, **p<0.01, ***p<001, ****p<0.0001.

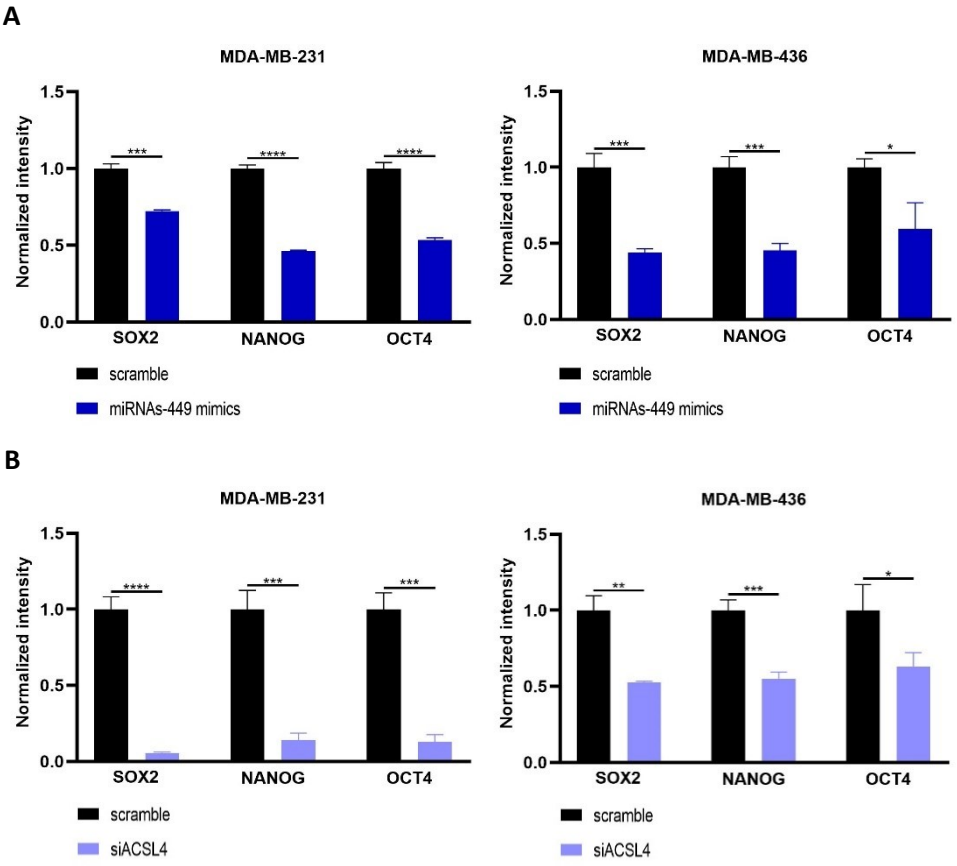

Figure S9: Bands densitometry for Western blot in figure 28. Band densitometry for figure (**A**) 28E and (**B**) 28F. Densitometry scores were normalized to GAPDH. Student T-test was used for statistical analyses. *p<0.05, **p<0.01, ***p<001, ****p<0.0001.

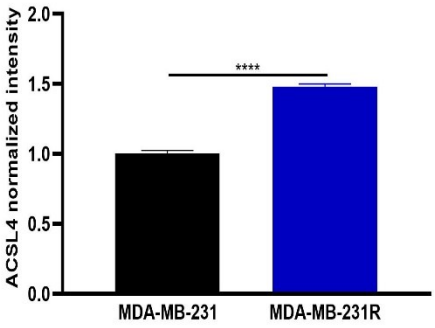

Figure S10: Bands densitometry for Western blot in figure 29C. Densitometry scores were normalized to GAPDH. Student T-test was used for statistical analysis. ****p<0.0001.

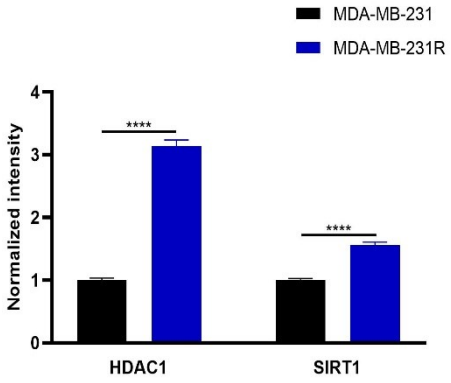

Figure S11: Bands densitometry for Western blot in figure 30B. Densitometry scores were normalized to GAPDH. Student T-test was used for statistical analyses. ****p<0.0001.

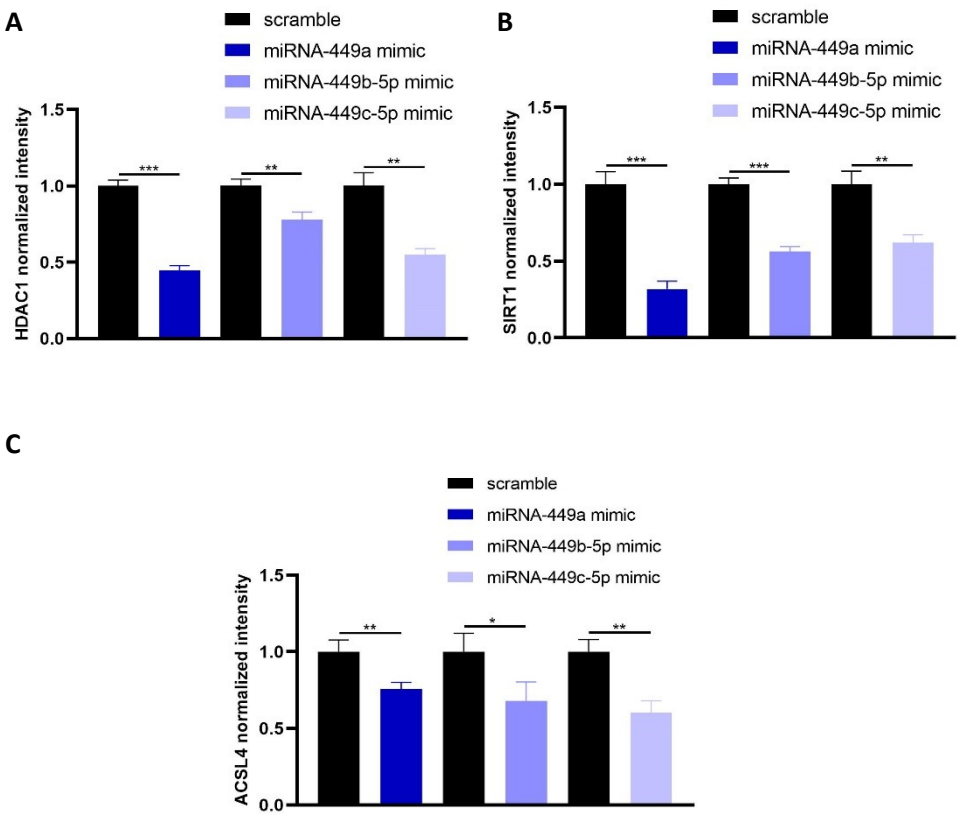

Figure S12: Bands densitometry for Western blot in figure 31. Band densitometry for figures (**A** and **B**) 31C and (**C**) 31E. Densitometry scores were normalized to GAPDH. Student T-test was used for statistical analyses. **p*<0.05, ***p*<0.01, ****p*<0.001.

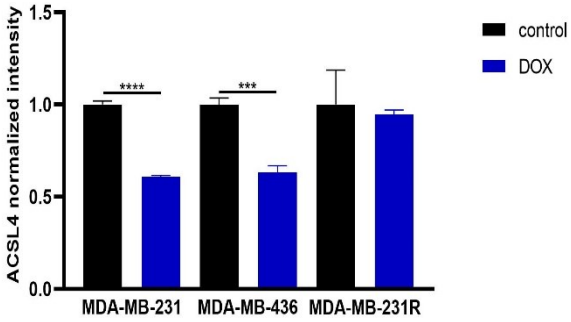

Figure S13: Bands densitometry for Western blot in figure 33C. Densitometry scores were normalized to GAPDH. Student T-test was used for statistical analyses. ****p*<0.001, *****p*<0.0001.

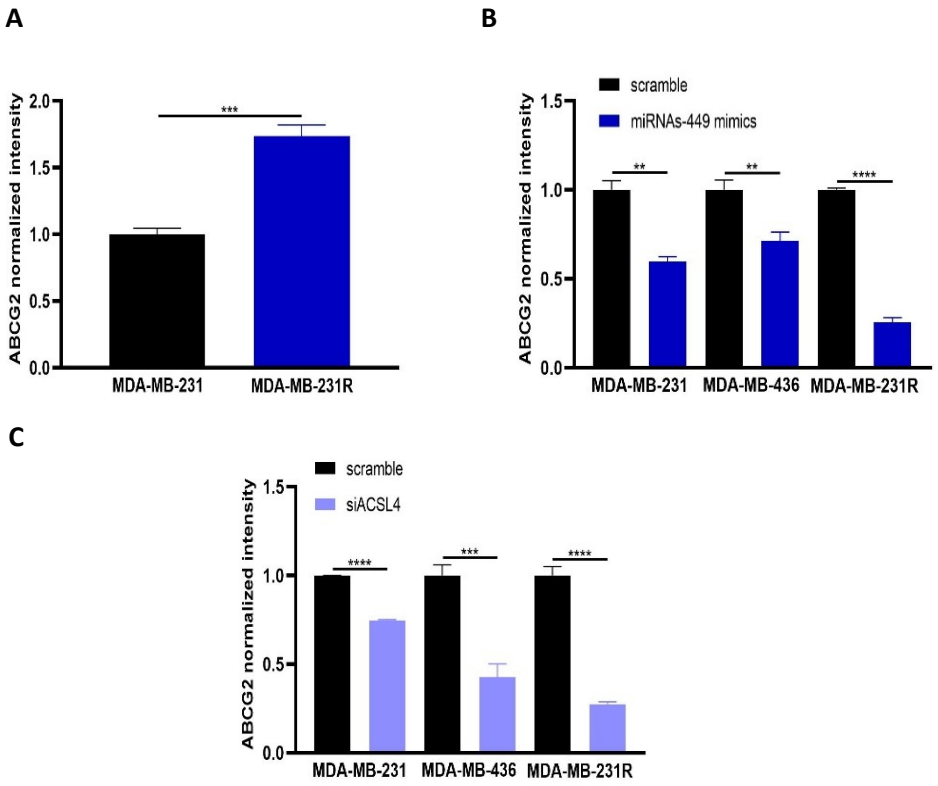

Figure S14: Bands densitometry for Western blot in figure 35. Band densitometry for figure (**A**) 35B, (**B**) 35C and (**C**) 35D. Densitometry scores were normalized to GAPDH. Student T-test was used for statistical analyses. ***p*<0.01, ****p*<001, *****p*<0.0001.

Supplementary tables

Table S1: Clinicopathological characteristics of TNBC patients and controls for miRNAs-449 analyses expression.

Characteristics	TNBC patients	Control
Number	55	23
Grade group, n (%)		
1	0(0%)	n.a.
2	11(20%)	
3	41(74.55)	
Unknown	3(5.45%)	
Clinical stage, n (%)		
1	13(23.64%)	n.a.
2	33(60%)	
3	8(14.54%)	
4	0(0%)	
Unknown	1(1.82%)	
Treatment, n (%)		
Neoadjuvant	37(67.27%)	n.a.
Adjuvant	0(0%)	
Neoadjuvant and Adjuvant	18(32.73%)	
RCB, n (%)		
0	22(40%)	n.a.
1	5(9.1%)	
2	16(29.1%)	
3	6(10.9%)	
Unknown	6(10.9%)	
Ki67, n (%)		
<30	4(7.27%)	n.a.
30-59.9	15(27.27%)	
≥60	33(60%)	
Unknown	3(5.46%)	
Regional lymph node metastasis, n (%)		
Yes	19(34.54%)	n.a.
No	35(63.64%)	
Unknown	1(1.82%)	
Distant metastasis, n (%)		
Yes	0(0%)	n.a.
No	54(98.18%)	
Unknown	1(1.82%)	

TNBC: Triple-negative breast cancer; RCB: Residual Cancer Burden; n.a: not applicable.

Table S2: Clinicopathological characteristics of TNBC patients and controls for *ACSL4* analysis expression.

Characteristics	TNBC patients	Control
Number	33	23
Grade group, n (%)		
1	0(0%)	n.a.
2	7(21.21%)	
3	25(75.76%)	
Unknown	1(3.03%)	
Clinical stage, n (%)		
1	8(24.24%)	n.a.
2	20(60.61%)	
3	5(15.15%)	
4	0(0%)	
Unknown	0(0%)	
Treatment, n (%)		
Neoadjuvant	21(63.63%)	n.a.
Adjuvant	0(0%)	
Neoadjuvant and Adjuvant	8(36.37%)	
RCB, n (%)		
0	17(51.51%)	n.a.
1	2(6.06%)	
2	9(27.27%)	
3	3(9.1%)	
Unknown	2(6.06%)	
Ki67, n (%)		
<30	3(9.1%)	n.a.
30-59.9	7(21.21%)	
≥60	23(69.69%)	
Unknown	0(0%)	
Regional lymph node metastasis, n (%)		
Yes	10(30.3%)	n.a.
No	22(66.67%)	
Unknown	1(3.03%)	
Distant metastasis, n (%)		
Yes	0(0%)	n.a.
No	33(100%)	
Unknown	0(0%)	

TNBC: Triple-negative breast cancer; RCB: Residual Cancer Burden; n.a: not applicable.

Table S3: Clinicopathological characteristics of relapse and non-relapse TNBC patients after chemotherapy treatment for *ACSL4* analysis expression.

Characteristics	TNBC no relapse patients	TNBC relapse patients
Number	12	20
Grade group, n (%)		
1	0(0%)	0(0%)
2	4(33.33%)	3(15%)
3	7(58.34%)	17(85%)
Unknown	1(8.33%)	0(0%)
Clinical stage, n (%)		
1	6(50%)	2(10%)
2	5(41.67%)	14(70%)
3	1(8.33%)	4(20%)
4	0(0%)	0(0%)
Unknown	0(0%)	0(0%)
Treatment, n (%)		
Neoadjuvant	11(91.67%)	14(70%)
Adjuvant	0(0%)	0(0%)
Neoadjuvant and Adjuvant	1(8.33%)	6(30%)
RCB, n (%)		
0	10(83.34%)	7(35%)
1	1(8.33%)	1(5%)
2	1(8.33%)	9(45%)
3	0(0%)	2(10%)
Unknown	0(0%)	1(5%)
Ki67, n (%)		
<30	1(8.33%)	1(5%)
30-59.9	3(25%)	4(20%)
≥60	7(58.34%)	15(75%)
Unknown	1(8.33%)	0(0%)
Regional lymph node metastasis, n (%)		
Yes	3(25%)	6(30%)
No	9(75%)	13(65%)
Unknown	0(0%)	1(5%)
Distant metastasis, n (%)		
Yes	0(0%)	0(0%)
No	12(100%)	19(95%)
Unknown	0(0%)	1(5%)

TNBC: Triple-negative breast cancer; RCB: Residual Cancer Burden; n.a: not applicable.

Table S4: **Bioinformatic analysis of miRNAs-449 target genes using miRWalk software**. ACSL4 bioinformatic analysis as miRNAs-449 (miRNA-449a, miRNA-449b-5p, and miRNA-449c-5p) direct target using miRWalk software. The database compares the results from 12 different miRNA–gene interaction prediction programs (miRWalk, Microt4, miRanda, mirbridge, miRDB, miRMap, miRNAMap, Pictar2, PITA, RNA22, RNAhybrid and Targetscan). SUM: Sum of bioinformatics programs that predicted each miRNA-gene interaction.

miRNA	Gene	EntrezID	RefSeqID	miRWalk	Microt4	miRanda	Mirbridge	miRDB	miRMap	miRNAMap	Pictar2	PITA	RNA22	RNAhybrid	Targetscan	SUM
hsa-miR-449a	ACSL4	2182	NM_022977	1	1	1	0	1	1	1	1	0	1	1	1	10
hsa-miR-449b-5p	ACSL4	2182	NM_022977	0	1	1	0	0	1	1	1	0	1	1	1	8
hsa-miR-449c-5p	ACSL4	2182	NM_022977	1	1	0	0	0	1	0	0	0	1	1	0	5